Strategies for Enhancing the Analytical Performance and Biocompatibility of Intravascular Amperometric Glucose Sensors

By

Alexander Keith Wolf

A dissertation submitted in partial fulfillment
of the requirements for the degree of
Doctor of Philosophy
(Chemistry)
in the University of Michigan
2016

Doctoral Committee:

Professor Mark E. Meyerhoff, Chair
Professor Robert T. Kennedy
Associate Professor Stephen Maldonado
Associate Professor Chuanwu Xi

2016

DEDICATION

This Work is Dedicated To:

My parents Keith W. Wolf, Jr. and Martha S. Wolf,
My grandparents Edward D. Simpson and Doris C. Simpson,
Keith W. Wolf, Sr. and Amy F. Wolf, and to
Irena F. Liu, Robert L. Yancy, and Hope M. Wolf
for their unending love and support.

ACKNOWLEDGEMENTS

Completion of this PhD research, would not have been possible without the help and support of many fantastic people in my life. First, and foremost, Dr. Meyerhoff, I would like to sincerely thank you for being wonderful advisor and mentor during my time as a graduate student at Michigan. I truly appreciate your encouraging and timely advice, in regards to both my research and professional career, infinite patience as I grew and developed from incoming grad student to senior researcher, and your immeasurable support and encouragement to persist through the many research challenges that I encountered while working on this research project. Being a part of your lab is being a member of your family, and you made each and every one of us in your lab a priority, taking time on late nights, weekends, and your holidays to help us with our conference abstracts, publication drafts, and research questions. I am humbled by your continued dedication to ensure that I always continue to learn new things and improve myself, and I am eternally grateful for the advice and wise words you've shared with me during my time here. I will carry the lessons you've taught me wherever life's journey carries me.

Thank you, especially, Dr. Robert Kennedy, Dr. Chuanwu Xi, and Dr. Stephen Maldonado for serving on my dissertation research committee. I very much appreciate your comments and suggestions, from candidacy to data meetings to defense, and I thank you very much for taking time from your schedules to serve a critical role in my progress toward a Ph.D.

I have been privileged to have the opportunity to work with many fantastic collaborators during my research at Michigan. Thank you, Terry Major, Dr. Megan Coughlin, Dr. Alvaro Rojas Pena, Dr. Robert Bartlett, Dr. Joseph Church, Dr. Azmath Mohammed, Marie Cornell, Salvatore Aiello, and Elena Perkins from the Extra-Corporeal Membrane Oxygenation (ECMO) lab in the Department of Surgery at the University of Michigan Medical School. It would have not been possible without your continued help animal prep, surgery, and vitals maintenance to collect the *in vivo* data from the rabbits and pigs. Terry and Megan, you were both invaluable resources with regards to advice on manuscript preparation and data analysis. Thank you so much, Dr. Stanley Stachelek and Dr. Robert J. Levy, my collaborators at the Children's Hospital of Philadelphia (CHOP) for conducting the CD47 surface immobilization on several sets of my glucose sensors as well as your helpful conference calls to discuss details of the CD47 immobilization protocol. Thank you, Dr. Megan Frost, for the collaboration project of writing the book chapter than overviewed glucose sensing technology which eventually became Chapter 1 of my thesis!

During my time as a member of the Meyerhoff lab, I have been incredibly fortunate to work with an amazing team of people! Whether it be brainstorming ideas to solve research obstacles, help proofreading documents, planning day trips or meals out for breaks, or exchanging life advice, they will always have a special place in my heart. Thank you to Dr. Laura Zimmerman, Dr. Natalie Crist, Dr. Bo Peng, Dr. Wenyi Ca, Dr. Elizabeth Brisbois (especially for all her help with SNAP synthesis), Dr. Andrea Bell, Dr. Si Yang, Alex Ketchum, Hang Ren (especially for your help with COMSOL modeling!), Zheng Zheng, Yaqi Wo, KyoungHa Cha, and Stephen Ferguson for sharing the graduate student experience with me. Thank you also to an exceptional group of post-doctoral researchers who helped mentor me and

offered many helpful suggestions on research and presentations, specifically Dr. Kebede Gemene, Dr. Lajos Hofler, Dr. Gary Jensen, Dr. Kun Liu, Dr. Dipankar Koley, Dr. Xuewei Wang, Dr. Gergely Lautner, Dr. Woonghee Lee, and Dr. Wen Wen. My lab experience was not complete without the opportunity to work with several undergraduate students. In particular, thank you to Eunsoo Yun, Alessandro Colletta, and Carly Warden for your help with glucose sensors. A very special thanks is due to Dr. Yu Qin and Dr. Xuewei Wang, as I am forever grateful for your help with glucose sensor design and conducting the *in vivo* animal experiments!

A very special thanks is also due to Roy Wentz, the master glass blower for the Chemistry Department at the University of Michigan. Your unique designs and solutions were invaluable to the Edwards transient NO project in Chapter 5. I am in awe of your hard work and extremely quick turnaround time on projects. Also, thanks to our accountants, Patti Fitzpatrick and Bo Zhao, who ensured that our orders were placed and delivered as quickly as possible. Thanks to Jon Boyd for his help in shipping sensors to Dr. Stachelek for the CD47 project.

I also had amazing mentors from instructors during my semesters as a Graduate Student Instructor. Thank you Dr. Jadwiga Sipowska, Dr. Amy Gottfried, and Dr. Brandon Rutolo for inspiring me to become a better instructor and truly enjoy my interactions with students. If I am to one day return to teaching, know that you inspired me to deeply care about my students as well as the information and experiments that I shared with them.

Outside of lab, I also had an amazing and invaluable group of friends to support and encourage me throughout my years as a graduate student. Thank you Robert Yancy, William Moore, Zach Powell, Alex Ketchum, Zheng Zheng, Dr. Broc Smith, Dr. Aaron White, Dr. Fangting Yu, Dr. Sung-He Yau, Dr. Lauren Soblosky, Dr. Jessica Gagnon, Dr. Brenden Arruda, Dr. Joshua Jasensky, Dr. Sabrina Peczonczyk, Richard Sutherland, and Thomas F. Blalock for

helping me through the rough times never letting me give up. Thank you to Rick Sanchez for your invaluable life advice and mentorship.

Finally, I want to thank my family for unquestioningly believing in me and encouraging me to always put forth my best effort. To my parents, sister, grandparents, aunts, uncles, cousins and my host family, Doug and Carol Gottliebsen, thank you for your care packages, home-cooked meals, cards, and encouraging words over the phone. I absolutely could not have completed this degree without you! Lastly, I would like say thank you to my wonderful girlfriend, Irena Liu, for your understanding and patience throughout all my late nights, weekends, holidays spent running experiments, and my many extended absences during the animal experiments. You all have made graduate school an amazing and unforgettable experience, and I can't wait to see all the exciting directions that life will take us next!

TABLE OF CONTENTS

LIST OF FIGURES

LIST OF ABBREVIATIONS

AFM	Atomic Force Microscopy
BSA	Bovine Serum Albumin
CGM	Continuous Glucose Monitoring
CNT	Carbon Nanotubes
DBHD	N,N'-Dibutyl-1,6-Hexanediamine
DBHD/N_2O_2	diazeniumdiolated dibutylhexyldiamine
DMHD/N_2O_2	(Z)-1-[N-methyl-N-[6-(N-methylammoniohexyl)amino]]-diazen-1-ium-1,2-diolate
DX	Dexamethasone
E2As	Elast-Eon Aliphatic Thermoplastic Polyurethane
FAD	Flavin Adenine Nucleotide
FDA	Food & Drug Administration
FITC	Fluorescein Isothiocyanate
FRET	Förster Resonance Energy Transfer
GOx	Glucose Oxidase
GPIb	Glycoprotein Ib
HAs	Humic Acids
HEP	Heparin
ICU	Intensive Care Unit (Hospital)
IV	Intravenous
LBL	Layer-By-Layer
LED	Light Emitting Diode
MC	Mast Cell
NADH	Nicotinamide Adenine Dinucleotide (Reduced Form)
NAF	Nafion
NDGA	Nordihydroguaiaretic Acid
NOA	Nitric Oxide Analyzer

OCP	Open Circuit Potential
PBS	Phosphate Buffered Saline
PCR	Polymerase Chain Reaction
PEG	Poly(Ethylene Glycol)
PFCI	Perfluorocarboxylic Acid Ionomer
PGH_2 and PGG_2	Prostoglandins
PHEMA	Poly(Hydroxyethyl Methacrylate)
PLA	Poly(Lactic Acid)
PLGA	Poly(Lactic-*co*-Glycolic Acid)
PSS	Polystyrene Sulfonate
PtTFPP	Platinum (II) Mesotetrakis(Penta-Fuorophenyl)Porphyrin
PU	Polyurethane
PVA	Poly(Vinyl Alcohol)
NO	Nitric Oxide
PVC	Poly(Vinyl Chloride)
RSNO	*S*-nitrosothiols
SEM	Scanning Electrode Microscopy
SG	Sol-Gel
SIRPα	Signal Recognition Transmembrane Protein α
SMCC	Succinimidyl 4-(N-maleimidomethyl)cyclohexane-1-carboxylate
SNAP	*S*-nitroso-*N*-acetylpenicillamine
TCEP	Tris(2-carboxyethyl)phosphine
THF	Tetrahydrofuran
UV	Ultraviolet
VEGF	Vascular Endothelial Growth Factor
vWF	von Willebrand's Factor

ABSTRACT

STRATEGIES FOR ENHANCING THE ANALYTICAL PEFORMANCE AND BIOCOMPATBILITY OF INTRAVASCULAR AMPEROMETRIC GLUCOSE SENSORS

by

Alexander K. Wolf

Chair: Dr. Mark E. Meyerhoff

Ensuring accurate analytical performance that can overcome the body's response to foreign objects is an integral part of developing improved *in vivo* biosensors. Blood contact from intravenous placement of such sensors readily results in surface clot formation, and blood-born electroactive species obscure the desired signal response. In this thesis, improvements of amperometric glucose sensor selectivity are combined with strategies to augment surface hemocompatibility with the aim of enhancing the *in vivo* analytical performance of such devices.

Annealing thin films and membranes of the sulfonated fluoropolymer Nafion causes morphological changes to the hydrophilic regions, altering their transport properties. Addition of a novel annealed Nafion layer to the electrode cavity of needle/catheter-type glucose sensors is shown to enhance selectivity over ascorbic and uric acid (<3 % of signal response for 5 mM glucose at typical levels of ascorbic and uric acid in blood) for a duration of at least 8 days.

The transmembrane CD47 protein is ubiquitously expressed in many cells as a marker of "self". A temporary "handshake" interaction with its cognate receptor on inflammatory response

cells (SIRPα) suppresses platelet activation. Herein, the outer polyurethane coatings of glucose sensors were functionalized with 85.0 ng/cm^2 of recombinant human CD47. *In vitro* calibrations confirm that immobilization has no adverse impact on the sensors' glucose response properties or selectivity against interference species.

Nitric oxide (NO) is a potent antithrombotic molecule, endogenously released by endothelial cells to prevent platelet activation and clot formation. Polymer layers of poly(lactic acid) containing the NO donor molecule diazeniumdiolated N,N'-dibutyl-1,6-hexanediamine (DBHD/N_2O_2) grant surface thromboresistance to glucose sensor surfaces by mimicking endogenous NO release from endothelial cells at a localized flux >0.5×10^{-10} mol cm^{-2} min^{-1} for at least 7 d. Intravascular amperometric glucose sensors prepared with such NO release coatings accurately trace modulations of *in vivo* glucose concentration within rabbit veins for 7 h. Preliminary *in vivo* glucose measurements for 20 h porcine veins are also examined and extensive *in vitro* investigations are conducted to identify sources of significant sensor calibration drift observed in the porcine model.

Finally, the Edwards GlucoClear, a commercial intermittent glucose sensing system, is configured for transient NO release. Preliminary data and diffusion modeling suggest that a source silicone rubber catheter sensor housing can be loaded with *S*-nitroso-*N*-acetylpenicillamine (SNAP), an NO releasing donor. NO released from the catheter partitions uniformly into the thin outer polyurethane sensor coating at a projected concentration of 6.77 x 10^{-5} M during a 5 min charging phase, enabling transient NO release above >0.5×10^{-10} mol cm^{-2} min^{-1} for a significant period (>5 min) after the sensor removal from the NO source, simulating *in vivo* blood contact. Rapid glucose response time and linearity of the sensors are preserved.

CHAPTER 1

CURRENT STATUS OF IN VIVO SENSORS FOR CONTINUOUS MONITORING OF CRITICAL CARE ANALYTES: BIOCOMPATIBILITY CHALLENGES AND POTENTIAL SOLUTIONS*

1.1 Introduction

Advances in electrochemical and optical sensors designed for specific ions (H^+, Na^+, K^+, Ca^{+2}, Cl^-), gases (PO_2, PCO_2), and low molecular weight biomolecules (*e.g.*, glucose, lactate, creatinine, urea, *etc*.) over the past 40 years have revolutionized the measurement of such species in the clinical setting, enabling rapid, near patient/point-of-care testing of such critical care analytes in undiluted blood samples.[1,2] However, nearly all existing sensor-based measurement systems require discrete samples of blood. Only a few commercial systems are designed for continuous monitoring capability either *in vivo* (for glucose monitoring in subcutaneous fluid[3,4]) or for short periods in blood within the bypass blood loops used during open-heart surgery (where blood clotting is prevented with high levels of anticoagulant).[5,6]

*Note: This chapter is adapted from the following book chapter that was coauthored by this Ph.D. candidate: M. C. Frost, A. K Wolf, and M.E. Meyerhoff, "In Vivo Sensors for Continuous Monitoring of Blood Gases, Glucose and Lactate," RSC Detection Science Series No. 2 Detection Challenges in Clinical Diagnostics, P. Vadgama and S. Peteu (Editors); The Royal Society of Chemistry, 2013.

Even the existing implantable sensors for glucose that are commercially available have significant limitations in their accuracy, requiring frequent calibration and confirmation of results *via* separate *in vitro* measurements of blood glucose using conventional glucometer test strips.[7–10]

Although there have been enormous efforts over the past 25 years by many companies to develop catheter-type sensors that could monitor blood gases (oxygen, carbon dioxide and pH) within arteries of critically ill patients using miniaturized electrochemical or optical sensors,[11–14] all of these efforts failed to produce a successful product. The lack of success in developing implantable chemical sensors that can provide reliable analytical results, especially for the blood gas test panel (PO_2, PCO_2, and pH), as well as for glucose and lactate (note: lactate levels are a major indicator of status for intensive-care patients[15–17]) can be attributed primarily to the biological response to the indwelling sensors.

In this chapter, the status of implantable chemical sensor technology for these analytes are reviewed. In addition, the fundamental biocompatibility problems inherent to both intravascular (placed in the blood stream) and subcutaneous (implanted under the skin) chemical sensors and new approaches aimed at solving these fundamental problems that might enable greatly enhanced analytical performance for indwelling chemical sensing devices are summarized.

1.2 Design of *In Vivo* Sensors

The basic requirements for sensors potentially useful for continuous real-time, *in vivo* measurements are: a) be of very small size (< 1 mm o.d.) for easy placement within a blood vessel (*i.e.*, artery for blood gases/pH; vein for glucose/lactate) or under the skin in

subcutaneous space (primarily for glucose); b) exhibit long-term analytical signal stability (limiting frequency of recalibration); c) cannot exude toxic chemicals into the patient; and d) provide reliable analyte values that correlate with conventional *in vitro* tests that use discrete blood samples, ideally such that analyte values reported by the implanted sensor can be used in place of discrete blood-test measurements to initiate appropriate medical therapy.

1.2.1 Sensing PO_2/PCO_2/pH in Blood

Miniaturized versions of both electrochemical (potentiometric and amperometric) and optical sensors have been employed to prepare intravascular devices. Figure 1.1 for illustrates the overall concept of intravascular blood-gas/pH sensors to monitor patients continuously. Optical sensors have certain advantages over electrochemical devices, including (1) ease of miniaturization using modern optical fibers; (2) potentially less electronic noise (no transduction wires); (3) potential long-term stability using ratiometric measurements at multiple wavelengths; and (4) no need for a separate reference electrode. These advantages promoted the development of optical sensor technology initially for the design of intravascular blood gas sensors using multiple optical fibers.[11]

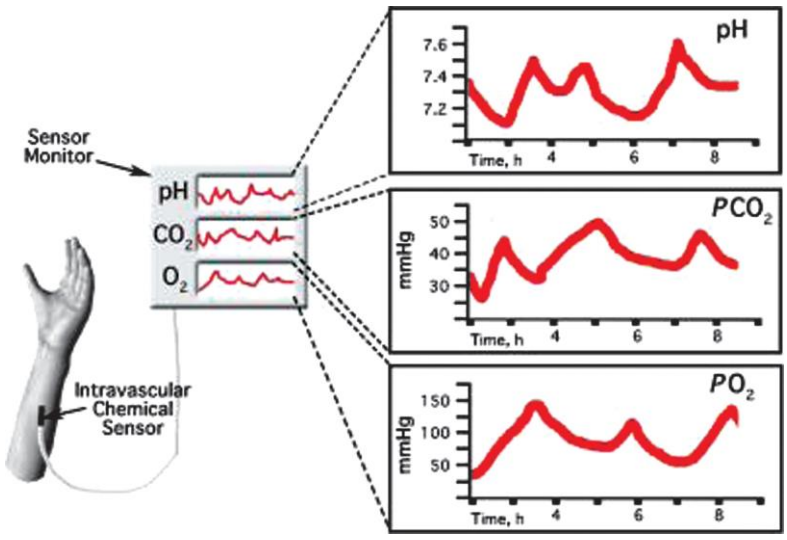

Figure 1.1. Overall concept of *in vivo* blood gas/pH patient monitoring system based on use of intravascular chemical sensors. Sensor inserted in to artery would be able to continuously monitor oxygen, carbon dioxide, and pH levels in arterial blood.

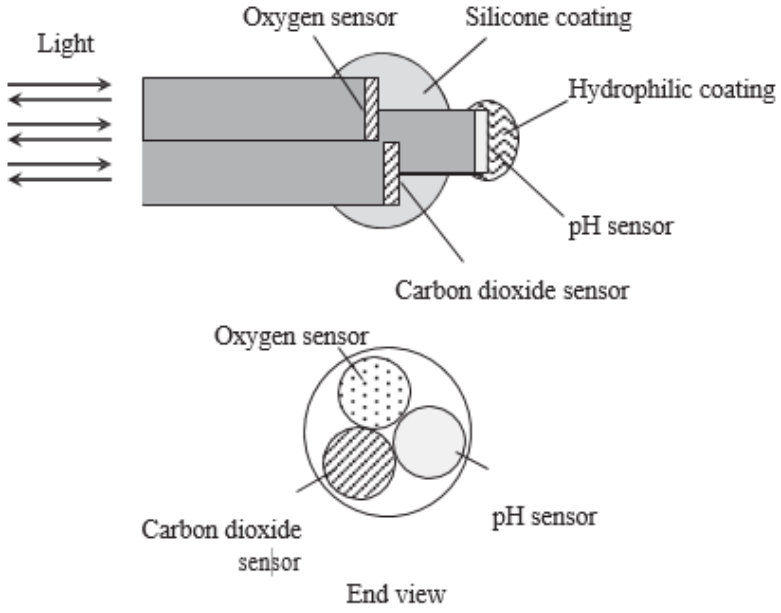

Figure 1.2. Schematic of intravascular optical blood-gas/pH sensing catheter configuration that uses three optical fibers to carry light to and from fluorescent dyes in sensing layers that enables optical detection of pH, PCO_2, and PO_2. This configuration is based on US Patent # 5,047,627 (1991).

In such systems, light is passed to and from the sensing site that contains immobilized dyes sensitive to the analyte species by the optical fibers and measures (by reflectance) the fluorescence or phosphorescence originating from the immobilized indicator at the distal end of the fibers (see Figure 1.2 for multifiber design for intravascular blood gas/pH sensing originally patented by Abbott Laboratories). Optical fiber sensors for PO_2 measurements are typically based on the immobilization of certain organic dyes, such as pyrene, diphenylphe- nanthrene, phenanthrene, fluoranthene, or metal ligand complexes, such as ruthenium[II] tris[dipyridine], or Pt and Pd metalloporphyrins within hydrophobic polymer films (*e.g.*, silicone rubber) in which oxygen is very soluble.[18,19] The fluorescence or phosphorescence of such species at a given wavelength is often quenched in the presence of paramagnetic species, including molecular oxygen. In the case of embedded fluorescent dyes, the intensity of the emitted fluorescence of such films will decrease in proportion to the PO_2 of the sample in contact with the polymer film. Optical-fiber oxygen sensors have also been developed using a luminophore platinum (II) mesotetrakis(penta-fluorophenyl)porphyrin (PtTFPP) complex embedded in different sol-gels.[20,21] The fluorescence of the PtTFPP is quenched in the presence of oxygen.

Optical sensors suitable for the determination of PCO_2 employ optical pH transducers (with immobilized indicators) as inner transducers in an arrangement quite similar to the classic Stow–Severinghaus style electrochemical PCO_2 sensor design. In this design, the pH-sensing layer is behind an outer gas permeable coating (*e.g.*, silicone rubber) that prevents sample proton access to the pH sensing layer (see Figure 1.3).[22] The addition of bicarbonate salt within the pH-sensing hydrogel layer creates the required electrolyte film layer, which varies in pH depending on the partial pressure of PCO_2 in equilibrium with the film. As the partial pressure

of PCO_2 in the sample increases, the pH of the bicarbonate layer decreases, and the corresponding decrease in the concentration of the deprotonated form of the indicator (or increase in the concentration of protonated form) is optically sensed. An alternate optical intravascular PCO_2 sensor was developed by Jin, *et al.*[23] using the fluorescence indicator 1-hydroxypyrene-3,6,8-trisulfonate that directly interacts with CO2.

Optical pH sensors require immobilization of appropriate pH indicators within thin layers of hydrophilic polymers (*e.g.*, hydrogels) because equilibrium access of protons to the indicator is essential. Fluorescein or 8-hydroxy-1,2,6-pyrene trisulfonate (HPTS) have often been used as the indicators and the fluorescence of the protonated or deprotonated form of the dyes can be used for sensing purposes.[24]

Jin and coworkers report the fabrication of an intra-arterial pH sensor based on fluorescence using N-allyl-4-piperazinyl-1,8-napthalimide and 2-hydroxyethyl methacrylate.[25] The sensors were tested in rabbits and showed appropriate response times ($t90$ ¼ 13.7 ± 0.8 s to 109.61 ± 4.06 s, depending on the conditions of the pH change) that are quite useful for real-time monitoring. One problem with respect to using immobilized indicators for accurate physiological pH measurements is the effect of ionic strength on the pKa of the indicator.[26] Because optical sensors measure the concentration of protonated or deprotonated dye as an indirect measure of hydrogen ion activity, variations in the ionic strength of the physiological sample have been known to influence the accuracy of the pH measurement.

While many of the prototypes for implantable blood gas monitoring developed in the 1980s/1990s were based on optical sensors that could be easily inserted in the radial artery of patients, miniaturized electrochemical sensors have also been described for *in vivo* sensing of

blood gases.[11–13] Electrochemical oxygen sensing catheters are based on the Clark-style oxygen sensing configuration (Figure 1.4), in which a platinum wire along with a Ag/AgCl or other reference electrode are placed within a narrow gas permeable tubing filled with an electrolyte solution.[11]

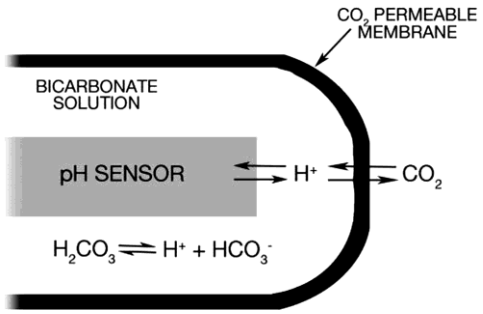

Figure 1.3. Basic *in vivo* PCO_2 sensing configuration that can be employed to detect carbon dioxide levels in blood using inner electrochemical or optical pH sensor.

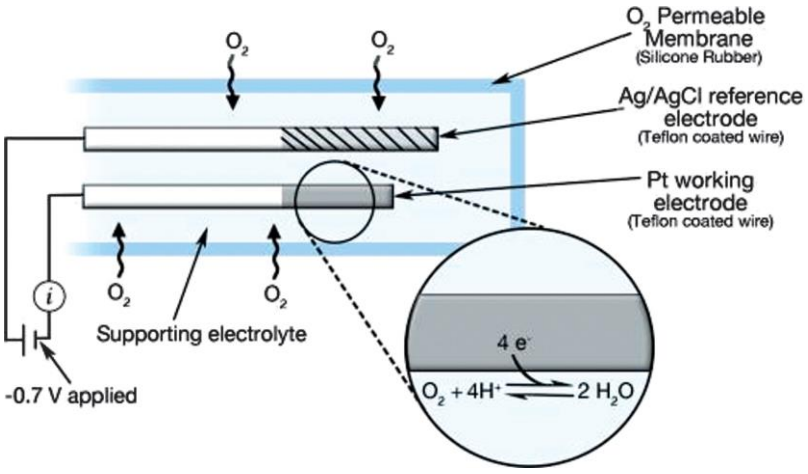

Figure 1.4. General design of implantable electrochemical PO_2 sensing catheter, where oxygen in sample permeates outer tubing wall of the catheter and is reduced electrochemically at working Pt wire electrode. The current flow is directly proportional to the PO_2 level in the blood stream.

For the electrochemical oxygen sensing catheters, oxygen within the blood stream diffuses through the walls of the tubing and is reduced electrochemically at the Pt working electrode *via* application of a – 0.6 to – 0.7 V *vs*. the Ag/AgCl reference electrode. The resulting current in the circuit is proportional to the *P*O2 levels in the blood.

Electrochemical *P*CO2 sensors suitable for intravascular sensing are typically prepared with miniature pH sensors, ideally non-glass potentiometric devices, made with metal oxides[27] or ionophore-based polymer membrane devices[28,29] that contain modified filling solutions. Carbon dioxide diffusion through the walls of a catheter tubing changes the pH within an inner bicarbonate filling solution. In one proposed *in vivo* sensor configuration, the pH ionophore tridodecylamine was impregnated into the walls of a dual lumen silicone rubber catheter tubing, with one of the lumens filled with buffer and the other with bicarbonate solution. The voltage between Ag/AgCl electrodes placed in each lumen is dependent on the PCO_2 level in the sample surrounding the tubing, since the wall between the two lumens is pH sensitive and detects the pH change within the lumen filled with the bicarbonate solution. If an external reference electrode is also employed, then the voltage between the Ag/AgCl wire in the buffered lumen *vs.* the external reference is related to the pH of the sample phase. Other recent work focused on electrochemical pH sensing includes a report by Makos, *et al.*[30] who developed a modified carbon-fiber electrode by the reduction of the diazonium salt Fast Blue RR on the fiber. The resultant sensor was capable of monitoring pH changes as small as 0.005 pH units. Huang and coworkers[31] report the fabrication of a flexible pH sensor utilizing a polymer substrate with an iridium oxide sensing layer, a sol-gel matrix, and an electroplated AgCl reference electrode. The ability to conform to a variety of shapes offers a wide range

of potential applications.

1.2.2 Sensing Glucose in Subcutaneous Tissue

The vast majority of sensors that can be implanted subcutaneously for continuous glucose monitoring (CGM) and lactate monitoring are electrochemical devices.[7,32–40] For glucose sensors, the enzyme glucose oxidase is most often employed as an immobilized catalyst on the surface of a suitable electrochemical transducer. Some configurations use amperometric oxygen sensors with glucose oxidase immobilized as layer on the outer surface. Glucose present in the bathing solution at the sensor reacts with oxygen *via* the enzyme, lowering the partial pressure of oxygen immediately adjacent to the outer gas-permeable membrane of the oxygen sensor. The decrease in PO_2 and concomitant current decrease is proportional to the level of glucose in the surrounding blood or tissue. However, typically, a second non-enzyme covered PO_2 sensor is required to monitor the level of PO_2 present in the sample phase. Similar configurations based on optical PO_2 sensors have also been reported.[41]

More often, implantable glucose sensors are fabricated using electrochemical oxidation of hydrogen peroxide (H_2O_2), produced by the immobilized glucose oxidase catalyzed reaction of glucose and oxygen. This is normally accomplished using a small surface area of platinum wire as the anode and an applied voltage of +0.6 to +0.7 V *vs.* an external Ag/AgCl electrode. Other physiological species (*e.g.*, ascorbic acid, uric acid, *etc*.) can be oxidized at this potential, so additional layers of membranes/coatings that decrease access of these species to the platinum surface are required. Specifically, the use of annealed Nafion membranes on implantable glucose sensors to select against these species is highlighted in Chapter 2 of this thesis. Further,

the outermost layer of such sensors requires a polymeric coating (illustrated in Figure 1.5) that restricts glucose diffusion[42] so that the glucose concentrations within the underlying immobilized enzyme layer are always less than the lowest levels of oxygen that might be present in the *in vivo* sample phase. This requirement greatly decreases the sensitivity of the devices to variations in localized oxygen levels and also enables the sensors to respond linearly to abnormally high levels of glucose (up to 20 mM) that might be present in blood or tissue of diabetic patients.

Another approach taken to prepare *in vivo* glucose sensors uses immobilized redox hydrogels in which tethered mediator sites (*e.g.*, ferrocene or Os(III) redox species) are able to accept electrons from the reduced form of the immobilized glucose oxidase enzyme after reaction with glucose.[43] These reduced mediators are then oxidized and hence the steady-state current is directly proportional to glucose concentration. The advantage of the mediator-based devices is that they partially reduce the need for outer membranes that carefully control the flux of glucose relative to oxygen. Further, the applied potential to the inner conductive electrode material can be less positive to reoxidize the mediator (compared to hydrogen peroxide), reducing the need for exclusion layers to block potential oxidizable species present in the *in vivo* milieu.

There have been a few optical-based glucose sensors reported with small size required for implantation.[44] These are usually fluorescent sensors that utilize glucose-binding proteins and fluorophore-labeled saccharides in a competitive binding mode behind membranes that are permeable to glucose.

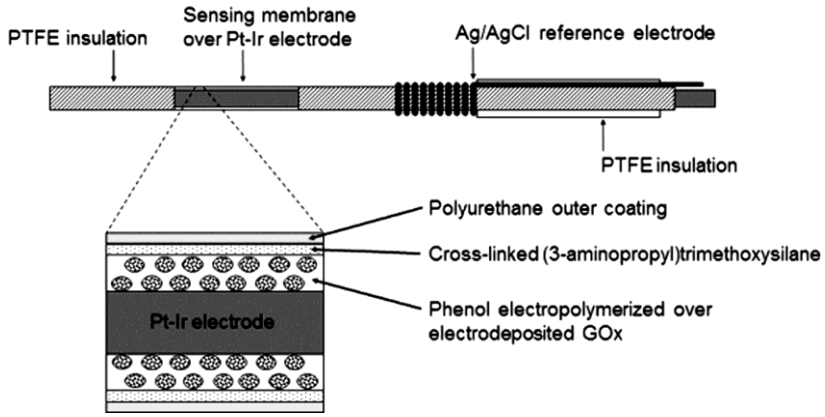

Figure 1.5. One design of subcutaneous or intravascular glucose sensors (diameter <0.6 mm), with glucose oxidase (GOx) immobilized over surface of Pt/Ir wire and a coiled Ag/AgCl reference electrode. The outer polyurethane layer decreases the rate of glucose access to enzyme layer, while allowing rapid diffusion of oxygen, that enables the sensor to exhibit a linear response to high levels of glucose (to 20 mM). The Pt/Ir electrode is poised at +0.65 V *vs.* Ag/AgCl to oxidize hydrogen peroxide generated from the enzymatic reaction.

(With permission from reference 11.)

Recent developments in electrochemical glucose sensors have branched in several directions from the second-generation sensors described above. Some continue to utilize the glucose oxidase/hydrogen peroxide enzyme electrodes, but they feature novel outer layers to limit glucose diffusion to extend the linear range and to extend the stability and lifetime of the sensors. Others have worked to eliminate electron-transfer mediators through the use of carbon nanotubes. Amperometric glucose sensors developed by Tipnis *et al.*[45] follow the standard design of immobilized glucose oxidase to generate hydrogen peroxide for oxidation. Glucose concentration is still determined from the measured steady-state current, but these sensors incorporate a layer-by-layer (LBL) assembled film as an outer coat to both limit glucose diffusion and minimize calcification, which can clog sensor pores or crack the outer membrane. LBL coatings of humic acids (HAs) and ferric chloride ($FeCl_3$) of various

thicknesses were compared to optimize the number of layers to tune glucose diffusion from the bulk to the sensor surface.[45] Lin *et al.* constructed sensors that utilized low density carbon nanotubes (CNT) for direct electron transfer between the enzyme and the electrode surface so that sensors neither required an electron mediator nor an outer glucose limiting layer.[46,47] These sensors had a large linear range (2–30 mM). Even more promising are sensors fabricated with carbon nanotube fibers, spun into nanoyarns.[48] The fibers are unwound at the tip to create a ‘‘brush’’ onto which glucose oxidase is immobilized and an outer polyurethane outer membrane is applied. These sensors exhibit limits of detection as low as 25 mM, although such low detection levels are not required for blood glucose measurements. Using nickel or copper nanoparticles to make a CNT array also lowered the limit of detection.[48]

Recent glucose sensors have also once again utilized optical detection to take advantage of technological developments in optical materials and the high degree of reversibility characteristic of optical sensors. Tierney *et al.* fabricated glucose sensors that function by covalent binding of an acrylamide-based hydrogel to the tip of an optical fiber.[49] The local glucose concentration swelled and contracted the phenylboronic acid within the hydrogel, changing the optical path length, which was measured by the optical fiber. What especially sets these optical sensors apart is their elimination of the need for a fluorescent molecule or tag. The sensors had high reversibility but could have interferences from glycoproteins, polysaccharides, elevated blood levels of lactate, and the common anticoagulants heparin and citrate. Sensor function was also significantly temperature dependent, as the difference between room and body temperature significantly affected the equilibrium swelling degree. Glucose sensors developed by Paek *et al.* utilize a reversible glucose binder, rather than a catalytic

enzyme reaction that consumes local glucose and optical detection, that would not suffer signal noise electromagnetic fields, and could use a detector that was spatially separated from the sensor.[50] The sensor functioned by competitive binding between glucose and a ligand conjugate for the immobilized glucose-selective protein (concanavalin A), which caused a detectable wavelength shift in the optical sensor. However, in order or preserve sensor lifetime for CGM and recycle the ligand conjugate, the sensing area must be separated from the sample by a semipermeable membrane selective for glucose diffusion. All of these sensors show promise in helping to extend the linear working range of glucose sensors and replace the sensitive glucose oxidase enzyme; however, the biocompatibility of these sensors to thrombosis and immune response from long-term *in vivo* implantation has yet to be assessed.

Despite tremendous advances in sensor design, however, none of these designs have yet achieved widespread use, and all existing commercial *in vivo* glucose sensors are either based on electrochemical detection of hydrogen peroxide or redox-mediator species. Indeed, Table 1.1 lists the current commercially available electrochemical glucose sensors, the lifetime of the sensor *in vivo*, and the suggested frequency of recalibration. The only FDA approved devices (by Medtronic-Minimed, Abbott Inc., Dexcom Inc.) require recalibration *in vivo* several hours after implantation (*via* repeated *in vitro* blood tests by the diabetic patient).[7–10] Even with such measures, the outputs of the devices are still not reliable enough for the patient to exclusively use values for monitoring glucose levels to decide on insulin doses.

Table 1.1. The current commercially available *in vivo* (all subcutaneous) electrochemical glucose sensors, sensor lifetime, and the suggested frequency of recalibration.

Company	*Sensor*	*Implantation time*	*Calibration frequency*
Abbott	FreeStyle Libre	5 days	no glucometer calibration required
			(1, 3, 24 h) not re-calibrated until new sensor implanted
Medtronic	Guardian	3 days	3–4 finger pricks/day (recommended), 1 per
	Enlite	6 days	12 hours required
Dexcom	G5	7 days	1 per 12 hours

1.2.3 Sensing Lactate in Blood

As mentioned above, continuous lactate measurements would be most useful in intensive-care units within hospitals since elevated lactate levels in blood are a negative predictor of a good outcome for such patients. Indeed, many critical-care doctors believe that trends in blood-lactate levels provide the best indicator of tissue oxygenation in patients, and when lactate levels continue to rise, therapy is failing, and patient survival rate is greatly decreased.[15–17] Hence, an intravenous catheter that could provide reliable real-time lactate concentrations would be highly desirable. Several indwelling lactate sensors have been reported,[51,52] and most are based on a design quite similar to the aforementioned glucose sensors, except that lactate oxidase is used as the immobilized enzyme. The enzyme produces hydrogen peroxide, and thus oxidation of this product species at a platinum, or other electrode material, provides the transduction method. Since levels of lactate are generally lower than glucose, controlling fluxes of lactate into the immobilized enzyme, relative to oxygen, is not quite as stringent,

although still important.

Recent developments in lactate sensors have also utilized both electrochemical and optical detection methods. While glucose sensor development has largely focused on applications for *in vivo* continuous monitoring for diabetic patients and patients under tight glycemic control, several recent lactate sensors have been designed for *in vitro* measurements of cell cultures, as increased lactate production has been identified as a cancer marker. A potentiometric sensor based on zinc-oxide nanorods was developed recently by Ibupoto *et al.* The ZnO nanorods were grown on gold-coated glass and lactate oxidase was subsequently immobilized on the surface.[53] The sensors showed excellent linear response range, stability for more than three weeks, and high selectivity over potential interfering species such as ascorbic acid, urea, glucose, galactose, and Mg^{2+} and Ca^{2+} ions. However, the sensor's response decreased at pH >8 and with temperatures above room temperature, necessitating a stable operating pH and temperature for the accurate and consistent measurements needed for a continuous monitoring system.

Zheng, *et al*. developed an optical-fiber nanosensor based on lactate dehydrogenase capable of measuring extracellular lactate concentration at the single-cell level. Lactate dehydrogenase immobilized at the tip of an aluminum-coated, heated/pulled optical fiber generates NADH as a fluorescent byproduct, directly proportional to the local lactate concentration. When excited by 360-nm UV light, the NADH fluoresces at 460 nm, allowing extremely sensitive and selective detection. While this promises to be an excellent technique for identifying cancerous cells *in vitro*, no plans have been made to use the sensors for implanted *in vivo* measurements.[54] Another very recent lactate sensor designed by Martín *et al*. utilizes genetically encoded Förster

resonance energy transfer (FRET) and fluorescence-based detection to measure local lactate extracellular concentration.[55] The sensor design proved extremely selective and very sensitive (single cell), but was pH sensitive and difficult to fabricate. Future *in vivo* lactate sensors, designed for continuous monitoring of patients to indicate health of critically ill patients may still utilize electrochemical detection, but could also benefit from the methods designed to improve the biocompatibility of implanted *in vivo* glucose measurements.

1.3 Biocompatibility Issues that Influence *In Vivo* Sensor Performance and Reliability

Several research teams actually fabricated prototype blood-gas/pH-sensing catheter products that were evaluated first in animals and then in humans.[13,56–59] Despite claims of success by some investigators, significant problems remain. A common observation for some sensors during *in vivo* studies is the performance pattern illustrated in Figure 1.6. Specifically, after a given period of time, sensor output signals often begin to deviate significantly from the values obtained for discrete blood samples analyzed *in vitro* on conventional laboratory instruments. The pattern is always the same, with intravascular sensor values for pH and PO_2 always lower than corresponding *in vitro* measurements and PCO_2 levels always higher than the corresponding *in vitro* values. This behavior was initially thought to arise exclusively from thrombus formation on the surface of implanted sensors, in which platelets and other entrapped metabolically active cells create a local environment that differs in PO_2, PCO_2 and pH levels compared to the bulk blood (due to cellular respiration). Although this effect will certainly be accentuated by the formation of a thick thrombus layer, even the adhesion of a single layer of metabolically active cells, *e.g.* platelets, could cause a local change in analyte

concentrations immediately adjacent to the surface of the device. Similar errors can be observed for glucose measurements, given the ability of cells to metabolize glucose, creating lower values near the surface of cell coated sensors.

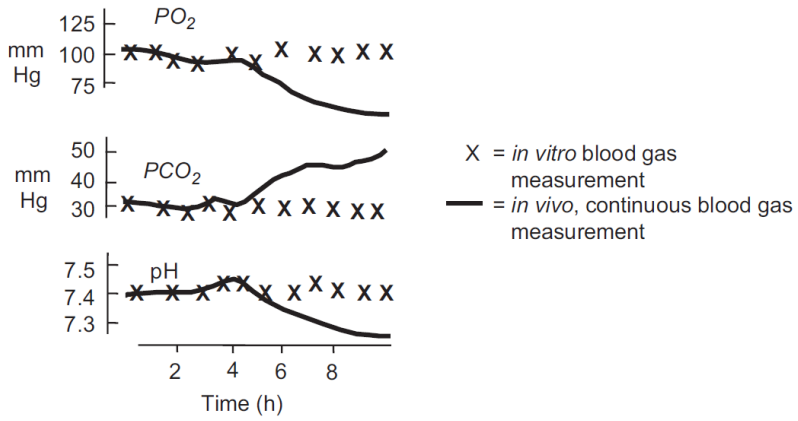

Figure 1.6. Overall concept of *in vivo* blood gas/pH patient monitoring system based on use of intravascular chemical sensors. Sensor inserted in to artery would be able to continuously monitor oxygen, carbon dioxide and pH levels in the atrial blood.

1.3.1 Details of Biological Response in Blood

Platelet adhesion and activation on foreign surfaces, such as the outer coatings of intravascular sensors, is primarily governed by the ability of platelets to recognize certain proteins that adsorb on the device surfaces once they are inserted into the bloodstream. Two proteins, von Willebrand's Factor (vWF) and fibrinogen, play key roles in this process.[60] vWF is a circulating protein that readily adsorbs to collagen and foreign materials that do not an have intact endothelial layer. Upon adsorption, vWF will bind with glycoprotein Ib (GPIb) on the surface of platelets to form the GPIb-V-IX complex, which allows platelet adhesion to the device surface.[61] Adherent and activated platelets release a host of factors that promote more platelet adhesion and accelerate the coagulation cascade including prostaglandins

(PGH_2 and PGG_2), Ca^{2+}, and thromboxane A_2.[62] Thomboxane A_2 promotes the presentation of GP IIb/IIIa on the surface of platelets that actively binds circulating fibrinogen, linking platelets together and locally converting fibrinogen to insoluble fibrin.[62] Fibrin entangles blood cells and forms the physical barrier that covers devices placed in blood. In addition to the role of platelets in coagulation, coagulation factor XII and platelet factor 3 (which is released by adherent platelets) will bind directly to the foreign surface and also convert prothrombin to thrombin, which will further promote the conversion of fibrinogen to fibrin (see Figure 1.7).[62] As mentioned above, even if significant blood clots are not formed, the presence of just a single layer of active platelets and other potential cells can alter the analyte concentrations near the surface of the implanted sensor, yielding inaccurate values compared to the concentration measured in the bulk blood phase. Within the realm of designing intravascular sensors, it is critical to be aware that the dynamic nature of this surface interaction is a significant challenge to obtaining accurate measurements of physiologically important analytes.

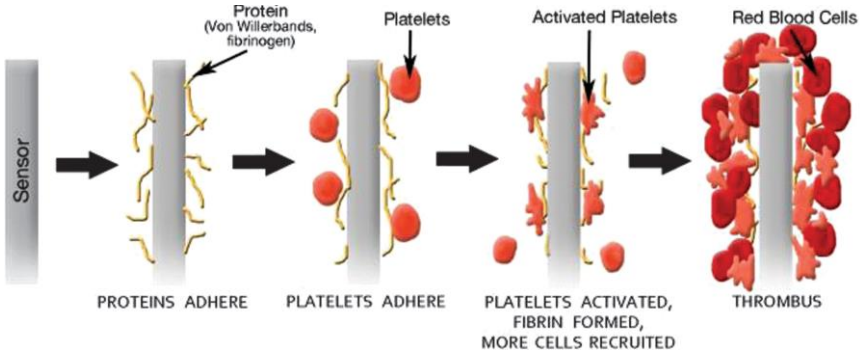

Figure 1.7. Physiological response to the outer surface of a sensor placed into the blood stream, ultimately causing activation of platelets and potentially thrombus formation on all or part of the sensor's surface. The coatings of cells on sensor surface can cause significant errors in the measurement of the target analytes.

1.3.2 Details of Biological Response in Subcutaneous Tissue

Sensors developed for real-time subcutaneous measurements, most notably electrochemical glucose sensors,[12–21] do not suffer from accuracy issues related to platelet activation and thrombus formation. However, such sensors are subject to their own unique biocompatibility problems that can influence the analytical performance of the implanted devices.[63,64] Specifically, a significant tissue inflammatory response to a large ''foreign body'' (*i.e.*, the sensor) can lead to encapsulation of the devices within a sheath of leukocytes, macrophages, and fibroblasts (see Figure 1.8). This sheath can alter local analyte levels (*e.g.*, glucose) *via* metabolic reactions (*e.g.*, inflamed tissues consume glucose at an accelerated rate[12,32,65,66]) and also greatly perturb mass transfer of the analyte to the sensor surface as well as between the blood and the interstitial fluid region. Such changes can effectively alter the calibration curve (*e.g.*, change sensitivity) for the device and can also greatly affect the lag time of the sensors response to varying glucose levels in the bulk blood.[12,32,67]

When foreign materials are placed in subcutaneous tissue, the inflammatory response poses significant challenges to stable sensor performance. Upon implantation of a sensor, an acute response occurs that lasts from minutes up to days.[68] As is the case with intravascular sensors, nearly instantly, proteins adsorb to the surface of the device. Due to the need to pass through vascularized tissue to place the sensors in subcutaneous tissue, both plasma and tissue proteins such as albumin, fibrinogen, complement factors, globulins, fibronectin, and vitronectin adsorb to the device.[68] Mast cells (MCs) present in subcutaneous tissue play a central role in regulating inflammation.[69,70] Upon injury, MCs will release a series of stored proinflammatory agents including vasoactive amine, chemotactic factors and proteases. As a

result of sustained stimulation, they will then synthesize and continue to release pro-inflammatory mediators that will recruit macrophages and lymphocytes. Additionally, they release vascular endothelial cell growth factor (VEGF) that is important for angiogenesis at the site of injury. MCs will also release cytokines that recruit and activate fibroblasts that will eventually participate in fibrous encapsulation.[69]

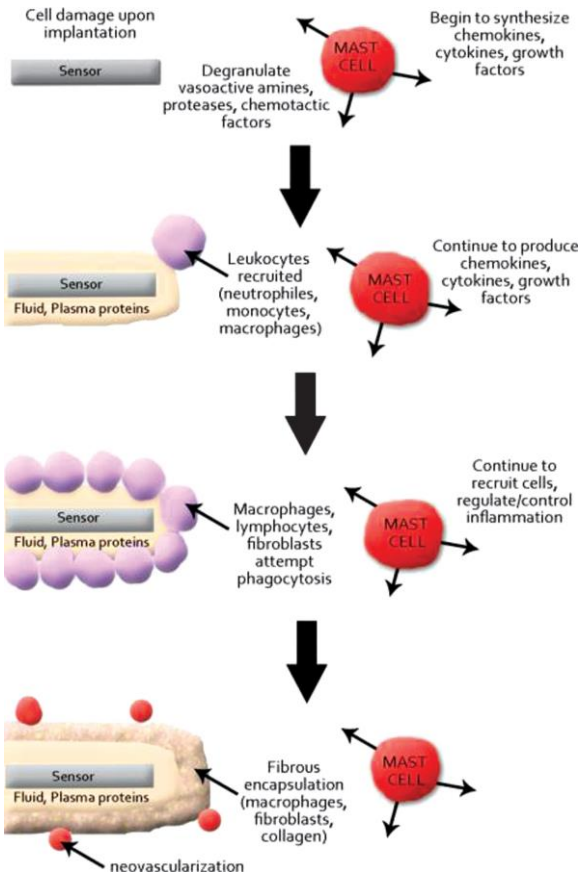

Figure 1.8. Schematic of inflammatory response process that takes place when a sensor, such as a glucose sensor, is placed subcutaneously. The increase in inflammatory cells in the area and the ultimate encapsulation of the device in a fibrous sheath creates a situation where levels of the analyte near the sensor surface do not reflect the concentrations in the blood.

Following initial protein adsorption and release of proinflammatory agents, neutrophils are recruited to the site of implantation and begin attempting to phagocytose and degrade the foreign device (in this case, the sensor).[71] This involves the release lysosomal proteases, reactive oxygen species, and chemokines that serve as potent signals to recruit cells to the wound site. Neutrophils will persist at the wound for 1–2 days before they are replaced by monocytes/ macrophages (monocytes excite the vasculature and mature into macrophages in tissue near the site of sensor implantation) and lymphocytes.[71] The macrophages become activated and release IL-12 and IL-23, reactive nitrogen and oxygen species (such as nitric oxide (NO), superoxides and H_2O_2), and proinflammatory cytokines.[72] Activated macrophages also continue to release chemoattractants to recruit more monocytes/macrophages. It has been shown that there is heterogeneous activation of macrophages, dependent on many factors that include the nature of the protein layer present and environmental signals that recruit monocytes from circulation.[73] The release of these active agents is intended to kill bacteria at the implantation site and biodegrade the foreign material that is in the subcutaneous tissue. These reactive species will additionally damage healthy tissue surrounding the implant and can lead to a state of chronic inflammation that ultimately leads to fibrous encapsulation of the sensor.

As the macrophages adhere to the protein-coated sensor, they undergo a cytoskeletal rearrangement in order to spread over the surface of the device. Adherent macrophages then fuse to form foreign-body giant cells (FBGCs) that further attempt to biodegrade the implanted device. After approximately 1–2 weeks, chronic inflammation leads to the deposition of a collagen matrix by fibroblasts to encapsulate the implant and isolate it from native tissue.[74]

The collagen layer thickness is partially dependent on factors such as the implant

texture, the protein layer adhered to the implant, and cells adhered to the protein layer. Additionally, movement of the sensor over time can change the thickness and level of inflammation around the implant. It is important to recognize that the material properties, topography, and placement *in vivo* affect the biological response to the implant, but the biological response itself will further influence long-term tissue response.[74] Again, this is a complicated and dynamic response that changes over time. This continuous change creates a highly challenging analytical environment in which reliable measurements must be made in order to make the use of implanted subcutaneous sensors for *in vivo* monitoring a clinical reality.

1.4 Strategies for Mediating Biological Response to Implanted Sensors

The commercial development of implantable chemical sensors for routine blood monitoring in humans has, at this point in time, reached an impasse of sorts. With only three commercial subcutaneous glucose sensors approved for limited use and no commercially available intravascular sensors, it appears that the combination of problems related to cell adhesion, thrombus formation, inflammatory response, *etc*. yielding poor *in vivo* sensor performance is a formidable challenge to overcome. Key to ultimate success in this field will be developing coatings that can prevent/resist the *in vivo* biocompatibility issues that play a dramatic role in the performance of implanted sensors. Fortunately, there has been significant fundamental research recently to address these issues. In the following section, new coatings that may provide a solution to the dynamic biocompatibility problems that have plagued all *in vivo* sensors developed to date will be discussed.

1.4.1 Materials Development for Improved Biological Response to Implanted Sensors

Considerable research over the last two decades has focused on designing materials that can be used to coat or fabricate sensors that are able to reduce the *in vivo* biological response that is responsible for loss of sensor function over time. An excellent review by Wisniewski and Reichert[75] details approaches that have been investigated to modify the materials surface properties to achieve this goal. Briefly, this review discusses use of hydrogels such as crosslinked poly(hydroxyethyl methacrylate) (PHEMA) or poly(ethylene glycol) (PEG) that allow water-soluble analytes to diffuse to the sensing element, and the hydrophilic nature of these materials is thought to improve biocompatibility. Phospholipid surface modification has been used in an attempt to mimic phospholipids present on cells in the body, thereby decreasing physiological response toward the sensor. Another approach is to apply thin Nafion (a chemically inert anionic compound that contains both hydrophobic and hydrophilic properties) coatings that show little adsorption of molecules from solution or use surfactants applied to sensor surfaces that have shown reduced protein adsorption. The use of natural materials such as modified cellulose has been shown to reduce compliment activation, covalent attachment of anti-fouling agents such as phenylenediamine, diols, and glycols seems to enhance biocompatibility. Additionally, using diamond-like carbons and controlling the topography of sensor coats also enhances biocompatibility and stability over time.

The development of biomimetic hydrogels for sensor coatings involves PHEMA-based membranes with PEG incorporated and crosslinked with tetraethyleneglycol diacrylate. Such a material has been reported by Justin and coworkers.[76] This UV-cured material was applied to microdisc electrode arrays, and it was shown that the diffusion coefficient of analyte was

decreased, and pH response of the material from 6.1 to 8.8 caused a change in the impedance signal obtained. This material is expected to improve biocompatibility of the coated sensor, but tuning of the porosity and crosslinking density is needed to preserve the sensor response. Silica based sol-gels (SG) have also been developed[77] that include the incorporation of either PEG (SG-PEG), heparin (SG-HEP), dextran sulfate (SG-DS), Nafion (SG-NAF), or polystyrene sulfonate (SG-PSS). The composite materials have been tested for toxicity *in vitro* with fibroblast cultures. The effect on cell proliferation was dependent on which additive was included. SG-DS showed the most promising results as glucose sensor coating when tested in BSA and serum, slowing the growth of fibroblasts on the surface of the hybrid material, while also allowing the best glucose response when coated on an amperometric sensor.

Work focused on controlling topography and stability of sensor coatings by Ju and coworkers[78] includes the development of a 3-dimensional porous type-I collagen scaffold crosslinked by nordihydroguaiaretic acid (NDGA) or glutaraldehyde (GA) that was applied to subcutaneous glucose sensors that were implanted for up to 28 days. The NDGA crosslinked collagen coatings showed a decrease in inflammation compared to bare implanted sensors.

Wang and coworkers[79] developed electrospun fibroporous polyurethane coatings for implantable glucose sensors. The authors were able to control the dimensions of the electrospun fibers and their density on the sensors to secure certain advantages including a stronger mechanical stability, a greater ability to elongate to accommodate the swelling enzyme layer on the sensor, a reduction in mechanical weak spots along the length of the coating, fibers that have excellent interconnected porosity, and a fiber structure that mimics natural extracellular matrix structure. Although this material has not been tested *in vivo* yet, the authors point out that

in vitro sensor performance was not adversely affected by the electrospun coating, and there is huge potential to apply biomimetic electrospun fibers to sensors once functioning of the fiber coating is validated. Ai, *et al*.[80] developed a perfluorocarboxylic acid ionomer (PFCI) that showed reduced cracking compared to the commonly used perfluorosulfonate ionomer membrane (PFSI). The advantage was realized because PFCI possess higher crystallinity and smaller ion clusters compared to PFSI, thereby reducing mineralization *in vivo* and reducing cracking, while maintaining the inert benefits of perfluoro materials.

1.4.2 Active Releasing Materials for Controlling Biological Response

Although the development of static materials that are more cognizant of potential biological response and biocompatibility problems is useful, it is unlikely that changing the chemistry of the material itself will alleviate biofouling and subsequent sensor failure when placed in the harsh, dynamic physiological environment. Work has also been undertaken that relies on more biomimetic approaches such as inclusion of specific surface active agents such as CD47 and drug eluting materials, both targeted at controlling explicit aspects of the inflammatory response. Stachelek, *et al*.[81] developed a material that appended a recombinant CD47 to poly(vinyl chloride) (PVC) or Tecothane, a polyether polyurethane (PU). CD47 is a transmembrane protein that binds to specific receptors on leukocytes and macrophages, which causes a downregulation of inflammatory cell attachment. The CD47-PU material was tested in a rat subdermal implant model for 70 days and showed significantly reduced number of attached cells associated with both acute and chronic inflammation. Chapter 3 in this thesis details preliminary results of demonstrating the functionalization of polyurethane outer coatings

on intravenous glucose sensors through immobilized recombinant CD47 protein does not affect the sensors' amperometric response to glucose, a collaborative research effort between the Stachelek and Meyerhoff research groups.

Several researchers have also proposed development of systems that will release the anti-inflammatory agent, dexamethasone (DX), and/or the angiogenic agent, vascular endothelial growth factor (VEGF). Norton *et al.*[82] developed a hydrogel system based on 2-hydroxyethyl methacrylate that released both DX and VEGF. The idea was to decrease inflammation and encourage angiogenesis around an implanted glucose sensor. Decreasing inflammation should decrease the thickness of the fibrous capsule and allow a stable background current to be reached more quickly, and increasing vasculature should help increase glucose flux to the sensor. It was found that DX alone did decrease inflammation after 2 weeks of implantation in rats. VEGF alone did increase vascularity of the fibrous capsule, but when DX and VEGF are released at the same time from the hydrogel, while there is still a decrease in inflammation, there is no increase in vascularization. After six weeks, there is no observable difference between the drug-releasing hydrogels and control implants, indicating that the positive effect is not maintained once the drug- release reservoir is depleted. Sung *et al.*[83] then investigated a similar approach by sequentially delivering DX and VEGF from a crosslinked PEG. The release of DX is faster (k_{DX} ¼ 0.5/day) and VEGF is slower (k_{VEGF} ¼ 0.4/day). The difference in delivery rate is enough to see a marked decrease in inflammation and increase in vascular density in an *ex ova* chick embryo after 8 days. This is significant because it points to the temporal importance of delivering agents in the appropriate sequence, thus more closely mimicking normal physiological conditions.

Bhardwaj and coworkers[84] tested the temporal effect of DX over much longer term implants by fabricating different poly(lactic-*co*-glycolic acid) (PLGA) microspheres that release DX for 30 days or PLGA/poly(vinyl alcohol) (PVA) composite microspheres that release DX over a 3-month period. The microspheres were implanted in rats to test for both acute and chronic inflammation. Sustained release of DX was achieved by combining microspheres, and the continued release did show suppression of inflammation for 3 months, while spheres that exhausted their drug after 30 days lost the ability to decrease inflammation. The same group then modified this approach and developed a system that dispersed PLGA microspheres in a crosslinked PVA hydrogel.[85] The motivation for this was that many different drugs in addition to the DX that was tested could be encapsulated in PLGA microspheres to impart a wide array of drug-release capability, and the PVA allows both analyte to diffuse to the sensor surface and drug to diffuse into the tissue immediately surrounding the sensor. The ‘‘smart’’ PLGA microsphere/PVA composite system showed good proof of concept tissue response when tested in both type-1 and type-2 diabetic rats for 1 month. Importantly, this system also recognizes the importance of tailoring the implanted material to the site of implantation and the specific medical condition under which the sensors are being used and holds the potential for incorporating additional biological mediators into the sensor coating.

Another very promising active agent for release from implanted sensors is nitric oxide (NO). Nitric oxide is a free radical-gas that is released endogenously in many physiological processes.[86] Namely, within the context of indwelling sensors, NO is a potent antithrombotic agent[87] and plays a role in mediating the inflammatory response in subcutaneous tissue.[88] NO is an important signaling molecule in shifting inflammation from acute stages to potentially

helping in enhancing wound healing. If NO can be released from intravascular or subcutaneous sensors at the appropriate levels and with good temporal control, evidence suggests that NO may radically reduce the biological response to these indwelling sensors.[89] A class of NO donor that has been extensively used for improving the biological response toward implanted sensors is diazeniumdiolates.[87–90] Figure 1.9 shows the structure of some examples of these molecules that have been used in polymeric materials to impart NO release to materials for sensor fabrication. Each diazeniumdiolate molecule will release 2 molecules of NO *via* thermal decomposition at 37 °C or a proton-mediated decomposition mechanism. The rate of decomposition can be controlled by changing the molecular structure of the parent compound used to form the diazeniumdiolate and/or by tuning the water uptake and pH of the polymer matrix in which the molecule is embedded. Initial work dispersed (Z)-1-[N-methyl-N-[6-(N-methylammoniohexyl)amino]]-diazen-1-ium-1,2-diolate (DMHD/N_2O_2), evenly through a PDMS matrix coated on an amperometric oxygen sensor.[90] This material showed greatly reduced thromobogenicity, but it was found that the hydrophilic DMHD/N_2O_2 leached out of the polymer matrix, presenting potential problems by allowing the parent diamine compound used to form the diazeniumdiolate (and present after NO release) to circulate in the body. Some diamine compounds are known to be carcinogenic.[91]

Because of the extremely promising results for inhibiting thrombus formation on the surface of the blood contacting device, work began to either covalently link the NO donor to the backbone of the polymer matrix used or to make the donor lipophilic enough that it would not exit the hydrophobic polymer matrix to enter the aqueous environment of blood.

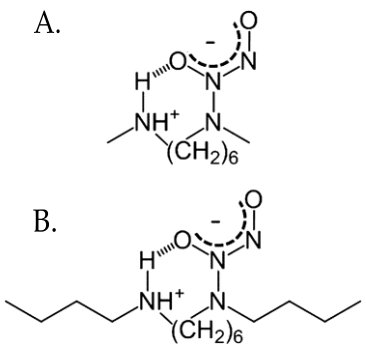

Figure 1.9. Chemical structures of two diazeniumdiolate type NO donor species that can be incorporated into polymers to coat implantable sensors, creating NO release surfaces that can reduce activation and adhesion of platelets in the blood stream and also decrease inflammatory response for subcutaneous sensors. (A) diazeniumdiolated dimethylhexanediamine; (B) diazeniumdiolated dibutyhexanediamine (DBHD/N_2O_2).

To this end, modified PDMS materials were developed that contained pendant secondary amines that could be converted to diazeniumdiolates and result in materials with different NO release properties. Zhang and coworkers[92] developed DACA/N2O2 and TACA/N_2O_2 PDMS that used diamine and triamino-containing crosslinking agents to react with hydroxyl-terminated PDMS chains. Once the crosslinked polymer was cured, it could be converted to the diazeniumdiolate by reacting in 5 atm of NO. Polyurethanes capable of releasing NO were reported by Reynolds, *et al.*[93] They developed two different methods to synthesize polyurethanes, containing pendent amines in different positions along the backbone of the PU that could be diazeniumdiolated, and these polyurethanes released NO for up to 6 days in aqueous solution at 37 °C. Underivatized PDMSs and PUs are routinely used as membranes for sensors (O_2, CO_2, glucose, lactate, *etc.*) and hence, adding the NO release capability to these polymers should be useful for improving the biological response to indwelling sensors.

Another approach to impart NO-release properties to polymers used for sensor fabrication

is to develop a more lipophilic analog of DMHD/N_2O_2 that replaces the methyl side groups with butyl side groups (DBHD/N_2O_2)[94] in an effort to alter the partition coefficient enough to keep the NO donor within the PDMS matrix in which it is dispersed. There are two distinct advantages to blending a discrete NO donor into the polymer matrix being used to fabricate a sensor over modifying materials to covalently attach NO donors. First, it provides the ability to alter the amounts of the NO donor blended into the material, depending on the level and reservoir of NO donor desired for a given application. Secondly, the base polymer matrix can be varied without changing the fundamental synthetic chemistry of the polymer itself. A limitation to this approach, however, is that the NO donor can still diffuse out of the polymer, albeit a greatly reduced risk compared to DMHD/N_2O_2. This diazeniumdiolate chemistry using DBHD/N_2O_2, modulated through pH control by poly(lactic acid) and a polyurethane top-coat, can be used to impart NO release from needle-type glucose sensors, thus bestowing thromboresistant properties to the sensors for intravenous implantation. *In vivo* analytical performance of these sensors is assessed in both 7 h rabbit models as well as 20 h pig experiments and is detailed in Chapter 4 of this dissertation.

An alternative, which allows similar advantages but reduces leaching, is the development of derivativized particle fillers with NO-releasing surface chemistry, such that these particles could be incorporated into different polymers, thereby imparting NO release capability to the material without changing the fundamental chemistry used to synthesize the matrix. These particles also have a much higher potential loading capacity and release of NO owing to the fact that they have more potential NO donating groups than just single molecules. Zhang and coworkers[95] developed a series of silica particles modified by covalent attachment of alkylamines to their surface that could be converted into diazeniumdiolates and subsequently

blended into different polymers. This yielded mechanically entrapped NO donors that were unable to leach from the polymer surface. Frost and Meyerhoff[96] also developed fumed silica particles derivatized with different S-nitrosothiols, another class of NO donor (*e.g.*, S-nitroso-cysteine, S- nitroso-N-acetylcysteine, and S-nitroso-N-acetylpenicillamine, or SNAP) that could impart NO-release ability with different release profiles compared to the diazeniumdiolate-based particle/polymer composites in response to Cu^{1}, or visible light when blended into plasticized PVC films. Although SNAP-based NO release as a solid outer layer is not easily transferable directly to glucose sensors, silicone rubber or PU catheters that have been impregnated with SNAP can be used to house implantable glucose sensors for intravenous placement. The thromboresistant behavior of these SNAP catheters can then preserve analytical accuracy of the sensors either by serving as an outer barrier between whole blood and the sensor's active cavity or potentially through transient NO, which can partition into the polyurethane outer coatings of the needle-type sensors during a flush of saline (since NO is rapidly scavenged by hemoglobin when whole blood is present).

There has also been extensive work to develop NO-releasing sol-gels (*i.e.*, xerogels) for potential implantable sensor applications.[97–100] Shin and Schoenfisch[97] note that these are attractive materials because they are synthesized under mild conditions and are chemically flexible and generally porous, facilitating diffusion of analytes through the matrix to the sensor. Marxer and coworkers[98,99] report the synthesis of sol-gels prepared by the hydrolysis and condensation of amine-functionalized alkoxysilanes and alkyl- trimethoxysilanes.

The crosslinked materials were exposed to 5 atm of NO to form diazeniumdiolate moieties covalently linked to the material. Four different aminosilanes (isobutyltrimethoxysilane,

(aminoethylaminomethyl)-phenethyltrimethoxysilane, (aminohexyl)aminopropyltrimethoxy-silane and N-[3-(trimethoxysilyl)propyl]diethylenetriamine) all had different storage and release properties, demonstrating the ability to achieve a wide range of NO- release profiles from this class of material. Shin *et al.*[100] embedded NO-releasing sol-gel particles into a polyurethane matrix to use as an NO-release coating for glucose sensors. Roughly 10–200 μm NO-releasing particles were obtained by grinding cured sol-gel monoliths synthesized by using (amino- hexyl) aminopropyltrimethoxysilane reacted with methyltrimethoxysilane or isobutyltrimethoxysilane. This further demonstrates the utility of these materials and the approach of incorporating NO release particles into a wide variety of polymer matrices to obtain composite materials that are able to release physiologically relevant levels of NO.

These materials that release bioactive agents show immense promise in controlling and mediating biological response around implanted sensors. One limitation all these materials possess, however, is a finite reservoir of active agent that is able to be released from materials preloaded with molecules such as VEGF, DX or NO. Since these materials also release their agents continuously once release is initiated, this limits the lifetime of a device. NO is, consequently, released even when it may not be needed to limit thrombosis, or even when a lower level of release may be adequate, and thus the total reservoir is exhausted sooner than need be. This unnecessary NO release limits the effective lifetime of the sensor.

In an effort to impart dynamic control over the level of NO released, RSNO- derivatized fumed silica particles imbedded in a hydrophobic polymer matrix showed dynamic NO release when illuminated with different intensities of light.[101] The hydrophobic polymer matrix excludes transition metal ions and ascorbate ions such that NO release is only initiated by

illumination, thereby providing a dynamic "on" trigger for controlling NO release.

Gierke *et al.*[102] have developed a modified polydimethylsiloxane with S-nitroso-N-acetyl-penicillamine (SNAP-PDMS) covalently attached to the crosslinking agent used to form the PDMS. This material, when coated onto declad optical fibers, enables the precise control over the level and duration of NO released in response to a programmed sequence of light generated by a wirelessly controlled LED light source (see Figure 1.10).[103] This system will permit control over NO release and allow detailed information to be obtained regarding the level and duration of NO needed to ensure controlled biological response in both blood contacting and tissue contacting sensor applications. Riccio and coworkers[104,105] developed RSNO-containing xerogels that also releases NO in response to illumination using incandescent bulbs of different wattages. These types of materials that are able to release NO in a dynamically controllable manner may offer a means to more closely mimic the physiological release of NO and have the potential to allow implanted sensors to reach a stable, interfacial blood/tissue response that may ultimately allow for widespread clinical utility.

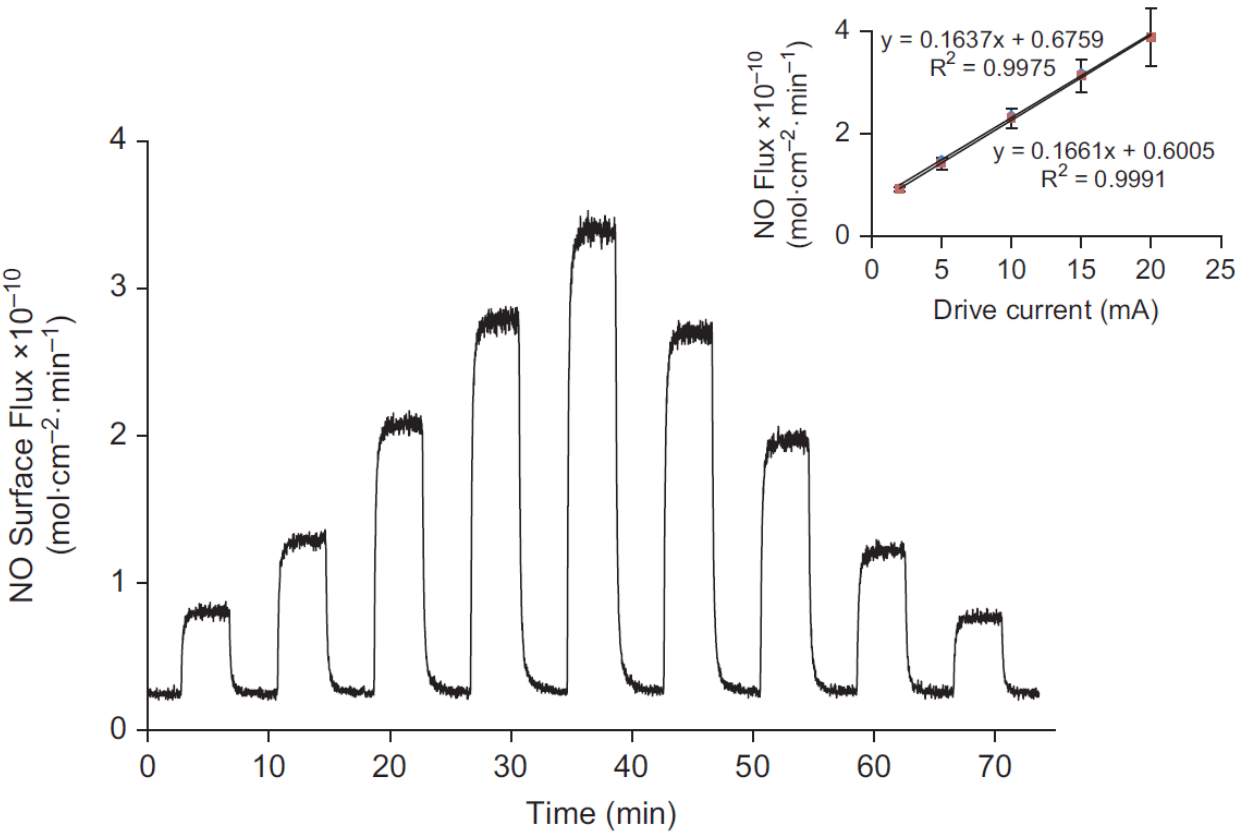

Figure 1.10. NO generated from S-nitroso-N-acetylpenicillamine-polydimethylsiloxane (SNAP-PDMS) coated on declad region of a 500 mm poly(methyl- methacrylate) (PMMA) optical fiber with drive current turned on and off and increasing with each step. The pulses used in this example were in 4 min intervals, light off and then light on with increasing light applied in each subsequent step from 2, 5, 10, 15 and 20 mA of I_{drive} applied and then 15, 10, 5, 2, and 0 mA applied to the LED *via* the ED. The corresponding surface fluxes of NO generated was 0.95 ± 0.04, 1.50 ± 0.13, 2.37 ± 0.33, 3.19 ± 0.45, 3.88 ± 0.57, 3.13 ± 0.13, 2.30 ± 0.19, 1.42 ± 0.12, and 0.91 ± 0.04 (allx10^{-10} mol · cm^{-2} · min^{-1}), respectively. The inset shows that the surface flux of NO generated is linearly related to the drive current applied to the LED illuminating the coated optical fiber and is identical whether I_{drive} is applied form 0–20 mA or 20–0 mA. Measurements were made at 22 °C with chemiluminescence detection. (From ref. 103 with permission.)

1.4.3 Materials to Mimic Biological Form and Function

To more fully mimic biological tissue such as intact endothelium, Zhou and Meyerhoff[106] created a trilayer system that combined NO release with surface-immobilized heparin. The idea is to more closely mimic the dual action of antiplatelet NO and anticoagulant heparin. Wu and

coworkers[107] later combined a continuously releasing NO PurSil^S layer top coated with a CarboSil® with surface-bound thrombomodulin and heparin that were shown to be biologically active. As material development produces more matrices that exhibit better biocompatibility, it is likely that combining these improved materials properties with controlled active agent release and immobilized bioactive molecules will lead to greatly enhanced performance of indwelling sensors.

An additional step toward creating longer-term implants would be to eliminate the dependence on the reservoir of active agent present in the implanted device. Klueh and coworkers[108] developed a system in which they genetically engineer cells to produce excess levels of VEGF. These cells were entrapped in the tip of a glucose sensor. The goal was to increase vascularization around the implanted sensor to allow ample diffusion of glucose to the sensor. When implanted in *ex ova* chick embryos, they were able to demonstrate a dramatic increase in the density of blood vessels present around the implant. This approach relies on the production of VEGF by cells *in situ* rather than a preloading of the sensor with the active agent. Another approach to avoid preloading donor molecules was demonstrated by Oh and Meyerhoff.[109] They developed a lipophilic catalytic copper-containing species that was incorporated into poly(vinyl chloride) (PVC) and demonstrated that RSNOs present in the bathing solution surrounding the material were decomposed to release NO catalytically. Hwang and Meyerhoff[110] then took a similar copper cyclen structure and tethered it to the surface of biomedical-grade polyurethane that was capable of spontaneously generating NO when in contact with blood. This approach offers the advantage of using already existing medical grade polymers and imparting them with NO-release properties. Cha and

Meyerhoff[111] then extended this by developing an immobilized organoselenium moiety that was able to catalytically generate NO from RSNOs present in plasma. These catalytic systems should be capable of nearly indefinite production of NO from their polymer surfaces because RSNOs are endogenously produced in the body and circulate in blood and intestinal fluid. As long as adequate levels of the endogenous RSNOs and reducing equivalents are present, the material will continue to generate physiological NO levels at the polymer/biological interface.

1.5 Summary

The goal of developing implantable blood gas, glucose, and lactate sensors that can provide reliable, real-time clinically relevant results remains elusive. While great advances have been made in the development of miniaturized electrochemical and optical sensors that have adequate sensitivity, selectivity and stability when operated *in vitro*, the placement of such devices in the *in vivo* environment creates a physiological response that greatly influences the quality of analytical results obtained. As summarized above, progress in this area mandates the development of appropriate sensor coating materials that can mitigate the normal activation of platelets and other cells when devices are placed intravascularly and the inhibition of the inflammatory response when sensors are placed subcutaneously. These coatings must be capable of diminishing the normal physiological responses to the implanted sensors, yet they cannot adversely affect analytical response properties, including response times, sensitivity to the target analyte, and selectivity of the sensor. A wide range of new, passive and active biomaterials coatings have been devised in recent years specifically to target the *in vivo* sensing challenge. In the end, it is likely that a combination of immobilized

agents and slow chemical release strategies will be needed to resolve the physiological response issues that have limited the analytical performance of implanted sensors to date. Continued research in this area during the coming years will hopefully achieve success and provide an array of new *in vivo* sensor tools that will enhance the quality of health care and disease management for millions of people worldwide.

1.6 Statement of Dissertation Research

In this thesis, a number of the strategies outlined above are selected with the intention of enhancing the biocompatibility of needle-type glucose sensors ultimately intended for intravenous implantation to aid in the tight glycemic control of ICU patients. Chapter 2 specifically details application of an annealed Nafion inner rejection layer on an inner Pt/Ir electrode surface area to enhance glucose sensor's selectivity over the electroactive interference species commonly encountered in whole blood. Daily assessment measurements of this layer's selectivity, specifically against ascorbic acid, uric acid, and acetaminophen were conducted yielding data supporting the hypothesis that the annealed Nafion layer maintains the sensor's selective behavior for at least 8 d, with less degradation in an aqueous buffer environment than a non-annealed Nafion counterpart layer.

Chapter 3 reports initial findings for a new collaborative research between the Meyerhoff lab (University of Michigan) and Dr. Stanley Stachelek (Children's Hospital of Philadelphia) aimed at functionalizing the outer polymer coating of the implantable glucose sensors with recombinant CD47 protein. This approach will potentially impart a "self" marker to the sensor surface, ultimately camouflaging it from foreign body response cells bearing the signal recognition transmembrane protein α (SIRPα). Preliminary data in Chapter 3 indicates that

glucose sensors can be successfully functionalized with recombinant CD47, and that the sensors retained their glucose linearity and glucose oxidase activity throughout the complete functionalization procedure.

Poly(lactic acid) layers containing dispersed diazeniumdiolates have been previously reported to provide NO release functionality to needle-type glucose sensors, and *in vivo* measurement within 7 h rabbit experiments.[112] Continuous measurements, in the form of a concentration vs. time trace plots are reported in Chapter 4 for sensors fabricated with this NO release chemistry and a new type of polyurethane outer coating (E2As Elast-eon). Further 20 h continuous measurements are reported for such sensors implanted within porcine blood vessels. Due to the difficulty with obtaining analytically accurate measurements in the latter case, long term *in vitro* stability measurement were conducted in bovine serum, and extensive *in vitro* testing for possible interference from administered intravenous drugs and NO scavenging effects from hemoglobin are reported via in vitro measurements in heparinized blood.

Chapter 5 summarizes efforts on a collaborative project with Edwards Life Sciences aimed to impart NO release capability to an existing commercial device designed for intermittent *in vivo* glucose measurement. Though the glucose sensors are fabricated without inherent NO release functionality, preliminary data in Chapter 5 shows that during the phase when the catheter housing the sensor is flushed with a buffered calibration solution, NO released from a surrounding catheter (which was previously impregnated with SNAP chemistry) can partition into the extremely thin polyurethane outer coating of the glucose sensor, and subsequently provide transient NO release behavior immediately afterward. Since the Edwards product measures glucose in blood only intermittently (every 5 min) by retracting blood over the sensor

housed potentially within an NO release catheter, this approach may provide adequate anticoagulant activity vs. using heparin within the calibration solution (current approach) that bathes the sensor when blood is not retracted over it.

Ultimately, while several of these projects are still within the preliminary data collection phase of *in vivo* evaluation, the data presented herein indicates the potential of annealed Nafion selective membranes, sensor surface CD47 functionalization, active NO releasing sensor surfaces, and transient NO release from an active surrounding catheter as viable biocompatibility/selectivity enhancement strategies to improve *in vivo* glucose sensor lifetime and performance.

1.7 Literature Cited:

(1) Gubala, V.; Harris, L.F.; Ricco, A. J.; Tan, M. X.; Williams, D. E. *Anal. Chem.*, 2012, 84, 487.
(2) P. St. Louis, *Clin. Biochem.* **2000**, *33*, 427.
(3) Myers, F. B.; Lee, L.P. *Lab Chip* **2008**, *8*, 2015.
(4) McGarraugh, G.; Bergenstal, R. *Diab. Technol. Ther.* **2009**, *11*, 145.
(5) Gelsomino, S.; Lorusso, R., Livi, U.; Romagnoli, S.; Romano, S.M.; Carella, R.; Lucà, F.; Billè, G.; Matteucci, F.; Renzulli, A.; Bolotin, G.; De Cicco, G.; Stefà no, P.; Maessen, J.; Gensini, G. F. *BMC Anesthesiol.* **2011**, *11*, 1.
(6) Bailey, D. H.; da Silva, E. J.; Cluton-Brock, T. H. *Anesthesia*, **2011**, *66*, 889.
(7) Kondepati, V. R.; Heise, H. M. *Anal. Bioanal. Chem.* **2007**, *388*, 545.
(8) Girardin, C. M.; Huot, C.; Gonthier, Delvin, M. E. *Clin. Biochem.* **2009**, *42*, 136.
(9) Cheyne, E.; Kerr, D. *Diabet. Metab. Res. Rev.* **2002**, *18(Suppl 1)*, S43.
(10) Kubiak, T.; Hermanns, N.; Schreckling, H. J.; Kulzer, B.; Haak, T. *Diabetic Med.*, **2004**, *21*, 487.
(11) Frost, M. C.; Meyerhoff, M. E. *Current Opin. Chem. Biol.* **2002**, *6*, 633.
(12) Frost, M. C.; Meyerhoff, M.E. *Anal. Chem.* **2006**, *78*, 7370.
(13) Ganter, M.; Zollinger, A. *Brit. J. Anaesth.* **2003**, *91*, 397.
(14) Meyerhoff, M. E. *Trends Analyt. Chem.* **1993**, *12*, 257.
(15) Holloway, P.; Benham, S.; St. John, A. *Clin. Chim. Acta.* **2001**, *307*, 9.
(16) Shapiro, R.; Howell, N.; Talmor, M.; Nathanson, D.; Lisbon, L.; Wolfe A.; Weiss, R. *J. Ann. Emerg. Med.* **2005**, *45*, 524.
(17) Valenza, F.; Aletti, G.; Fossali, T.; Chevallard, G.; Sacconi, F.; Irace, M.; L. Gattinoni, *Crit. Care* **2005**, *9*, 588.
(18) Mahutte, C. K.; Sasson, C. S. H.; Muro, J. R.; Hansmann, D. H.; Maxwell, T.P.; Miller, W. W.; Yafuso, M. *J. Clin. Monitor.* **1990**, *6*, 147.
(19) Amao, Y. *Microchim. Acta* **2003**, *143*, 1.
(20) Yeh, T.-S.; Chu, C.-S.; Lo, Y.-L. Sens, *Actuators B* **2006**, *119*, 701.
(21) Chu, C.-S.; Lo, Y.-L. Sens, *Actuators B* **2010**, *151*, 83.
(22) Severinghaus, J. W. *Ann. NY Acad. Sci.* **1968**, *148*, 115.
(23) Jin, W.; Jiang, J.; Song, Y.; Bai, C. *Res. Physiol. Neurobiol.* **2012**, *180*, 141.
(24) Nivens, D. A.; Schiza, M. V.; Angel, M. *Talanta* **2002**, *58*, 543.
(25) Jin, W.; Jiang, J.; Wang, X.; Zhu, X.; Wang, G.; Song, Y.; Bai, C. *Res. Physiol. Neurobiol.* **2011**, *177*, 183.
(26) Offenbacher, H.; Wolfbeis, O. S.; Furlinger, E. *Sens. Actuators* **1986**, *9*, 73.
(27) Kinlen, P. J.; Heider, J. E.; Hubbard, D. E. *Sens. Actuators B* **1994**, *22*, 13.
(28) Telting-Diaz, M.; Collison, M. E.; Meyerhoff, M.E. *Anal. Chem.* **1994**, *66*, 576.
(29) Meruva, R. K.; Meyerhoff, M. E. *Biosens. Bioelectron.* **1997**, *13*, 201.
(30) Makos, M. A.; Omiatek, D. M.; Eweing, A. G.; Heien, M. L. *Langmuir* **2010**, *26*, 10386.
(31) Huang, W.-D.; Cao, H.; Deb, S.; Chiao, M.; Chiao, J. C. Sens, *Actuators A* **2011**, *169*, 1.
(32) Wilson, G. S.; Gifford, R. *Biosens. Bioelectron.* **2005**, *20*, 2388.
(33) Mo, J. W.; Smart, W. *Front. Biosci.* **2004**, *9*, 3384.
(34) Ward, W. K.; Jansen, L. B.; Anderson, E.; Reach, G.; Klein, J. C.; Wilson, G. S. *Biosens. Bioelectron.* **2002**, *17*, 181.
(35) Wang, J. *Electroanalysis* **2001**, *13*, 983–988.
(36) Koschchinsky, T.; Heinemann, L. *Diabet. Metab. Res. Rev.* **2001**, *17*, 113.
(37) Choleau, C.; Klein, J. C.; Reach, G.; Aussedat, B.; Demaria-Pesce, V.; Wilson, G. S.; Gifford, R.; Ward, W. K. *Biosens. Bioelectron.* **2002**, *17*, 647.
(38) Waeger, P.; Hummel, M. *Diabet. Stoffwechsel und Herz* **2008**, *17*, 385.

(39) Tubiana-Rufi, N.; Riveline, J. P.; Dardari, D. *Diabet. Metab* **2007**, *33*, 415.
(40) Hirsch, I. B.; Armstrong, D.; Bergenstal, R. M.; Buckingham, B.; Childs, B. P.; Clarke, W. L.; Peters, A.; Wolpert, H. *Diabet. Technol. Ther.* **2008**, *10*, 232.
(41) McNichols, R. J.; Cote, G. L. *J. Biomed. Opt.*, **2000**, *5*, 5.
(42) Wang, J. *Talanta* **2008**, *75*, 636.
(43) Heller, A. *Current Opin. Chem. Biol.* **2006**, *6*, 664.
(44) Marvin, J. S.; Hellinga, H. W. *J. Am. Chem. Soc.* **1998**, *120*, 7.
(45) Tipnis, R.; Vaddiraju, M.; Jain, F.; Burgess, D.; Papadimitrakopoulos, F. *J. Diabet. Sci. Technol.* **2007**, *2*, 193.
(46) Lin, Y.; Taylor, S.; Li, H.; Fernando, K .A. S.; Qu, L.; Wang, W.; Gu, L.; Zhou B.; Sun, Y. P. *J. Mater. Chem.* **2004**, *14*, 527.
(47) Lin, Y. H.; Lu, F.; Tu Y.; Ren, Z. F. *Nano Lett.* **2004**, *4*, 191.
(48) Zhu, Z.; Garcia-Gancedo, L.; Flewett, A.; Xie, H.; Moussy F.; Milne, W. *Sensors*, **2012**, *12*, 5996.
(49) Tierney, S.; Falch, B.; Hjelme D.; Stokke, B. *Anal. Chem.* **2009**, *81*, 3630.
(50) Paek, S.; Cho, I.; Kim, D.; Jeon, J.; Lim, G.; Paek, S. *Biosens. Biolectron.* **2013**, *40*, 38.
(51) Hu, Y.; Zhang, Y.; Wilson, G. S. *Anal. Chim. Acta* **1993**, *281*, 503.
(52) Baker, D. A.; Gough, D. A. *Anal. Chem.* **1995**, *67*, 1536.
(53) Ibupoto, Z.; Shah, S.; Kuhn, K.; Willander, M. *Sensors* **2012**, *12*, 2456.
(54) Zheng, X.; Yang, H. Li, C. *Anal. Chem.* **2010**, *82*, 5082.
(55) Martín, A.; Ceballo, S.; Ruminot, I.; Lerchundi, R.; Frommer W.; Barros, L. *Plos One* **2013**, *8*, 1.
(56) Venkatesh, B.; Clutton-Brock, T. H.; Hendry, S. P. *J. Med. Eng. Technol.* **1994**, *18*, 165.
(57) Venkatesh, B.; Clutton-Brock, T. H.; Hendry, S. P. *J. Cardiothorac. Vasc. Anesth.* **1995**, *9*, 412.
(58) Venkatesh, B.; Clutton-Brock, T. H.; Hendry, S. P. *Crit. Care Med.* **1994**, *22*, 588.
(59) Divers, S.; Marshall, W.; Foster-Smith, R. in *Proceedings of the Conference on Electrolytes, Blood Gases and Other Critical Analytes* Burritt, M. Sena, S. F. D'Orazio, P., Eds., AACC: Washington, D.C., **1992** pp. 1–9.
(60) Gorbet, M. B.; Sefton, M. V. *Biomaterials* **2004**, *25*, 5681.
(61) Dörmann, D.; Clemetson, K. J.; Kehrel, B. E. *Blood* **2000**, *96*, 2469.
(62) Dee, K. C.; Puleo, D. A.; Bizios, R *An Introduction to Tissue-Biomaterial Interactions*, John Wiley & Sons, Inc., Hoboken, New Jersey, USA, **2002**, *4*, pp 68–81.
(63) Nichols, S. P.; Koh, A.; Storm, W. L.; Shin, J. H.; Schoenfisch, M .H. *Chem. Rev.* **2013**, *113*, 2528.
(64) Zhu, Z.; Garcia-Gancedo, L.; Flewitt, A. J.; Xie, H.; Moussy, F.; Milne, W. I. *Sensors* **2012**, *12*, 5996.
(65) Anderson, J. M. *Cardiovasc. Path.* **1993**, *2*, 33S.
(66) Daley, J. M.; Shearer, J. D.; Mastrofrancesco, B.; Caldwell, M. D. *Surgery* **1990**, *107*, 187.
(67) Baker, D. A.; Gough, D. A. *Anal. Chem.* **1996**, *68*, 1292.
(68) Anderson, J. M.; Rodriguez, A.; Chang, D. T. *Semin. Immunol.* **2008**, *20*, 86.
(69) Klueh, U.; Kaur, M.; Qiao Y.; Kreutzer, D. L. *Biomaterials*, **2010**, *31*, 4540.
(70) Thevenot, P. T.; Baker, D. W.; Weng, H.; Sun, M.-W.; Tang, L. *Bio- materials* **2011**, *32*, 8394.
(71) Bryers, J. D.; Giachelli C. M.; Ratner, B. D. *Biotechnol. Bioeng.* **2012**, *109*, 1898.
(72) Chang, D. T.; Jones, J. A.; Meyerson, H.; Colton, E.; Kwon, I. K.; Matsuda, T.; Anderson, J. M. *J. Biomed. Mater. Res.* **2008**, *87A*, 676.
(73) Anderson, J. M. *Ann. Rev. Mater. Res.*, **2001**, *31*, 81.
(74) Helton, K. L.; Ratner, B. D.; Wisniewski, N. A. *J. Diabet. Sci. Technol.* **2011**, *5*, 632.
(75) Wisniewski, N. A.; Reichert, M. *Colloid Surf. B: Biointerfaces* **2000**, *18*, 197.
(76) Justin, G. F; Rahman, S.; Guiseppi-Elie, A. R. A. *A. Biomed. Microdevices* **2009**, *11*, 103.
(77) Kros, A.; Gerritsen, M.; Sprakel, V. S. I.; Sommerdijk, N. A. J. M.; Jansen, J. A.; Nolte, R. J.

M. *Sens. Actuators B*, **2001** *81*, 68.
(78) Ju, Y. M.; Yu, B.; West, L.; Moussy Y.; Moussy, F. *J. Biomed. Mater. Res.* **2009**, *92A*, 650.
(79) Wang, N.; Burugapalli, K.; Song, W.; Halls, J.; Moussy, F.; Ray, A.; Zheng, Y. *Biomaterials* **2013**, *34*, 888.
(80) Ai, F.; Wang, Q.; Yuan, W. Z.; Li, H.; Chen, X.; Yang, L.; Zhang, Y.; Pei, S. *J. Mater. Sci.* **2012**, *47*, 5181.
(81) Stachelek, S. J.; Finely, M. J.; Alferiev, I. S.; Wang, F.; Tsai, R. K.; Eckells, E. C.; Tomczyk, N.; Connolly, J. M.; Discher, D. E.; Eckmann, D. M.; Levy, *R.J. Biomaterials* **2011**, *32*, 4317.
(82) Norton, L. W.; Koschwanez,H. E.; Wisniewski, N. A.; Klitzman, B.; Reichert, W. M. *J. Mater. Res.* **2007**, *81A*, 858.
(83) Sung, J.; Barone, P. W.; Kong, H.; Strano, M. S. *Biomaterials*, **2009** *30*, 622.
(84) Bhardwaj, U.; Sura, R.; Papadimitrakopoulos, F.; Burgess, D. J. *Int. J. Pharmaceut.* **2010**, *384*, 78.
(85) Wang, Y.; Papadimitrakopoulos, F.; Burgess, D. *J. Control. Release* **2013**, *169(3)*, 341.
(86) Moncada, S. *Ann. NY Acad. Sci.* **1997**, *811*, 60.
(87) Radomski, M. W.; Palmer, R. M. J.; Moncada, S. *Biochem. Biophys. Res. Commun.* **1987**, *148*, 1482–1489.
(88) Nichols, S. P.; Koh, A.; Brown, N. L.; Rose, M. B.; Sun, B.; Slomnerg, D. L.; Riccio, D. A.; Klitzman, B.; Schoenfisch, M. H. *Biomaterials* **2012**, *33*, 6305.
(89) Wu, Y.; Meyerhoff, M. E. *Talanta* **2008**, *75*, 642.
(90) Mowery, K. A.; Schoenfisch, M. H.; Baliga, N.; Wahr, J. A.; Meyerhoff, M. E. *Electroanalysis* **1999**, *11*, 681.
(91) Mowery, K. A.; Schoenfisch, M. H.; Saavedra, J. E.; Keefer, L. K.; Meyerhoff, M. E. *Biomaterials* **2000**, *21*, 9.
(92) Zhang, H.; Annich, G. M.; Miskulin, J.;Osterholzer, K.; Merz, S. I.; Bartlett, R. H.; Meyerhoff, M. E. *Biomaterials* **2002**, *23*, 1485.
(93) Reynolds, M. M.; Hrabie, J. A.; Oh, B. K.; Politis J. K; Citro, M. L.; Keefer, L. K.; Meyerhoff, M.E. *Biomacromolecules* **2006**, *7*, 987.
(94) Major, T. C.; Brant, D. O.; Reynolds, M. M.; Bartlett, R. H.; Meyerhoff, M. E.; Handa, H.; Annich, G. M. *Biomaterials* **2010**, *31*, 2736.
(95) Zhang, H.; Annich, G. M.; Miskulin, J.; Staniewwicz, K.; Osterholzer, K.; Merz, S. I.; Bartlett, R. H.; Meyerhoff, M. E. *J. Am. Chem. Soc.* **2003**, *125*, 5015.
(96) Frost, M. C.; Meyerhoff, M. E. *J. Biomed. Mater. Res.* **2005**, *72A*, 409.
(97) Shin, J. H.; Schoenfisch, M. H. *Analyst* **2006**, *131*, 609.
(98) Marxer, S. M.; Rothrock, A. R.; Nablo, B. J.; Robbins, M. E.; Schoenfisch, M. H. *Chem. Mater.* **2003**, *15*, 4193.
(99) Marxer, S. M.; Robbins, M. E.; Schoenfisch, M. H. *Analyst* **2005**, *130*, 206.
(100) Shin, J. H.; Marxer, S. M.; Schoenfisch, M. H. *Anal. Chem.* **2004**, *76*, 4543.
(101) Frost, M.C.; Meyerhoff, M. E. *J. Am. Chem. Soc.* **2004**, *126*, 1348.
(102) Gierke, G. E.; Nielsen, M.; Frost, M. C. *Sci. Technol. Adv. Mater.* **2011**, *12*, 055007.
(103) Starrett, M. A.; Nielsen, M.; Smeenge, D. M.; Romanowicz, G. E.; Frost, M. C. *Nitric Oxide* **2012**, *27*, 228.
(104) Riccio, D. A.; Dobmeier, K. P.; Hetrick, E. M.; Privett, B. J.; Paul, H. S.; Schoenfisch, M. H., *Biomaterials* **2009**, *30*, 4494.
(105) Riccio, D. A.; Coneski, P. N.; Nichols, S. P.; Broadnax A. D.; Schoenfisch, M. H. *Appl. Mater. Interfaces* **2012**, *4*, 796.
(106) Zhou, Z.; Meyerhoff, M. E. *Biomaterials* **2005**, *26*, 6506.
(107) Wu, B.; Gerlitz, B.; Grinnell, B. W.; Meyerhoff, M. E. *Biomaterials* **2007**, *28*, 4047.

(108) Klueh, U.; Dorsky, D. I.; Kreutzer, D. L. *Biomaterials* **2005**, *26*, 1155.
(109) Oh, B. K.; Meyerhoff, M. E. *J. Am. Chem. Soc.* **2003**, *125*, 9552.
(110) Hwang, S.; Meyerhoff, M. E. *Biomaterials* **2008**, *29*, 2443.
(111) Cha, W.; Meyerhoff, M. E. *Biomaterials* **2007** *28*, 19.
(112) Yan. Q; Major, T. C.; Bartlett, R. H.; Meyerhoff, M. E. *Biosens. Bioelectron.* **2011**, *26,* 4276.

CHAPTER 2

IMPROVED GLUCOSE SENSOR SELECTIVITY OVER ELECTROACTIVE INTERFERENCE SPECIES WITH ANNEALED NAFION AS AN INNER REJECTION LAYER

2.1 Introduction

As highlighted in Chapter 1, accurate real-time measurement of blood glucose levels within critically ill hospital patients in intensive care units is a niche that can be filled by the development of intravenous blood glucose sensors. Such monitoring could not only decrease potential complications for diabetic patients, but also offers better outcomes for non-diabetic patients, both benefiting from tight glycemic control. Miniaturized glucose sensors have been developed in academic labs for intravenous use and in commercialized products for measurement in subcutaneous interstitial/brain fluid matrices; however, achieving good biocompatibility and high selectivity over potential interference species are the primary obstacles that have prevented widespread clinical applications of such intravascular devices for ICU patients.

First generation glucose sensors function by electrochemical oxidation of hydrogen peroxide (H_2O_2) produced by the glucose oxidase enzyme which is immobilized onto the sensor surface. In the absence of inner selectivity enhancement layers, the steady-state current generated from the oxidation of H_2O_2 is proportional to the bulk glucose concentration in the buffered solution, blood, or fluid surrounding the sensor. However, other naturally-occurring electroactive species

(ascorbate and urate) are present in biological fluids, and these are typically oxidized at the operating potential of such glucose sensors (e.g., +0.600V vs. Ag/AgCl reference), creating an overall oxidation current in which it is difficult to distinguish the component currents of each individual oxidation reaction. Without using methods to achieve preferential oxidation of H_2O_2 generated from glucose at the working wire electrodes of such devices, the accuracy of these glucose sensors is poor, yielding falsely elevated values for glucose in the blood or subcutaneous fluid.

Previous glucose sensor designs have featured two types of selectivity enhancing layers. The first layer, is typically a coating of Nafion that provides selectivity against negatively-charged electroactive species, such as ascorbate and urate. The second layer is an electropolymerized film formed by the oxidation of the monomers 1,3-diaminobenzene and resorcinol, which forms on an inner Pt/Ir electrode surface only within the pores in the Nafion layer. This electrochemically formed polymer layer is designed to select based on size-exclusion, reducing the oxidation signal generated from the neutrally-charged electroactive interference species such as acetaminophen, an analgesic commonly administered to hospital patients. A variety of electropolymerized films were examined in the work reported by Carelli, et al. in 1993 by exploring a range of scanning potential ranges, scan rate, polymerization time duration, and composition of monomers which were subsequently ranked by their selectivity of H_2O_2 oxidation over ascorbate, urate, and acetaminophen.[1] In 2011, Yan, et al. adapted a specific electropolymerized film protocol (monomers, potential scan range, scan rate, reaction duration) for use as a selective layer for implantable glucose sensors.[2] The electropolymerization process occurred over 18 h using repeated cyclic voltammetric scans (range: 0.000 to +0.830V vs. Ag/AgCl reference; scan rate: 0.002 V/s), and the progress of the reaction was monitored by observing the decreasing peak

current, indicating the formation of a non-conducting polymer on the sensor surface. However, these electropolymerized films are vulnerable to partial structural decomposition with sustained exposure to aqueous solutions and can gradually lose selective functionality over time.

Kwon, et al. demonstrated, on a macro scale, that annealing Nafion films (~50-170mm thickness) above their glass transition temperature range (above the 100-150°C) causes significant change in conducting ionic channel structure and the ionic activity at the membrane surface.[3] To date, there are no published findings on application of such annealed Nafion layers for use in creating *in vivo* glucose sensors with enhanced selectivity. In this chapter, the concept of utilizing an annealing process of thin Nafion films, pre-applied to the glucose sensors before application of electropolymerized films, is shown to enhance selectivity over ascorbate and urate, indicating less structural decomposition, and ultimately, extended glucose sensor lifetimes.

2.2 Experimental

2.2.1 Materials

Glucose oxidase (Type VII, from *Aspergillus niger*), d(+)-glucose, glutaraldehyde, bovine serum albumin (BSA), iron (III) chloride ($FeCl_3$), 37% hydrochloric acid (HCl), L-ascorbic acid, uric acid (sodium salt), acetaminophen, Nafion (5 wt % solution in lower aliphatic alcohols/H_2O mixture), 1,3-diaminobenzene, resorcinol, tetrahydrofuran (THF), N,N'-dibutyl-1,6-hexanediamine (DBHD) were all obtained from Sigma-Aldrich (St. Louis, MO). Sodium phosphate dibasic heptahydrate ($Na_2HPO_4 \cdot 7H_2O$), sodium phosphate monobasic monohydrate ($NaH_2PO_4 \cdot H_2O$) were purchased from Amresco, Inc. (Solon, OH). Sodium chloride (NaCl) is a product of Research Products International Corp. (Mt. Prospect, IL). Potassium chloride is from Fisher Scientific (Pittsburgh, PA). Teflon-coated platinum/iridium and silver wires are products

of A-M Systems (Sequim, WA). E2As Elast-Eon polyurethane was a gift from Aortech Biomaterials. Diazeniumdiolated DBHD (DBHD/N_2O_2) was synthesized by treating DBHD with 80 psi nitric oxide (NO) gas purchased from Cryogenic Gases (Detroit, MI) at room temperature for 24 h, as previously described.[4]

2.2.2 Sensor Fabrication

Glucose sensor design (see Fig. 2.1) was based on previous configurations[2,4-6] by first cutting a 1-mm length cavity in the Teflon coating of a platinum/iridium wire (outer diameter = 0.2 mm). A Nafion coating was then applied to the cavity, and then the wires were annealed at 170°C for 1.5 h and then gradually cooled to 35°C using a Fisher Scientific Isotemp oven to enhance sensor selectivity against negatively-charged electroactive interference species, such as ascorbic and uric acid. Control sensors were dried at 37.5°C, rather than annealed. Then *via* a CV electropolymerization process (cycling voltage between 0 and +0.830 V at 0.002 V/s for 18 h) a layer of polymerized resorcinol and *m*-phenylenediamine[2,7] was applied to the cavity to help further reject electroactive neutral interference species, such as acetaminophen, from reaching the inner Pt/Ir surface. A silver/silver chloride (Ag/AgCl) wire electrode was tightly wrapped around the sensor to serve as an electrochemical reference, and heat-shrinkable polyester tubing was applied to secure the reference wire in place. Glucose oxidase was then immobilized within the cavity using glutaraldehyde. An outer polymer layer was then applied to the sensor's surface using a wire loop: a 2% (wt/vol) Elast-Eon E2As polyurethane in THF was applied as a top coat to modulate the NO release and also control the sensor's linear detection range for glucose by restricting glucose diffusion into the immobilized enzyme layer. E2As polyurethane was chosen for these studies since it had been previously used with positive success as an NO release coating

to prevent platelet activation and clotting within a rabbit model for extracorporeal circulation.[8] A diagram of the fully-assembled sensor is shown below in Figure 2.1.

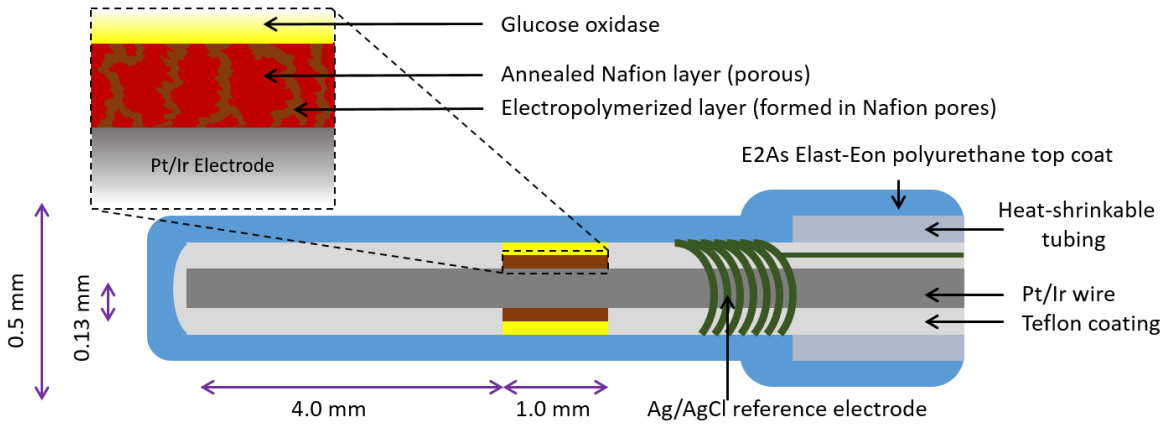

Figure 2.1. Configuration of annealed Nafion-based intravascular glucose sensor with expanded inset of electroactive interference rejection layer.

2.2.3 Analytical In Vitro Performance of Annealed Glucose Sensors

Glucose sensors were calibrated using 4-channel BioStat potentiostats (ESA Biosciences Inc., Chelmsford, MA). The potential applied to the inner Pt/Ir wire was +0.600 V vs. Ag/AgCl reference in a 0.1 M phosphate buffered saline (PBS), pH 7.4, test solution at 37.5°C.

To evaluate the selectivity of the sensors over naturally occurring electroactive interference species such as ascorbic acid, uric acid, and acetaminophen, injections of near maximum *in vivo* concentrations of these species were made into the *in vitro* test cell (thermostat-controlled glass beaker) during the glucose calibrations (from 1.0 – 20.0 mM). The % error for these sensors was calculated by dividing the current response from an injection of interference species (0.5 mM for ascorbic acid, 0.33mM for uric acid, and 0.2 mM for acetaminophen[9] by the current signal recorded for 5.0 mM glucose, the average normal level of glucose in blood. A threshold was established to

determine effective selectivity: the current from a specific interference species should not exceed 5% of the current response observed for 5.0 mM glucose[10]. The selectivity test was repeated and monitored over 14 days to evaluate the stability of the selectivity layers. Comparisons in stability were evaluated between sensors with the annealed Nafion layers and the control group of sensors, which were fabricated with non-annealed Nafion.

2.2.4 Additional In Vitro and In Vivo Evaluation of Annealed Glucose Sensors

Some experimental results detailed in Chapters 3 and 4 of this thesis document continued to use the annealed Nafion layer for extended selectivity over interference species due to the conclusions drawn from results presented in this chapter.

2.3 Results and Discussion

2.3.1 Extended In Vitro Glucose Sensor Stability

Figure 2.2 displays a selectivity comparison of eight glucose sensors prepared with annealed Nafion layers and six glucose sensors fabricated with non-annealed Nafion layers over ascorbic acid through an experimental period of 8 d. The values for selectivity represent the average change in sensor response current for an injection of 0.5 mM ascorbic acid, the maximum biological concentration, divided by the current change recorded for an injection of 5.0 mM glucose. The line at 0.05 represents the 5% threshold for selectivity tolerance for a sensor over a particular electroactive interference species. For the glucose sensors made with annealed, Nafion, selectivity under the selectivity threshold for ascorbic acid is maintained for the duration of the testing. These sensors also have a lower variability in their selectivity, which is maintained throughout the testing period.

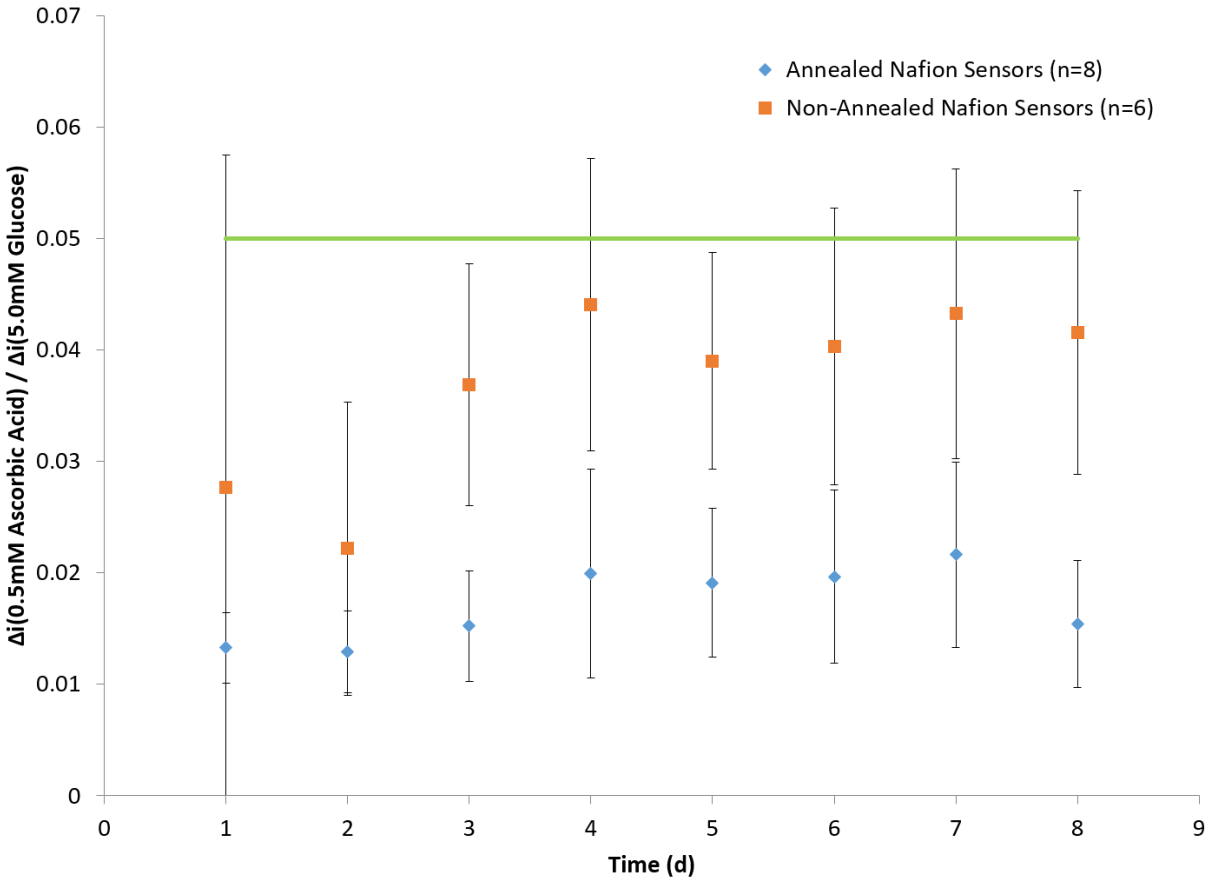

Figure 2.2. *In vitro* comparison of selectivity over ascorbic acid (0.5 mM) between glucose sensors fabricated with annealed Nafion layers and those with non-annealed Nafion layers.

Figure 2.3 highlights the selectivity comparison of the same eight annealed Nafion glucose sensors versus six non-annealed glucose sensors over uric acid, another common electroactive interference species found in blood and bearing a negative charge. The glucose sensors fabricated with annealed Nafion sensors maintain excellent selectivity (< 3%) with a very tight standard deviation, accounting for variation between different sensors, for the duration of the 8 d of testing. In contrast, those glucose sensors with non-annealed Nafion layers have a larger variability in their responses, and some do cross the 5% threshold of interference species response during the evaluation period.

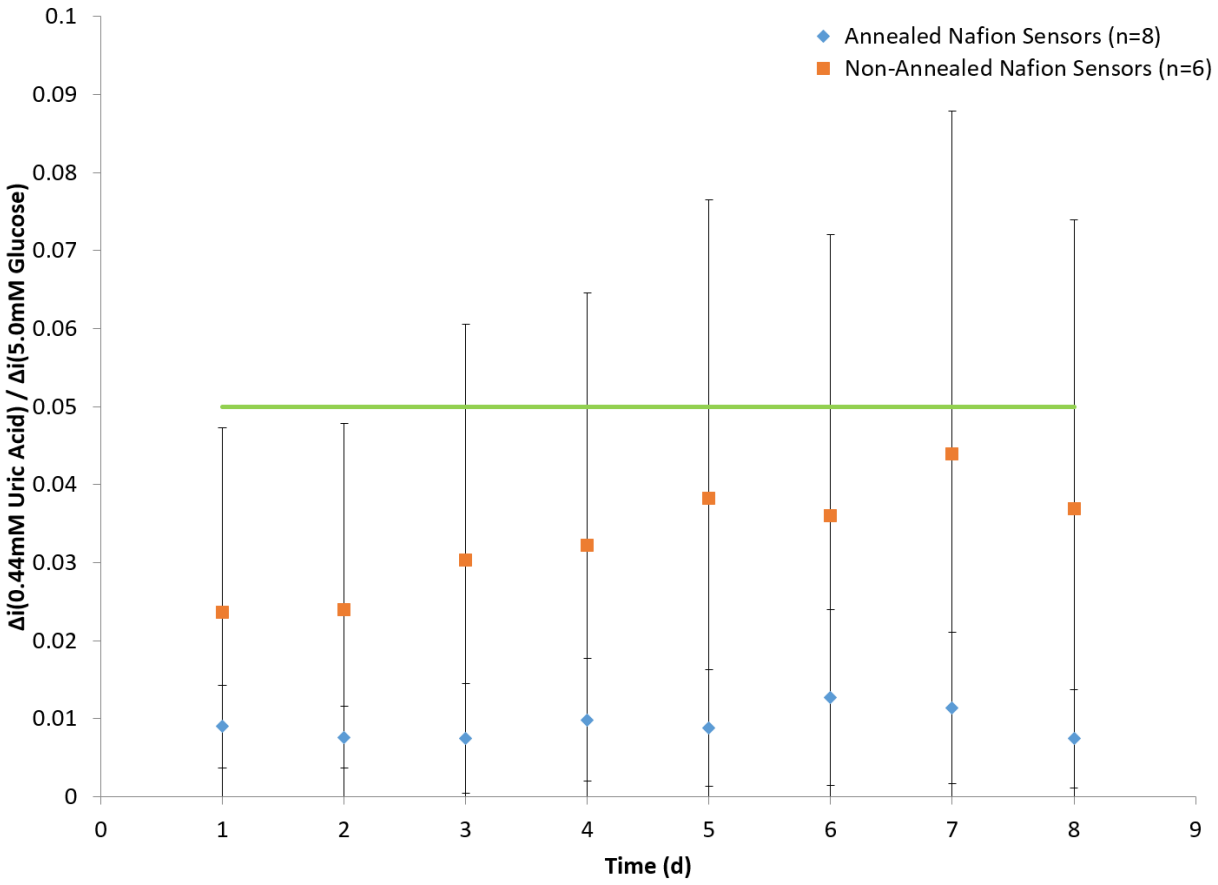

Figure 2.3. *In vitro* comparison of selectivity over uric acid (0.44 mM) between glucose sensors fabricated with annealed Nafion layers and those with non-annealed Nafion layers.

Figure 2.4 compares the selectivity of the eight annealed Nafion glucose sensors with non-annealed sensors over acetaminophen. A common analgesic, acetaminophen is not a naturally occurring species, but may be present in hospitalized patients, which is the target application for intravenous CGM sensors. It is a neutral molecule, and is primarily selected against by the size exclusion properties of the electropolymerized layer of the glucose sensors. Interestingly, several commercial subcutaneous CGM systems encourage users of their glucose sensors to refrain from consuming acetaminophen while using the system, especially during their periods of instrument calibration.[11] Both the annealed and non-annealed sensors in Figure 2.4 have similar selectivity

against acetaminophen throughout the testing time, although the standard deviation, indicating variability between the sensors, is smaller for the annealed sensors. The dissertation thesis work of Dr. Qinyi Yan indicates that $< 7\%$ may be a more appropriate threshold cutoff for signal from acetaminophen oxidation.[10] Otherwise, hospitalized patients could be given an alternative medication for pain relief while using these sensors for blood glucose monitoring.

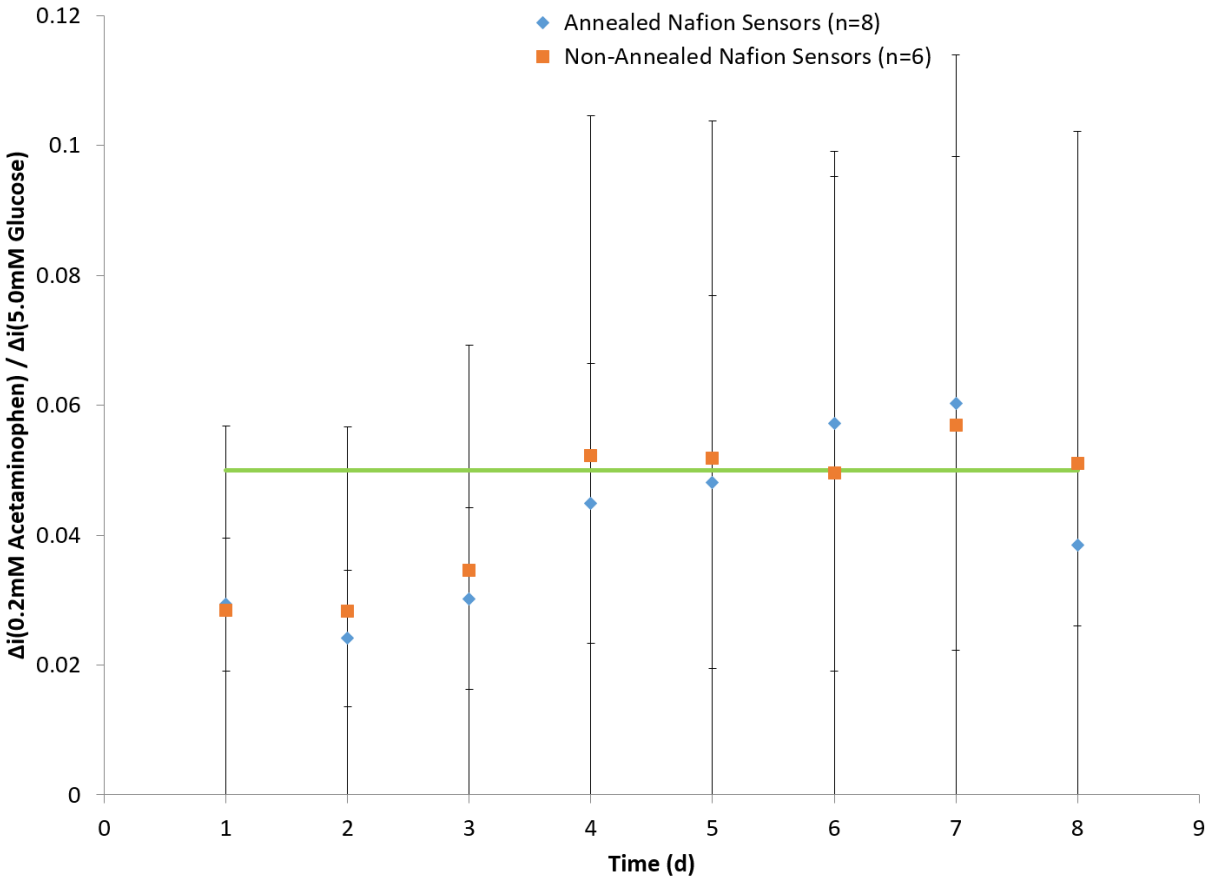

Figure 2.4. *In vitro* comparison of selectivity over acetaminophen between glucose sensors fabricated with annealed Nafion layers and those with non-annealed Nafion layers.

Since the glucose sensors fabricated with annealed Nafion layers maintained better selectivity over two of the three major electroactive interference species found in blood than did those with previously-described non-annealed Nafion, these experiments indicate that annealed Nafion-based glucose sensors can maintain reasonably good selectivity over the expected lifetime of the sensor

of approximately 7 d. The lack of improved selectivity over acetaminophen is likely based on the fact that its diffusion through Nafion is not impeded based on the properties of the Nafion layer that change as a function of the annealing process, and its access to the underlying Pt/Ir electrode is governed more by its permeability through the electropolymerized organic layer. In particular, it appears that the better rejection over ascorbate and urate in the case of the annealed Nafion layer may be due to slightly smaller hydrophilic channels within the structure of the Nafion layer that are formed by reorganization of the anionic sulfonate groups within Nafion. Slightly smaller channels would enhance the transference numbers for cations vs. anions, especially larger anions such as ascorbate and urate. Recently published studies of Nafion thin films and membranes have confirmed physical morphological changes that occur during treatment at elevated temperatures. Annealing (at 160°C) commercially-produced Nafion films that were 254 μm in thickness demonstrated significant changes in oxygen gas permeability based on morphological changes to the hydrophilic channels of the membrane.[12] A study of 6-μm thick Nafion films cast on quartz slides demonstrated that annealing the films caused distinct physical changes in the hydrophilic channels of the membranes, specifically the formation of sulfonic acid anhydrides, as evidenced by attenuated total reflection infrared spectroscopy (ATR-IR).[13]

2.4 Conclusions and Future Directions

A major obstacle to continuous glucose monitoring in blood with electrochemical enzymatic glucose sensors is the oxidation of electroactive species at the operational applied voltage range for the sensor, leading to incorrect glucose readings. Annealing the Nafion layers of such glucose sensors enhances their selectivity, especially over the negatively charged ascorbic and uric acid species in comparison to previous sensor designs that included Nafion but did not involve the annealing process. This selectivity enhancement is maintained over the course of at least 8 d,

indicating that with regard to the sensor lifetime, such sensors are expected to maintain their selective properties to match the duration of nitric oxide (NO) release once additional outer layers were added to the sensor surface (see Chapter 4). The smaller standard of deviation for the annealed Nafion sensors, which is also maintained for the 8 d duration, indicates that there is less performance variability between individual sensors, [6]

Annealed Nafion has been previously reported to yield much thicker, large scale films for other applications (e.g. examining the topographical structure via AFM and ionic channel selectivity properties),[3] but their application to create improved glucose sensors has not yet been reported. Due to the success of these experiments, further sensors discussed in Chapters 3 and 4 that employ outer layers to enhance biocompatibility were fabricated with annealed Nafion layers. Of particular interest, once the annealed Nafion glucose sensors were combined with NO releasing layers, they could be evaluated for glucose measurement performance within heparinized blood *in vitro* on the benchtop, as well as *in vivo* assessment when implanted within the blood vessels of rabbits or pigs.

2.5 Literature Cited

(1) Carelli, I.; Chiarotto, I.; Curulli, A.; Palleschi, G. *Electrochim Acta* **1996**, *41*, 1793.
(2) Yan, Q. Y.; Major, T. C.; Bartlett, R. H.; Meyerhoff, M. E. *Biosens Bioelectron* **2011**, *26*, 4276.
(3) Kwon, O.; Wu, S. J.; Zhu, D. M. *J Phys Chem B* **2010**, *114*, 14989.
(4) Batchelor, M. M.; Reoma, S. L.; Fleser, P. S.; Nuthakki, V. K.; Callahan, R. E.; Shanley, C. J.; Politis, J. K.; Elmore, J.; Merz, S. I.; Meyerhoff, M. E. *J Med Chem* **2003**, *46*, 5153.
(5) Yan, Q. Y.; Peng, B.; Su, G.; Cohan, B. E.; Major, T. C.; Meyerhoff, M. E. *Anal Chem* **2011**, *83*, 8341.
(6) Bindra, D. S.; Zhang, Y. N.; Wilson, G. S.; Sternberg, R.; Thevenot, D. R.; Moatti, D.; Reach, G. *Anal Chem* **1991**, *63*, 1692.
(7) Geise, R. J.; Adams, J. M.; Barone, N. J.; Yacynych, A. M. *Biosens Bioelectron* **1991**, *6*, 151.
(8) Brisbois, E. J.; Handa, H.; Major, T. C.; Bartlett, R. H.; Meyerhoff, M. E. *Biomaterials* **2013**, *34*, 6957.
(9) Zhang, Y. N.; Hu, Y. B.; Wilson, G. S.; Moattisirat, D.; Poitout, V.; Reach, G. *Anal Chem* **1994**, *66*, 1183.
(10) Yan, Q. Doctor of Philosophy Dissertation (Chemistry), University of Michigan, 2011.
(11) http://www.dexcom.com/sites/dexcom.com/files/international/user_guides/G5-Mobile-UG-OUS-Eng-mmol.pdf Dexcom, Inc. 2015; Vol. 2015.
(12) Evans, C. M.; Singh, M. R.; Lynd, N. A.; Segalman, R. A. *Macromolecules* **2015**, *48*, 3303.
(13) Singhal, N.; Datta, A. *J Phys Chem B* **2015**, *119*, 2395.

CHAPTER 3

POTENTIAL FOR ENHANCING GLUCOSE SENSOR SURFACE THROMBORESISTANCE BY UTILIZING RECOMBINANT CD47 PROTEIN FUNCTIONALIZATION: A PRELIMINARY COMPATABILITY STUDY

3.1 Introduction

As highlighted in Chapters 1 and 2, accurate real-time measurement of blood glucose in intensive care unit (ICU) patients requires the development of needle-type intravenous blood glucose sensors. Such monitoring not only decreases potential complications for diabetic patients, but also offers better outcomes for non-diabetic patients, both benefiting from tight glycemic control. Miniaturized glucose sensors have been developed in academic labs for intravenous use and in commercialized products for measuring in subcutaneous interstitial/brain fluid matrices; however, biocompatibility is the primary obstacle to widespread use and application.

As illustrated in Figure 3.1, thrombosis of the sensor surface is a potential problem when the device comes into physical contact with fresh, flowing blood. In blood, the body's coagulation system will quickly respond to the implantation of a foreign material, such as a chemical catheter. Surface protein adsorption occurs within minutes, which can lead to the activation of the coagulation cascade (e.g., platelet activation) and clot formation around the working area of the sensor. Platelets and red blood cells that compose these clots increase diffusion time from the bulk blood to the electrode surface, resulting in increased response times or unpredictable sensor signal

drift. These cells also consume glucose and oxygen, which cause the local concentrations of these species to differ from the bulk blood concentrations, resulting in analytical performance errors.

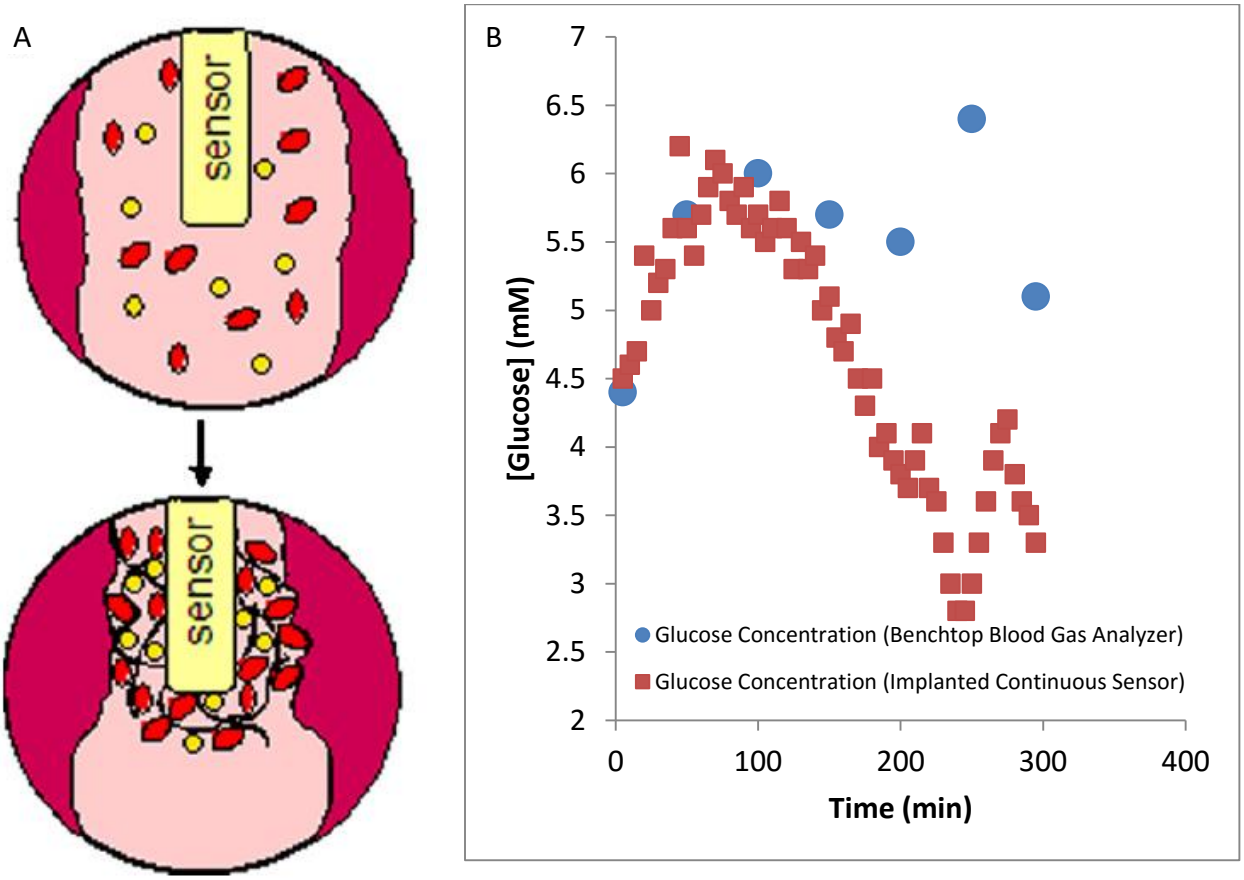

Figure 3.1. Illustration of thrombosis formation on the sensor surface during an *in vivo* experiment (A) and simulation of declining glucose sensor analytical performance after clot formation, as compared to benchtop point-of-care device (B). The red squares represent frequent measurements made by a continuously or intermittently monitoring glucose sensor, which correlate at the start of the experiment with the less frequent, discrete measurements made by the benchtop blood gas analyzer. However, after surface thrombus formation occurs (after 150 minutes), the continuous sensor measurements significantly deviate from the blood gas measurements.

One method to prevent clot formation on polymer surfaces is to functionalize the material with biocompatible molecules or native proteins, with the goal of camouflaging the implanted device against the typical thrombotic response. Our collaborators, Dr. Robert J. Levy and Dr. Stanly

Stachelek, at the Children's Hospital of Philadelphia have pioneered the attachment of recombinant CD47 protein onto poly(vinyl chloride) and polyurethane surfaces and have found that such treatment significantly reduces human neutrophil and human monocyte derived macrophage attachment to those surfaces, respectively.[1] They have further demonstrated that reduced platelet and neutrophil activation occurs in blood when contacting CD47 functionalized polymer surfaces.[2] Naturally-occurring CD47 is a transmembrane protein that is ubiquitously expressed in many mammalian cells (Fig. 3.2). When immune cells or platelets bearing the SIRPα transmembrane protein come into contact with the Ig extracellular domain of its cognate ligand, CD47, a temporary "handshake" interaction occurs between the CD47 and SIRPα, and prompting immune response cells such as thrombocytes, leukocytes, and macrophages to recognize the surface as "self" and thus do not trigger pathways activate the immune or the coagulation cascades (Fig. 3.3)[1]. Initially, CD47 became a protein of interest when it was found to be upregulated in malignant cancerous cells, giving the cells "camouflage" or "cloaking" against phagocytosis.[3,4] This resistance to phagocytosis was then successfully transferred to artificial structures such as perfluorocarbon emulsions (PFC) and to both μm-and nm-sized polystyrene beads.[5-10] More recent studies into the specific inflammatory response pathways and mechanisms affected by the "handshake" interaction between CD47 and SIRPα show that CD47 provides a global inflammatory inhibition, which extends beyond only localized resistance to phagocytosis.[11]

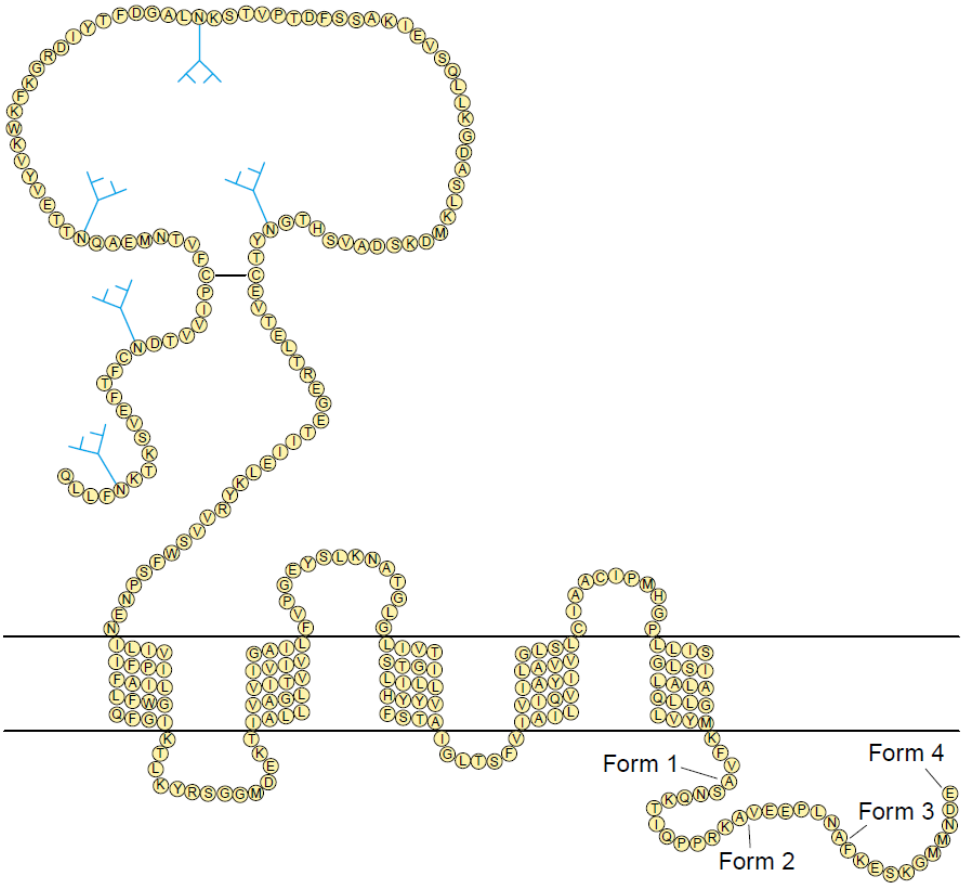

Figure 3.2. Transmembrane and extracellular domains of naturally-occurring CD47 protein (figure adapted from Brown, et al., *Trends Cell Biol*. 2001).[12]

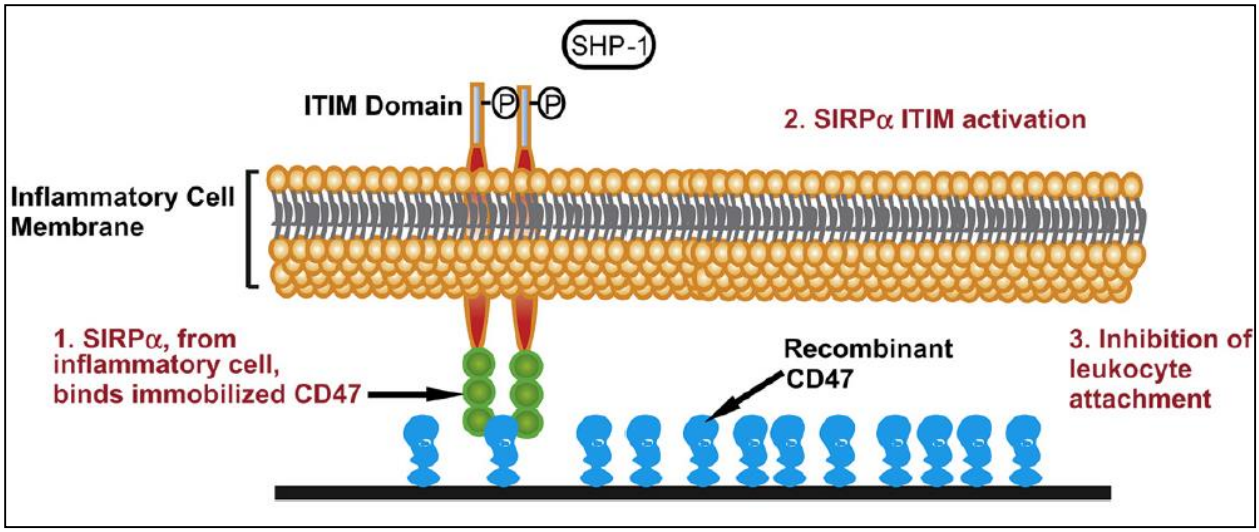

Figure 3.3. Concept and molecular mechanism of the temporary "handshake" interaction between recombinant CD47 immobilized on a polymer surface and the SIRPα domain found on an inflammatory cell membrane (figure adapted from Finley, et al., *Biomaterials* 2011).[1]

Thus, the ability of the CD47 extracellular membrane to confer "self" status to a synthetic polymer surface makes it an attractive method of potentially enhancing the biocompatibility of implantable catheters and sensors, provided that a sufficient CD47 surface density can be achieved. In the case of implantable chemical sensors, it must first be demonstrated that immobilization of CD47 on functional sensors does not alter the analytical response of such devices. In this chapter, the glucose sensors described in Chapters 2 that featured outer E2As polyurethane coatings are examined for their ability to be surface functionalized with CD47 and the effect of such an immobilization process on the electrochemical response to glucose is herein evaluated.

3.2 Experimental

3.2.1 Materials

Glucose oxidase (Type VII, from *Aspergillus niger*), d(+)-glucose, glutaraldehyde, bovine serum albumin (BSA), iron (III) chloride ($FeCl_3$), 37% hydrochloric acid (HCl), L-ascorbic acid, uric acid (sodium salt), acetaminophen, Nafion (5 wt % solution in lower aliphatic alcohols/H_2O mixture), 1,3-diaminobenzene, resorcinol, tetrahydrofuran (THF), N,N'-dibutyl-1,6-hexanediamine (DBHD) were all obtained from Sigma-Aldrich (St. Louis, MO). Sodium phosphate dibasic heptahydrate ($Na_2HPO_4 \cdot 7H_2O$), sodium phosphate monobasic monohydrate ($NaH_2PO_4 \cdot H_2O$) were purchased from Amresco, Inc. (Solon, OH). Sodium chloride (NaCl) was a product of Research Products International Corp. (Mt. Prospect, IL). Potassium chloride was obtained from Fisher Scientific (Pittsburgh, PA). Teflon-coated platinum/iridium and silver wires were products of A-M Systems (Sequim, WA). E2As Elast-Eon polyurethane was a gift from Aortech Biomaterials (Weybridge, Surrey, UK).

3.2.2 Sensor Fabrication

The glucose sensor configuration was based upon previous designs[13-16] and the devices were prepared by first cutting a 1-mm length cavity in the Teflon coating of the platinum/iridium wire (outer diameter = 0.2 mm). A Nafion coating was then applied to the cavity, and then the wires were annealed at 170°C for 1.5 h, and then gradually cooled to 35°C using a Fisher Scientific Isotemp oven to enhance sensor selectivity against negatively-charged electroactive interference species, such as ascorbic and uric acid. Then *via* a CV electropolymerization process (cycling voltage between 0 and +0.830 V at 0.002 V/s for 18 h) a layer of polymerized resorcinol and *m*-phenylenediamine[13,17] was applied to the cavity to help reject neutral electroactive interference

species, such as acetaminophen, from reaching the Pt/Ir surface. A silver/silver chloride (Ag/AgCl) wire electrode was tightly wrapped around the sensor to serve as an electrochemical reference, and heat-shrinkable polyester tubing was applied to secure the reference wire in place. Glucose oxidase was then immobilized within the cavity using glutaraldehyde, as previously published.[13,14,18] An outer polymer layer was then applied to the sensor's surface using a wire loop. This layer consisted of 2% (wt/vol) Elast-Eon E2As polyurethane in THF and it was applied as a top coat to modulate the NO release and also control the sensor's linear detection range for glucose by restricting glucose diffusion into the enzyme layer. The E2As polyurethane outer coating was previously used with success to prepare an NO release inner coating to prevent platelet activation and clotting within a rabbit model for extracorporeal circulation.[19] Sensors (see Figure 3.4) were calibrated within the operational range of glucose sensors (1.0 – 20.0 mM) to ensure good analytical performance before modification, and subsequently dried before shipping to Dr. Stachelek at CHOP for CD47 surface functionalization. Control sensors that were not CD47 functionalized were also prepared from the same batch, kept in the University of Michigan Chemistry Department, and tested for analytical performance at the same time as the sensors modified with CD47 at CHOP to ensure that sensor age did not adversely affect glucose sensor response properties.

A diagram of the fully-assembled sensor is shown below in Figure 3.4:

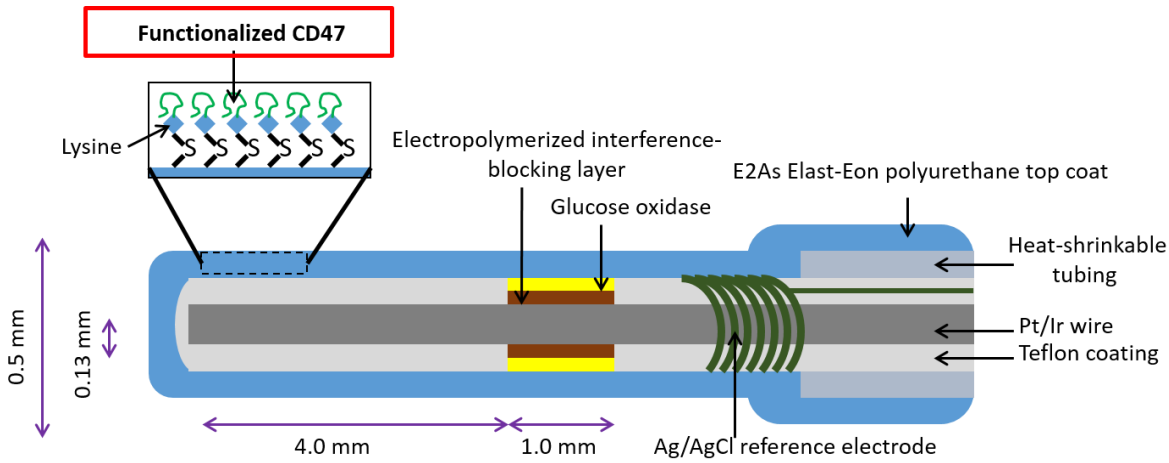

Figure 3.4. Configuration of annealed Nafion glucose sensors with surface functionalized recombinant CD47 protein.

3.2.3 Recombinant CD47 protein production and purification (performed by Dr. Stanly Stachelek at the Children's Hospital of Philadelphia, as described in Finley, et al. Biomaterials 2012).[2]

A modification of the previously published methodology was used to produce recombinant human CD47 from human whole blood.[1,2] Briefly, the extracellular domain of human CD47 (GenBank accession number NM_174708) was amplified from human cDNA using gene specific primers. Forward Primer: 5' – ATAAGCTTATGTGGCCCCTGG - 3'. Reverse Primer: 5' - GCGGATCCTCTGGTTCAACCCT – 3'. The PCR conditions were as follows: 95°C for 30 s denaturation, 59°C for 45 s annealing, and 72°C for 1 min extension for a total of 35 cycles. The PCR product was ligated into a thymidine/adenine vector containing the rat CD4 domains 3 and 4 (rCD4D3+4) coding sequence. A poly-lysine coding sequence (L) was cloned into the vector at the three prime end of the rat CD4 sequence to aid in protein purification and appendage to the polymeric surfaces. The expression cassette (5' - hCD47-rCD4d3+4-Biotin – 3' or 5' - hCD47-rCD4d3+4-Poly-Lysine – 3') was then sub-cloned into pcDNA5-FRT (Invitrogen, Carlsbad, CA) by digesting vector and insert with Hind III and BamHI and then ligating using T4 DNA ligase. All vectors were sequenced by the Children's Hospital of Philadelphia Research Institute Nucleic

Acid Facility and confirmed to be free of coding errors and in-frame for accurate protein production. The pcDNA5-FRThCD47- rCD4d3+4-Biotin (hCD47B) and pcDNA5-FRT-hCD47-rCD4d3+4-Poly-Lysine (hCD47L) were co-transfected with pOG44, used to transiently provide the recombinase enzyme required for integration of the hCD47-rCD4d3þ4 into the genomic DNA of the host cell, into CHO Flp-In cells to allow for genomic integration of the expression cassette. Recombinant protein was isolated from the cell culture medium, concentrated, desalted, and purified using an avidin protein purification column or anti-CD47 amino-link protein purification column both obtained from Thermo Fisher Scientific (Wilmington, DE). Protein concentration and purity were analyzed by the Bradford assay and SDS-PAGE Western blot analysis.

3.2.4 Appending of poly-lysine tagged recombinant proteins to synthetic polymeric surfaces (performed by Dr. Stanly Stachelek at the Children's Hospital of Philadelphia, as described in Finley, et al. Biomaterials 2012)[2]

Polyurethane coated glucose sensors were reacted with 2-pyridyldithio-, benzophenone- and carboxymodified polyallylamine (PDT-BzPh) and reduced with tris(2-carboxyethyl)phosphine TCEP to obtain a thiol reactive surface, as previously described.[1,2] The poly-lysine tail of the recombinant CD47L protein was reacted with succinimidyl 4-(N-maleimidomethyl) cyclohexane-1-carboxylate (SMCC) for 1 h to form thiol-reactive groups. SPDP was removed via a desalting protein cut off column and the poly-lysine CD47 protein was incubated with the synthetic surface overnight at 4°C. Figure 3.5 is provided as an illustration of the chemistry described in this section. Confirmation of recombinant protein attachment was determined by conjugation with a FITC-tagged antibody specific for human CD47 (BD Biosciences, Franklin Lakes, NJ).

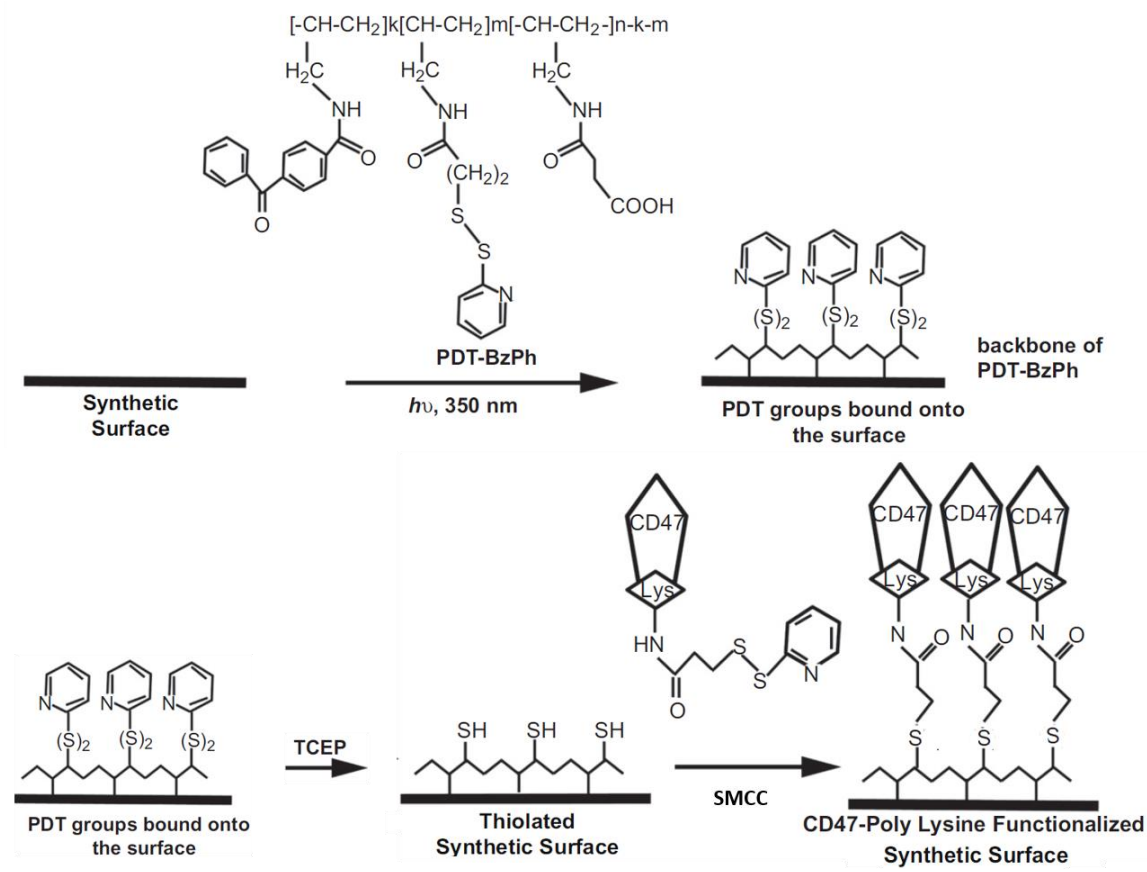

Figure 3.5. Mechanism of recombinant CD47 functionalization of polyurethane surface coating of functional glucose sensors.

3.2.5 Analytical In Vitro Performance of Annealed Glucose Sensors

Glucose sensors were calibrated using a 4-channel BioStat potentiostats (ESA Biosciences Inc., Chelmsford, MA). The potential applied to the working Pt/Ir wire of the sensors was +0.600 V vs. Ag/AgCl reference in 0.1 M phosphate buffered saline (PBS), pH 7.4, at 37.5°C. It was critical to measure the sensor response before and after CD47 functionalization, to ensure that glucose oxidase activity was retained throughout the CD47 attachment procedure and transit between laboratories.

As previously described (see Chapter 2), the selectivity of the CD47 modified and corresponding control sensors over naturally occurring electroactive interference species (ascorbic acid and uric acid), was evaluated by injecting near maximum *in vivo* concentrations of these interference species into the *in vitro* cell during the glucose calibrations (from 1.0 – 20.0 mM). The % error for these sensors was calculated by dividing the current response from an injection of interference species (0.5 mM for ascorbic acid and 0.33mM for uric acid[20] by the current signal recorded for 5.0 mM glucose. A threshold was established to determine effective selectivity. The threshold was defined as the current from a specific interference species should not exceed 5% of the current response from a 5.0 mM glucose. The selectivity test was repeated and monitored over a 14-d period to evaluate the stability of the selectivity layers. Comparisons in stability were evaluated between the CD47 modified sensors and the control group of sensors, which were kept in storage in the University of Michigan Chemistry Department and not CD47 functionalized.

3.3 Results and Discussion

3.3.1 Assessment of Glucose Oxidase Activity of CD47 Modified Sensors Before and After CD47 Functionalization

As shown in Figure 3.6 (a-d), four CD47 glucose sensors that were successfully modified with recombinant CD47 protein retained their glucose linearity, and therefore, their glucose oxidase activity throughout the complete functionalization procedure (Section 3.2.4). Dr. Stachelek reported that via fluorescence intensity assay, a coating of 85.0 ng/cm^2 of CD47 had been successfully deposited onto the glucose sensor surfaces, indicating that E2As is an acceptable candidate polymeric surface material for CD47 modification. The variations in the slopes of the

different sensors is primarily due to variations in the thickness of the outer polyurethane coating, which is difficult to control using the manual loop casting method employed.

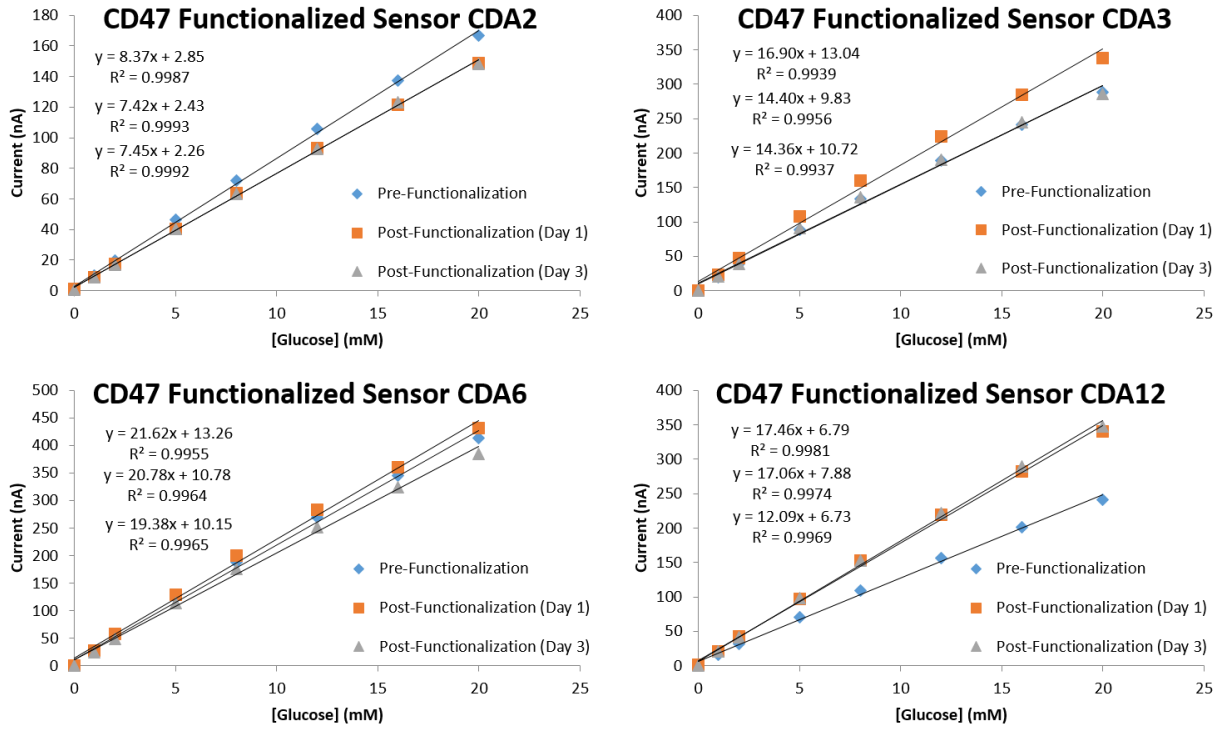

Figure 3.6. Glucose sensor calibration data prior to and after CD47 surface functionalization.

Figure 3.7 shows the same glucose calibrations performed on control glucose sensors that did not undergo the CD47 surface functionalization. The preservation of linearity and glucose oxidase activity indicates that any perceived change in glucose oxidase activity in the CD47 functionalized sensors was not due to age of the sensors.

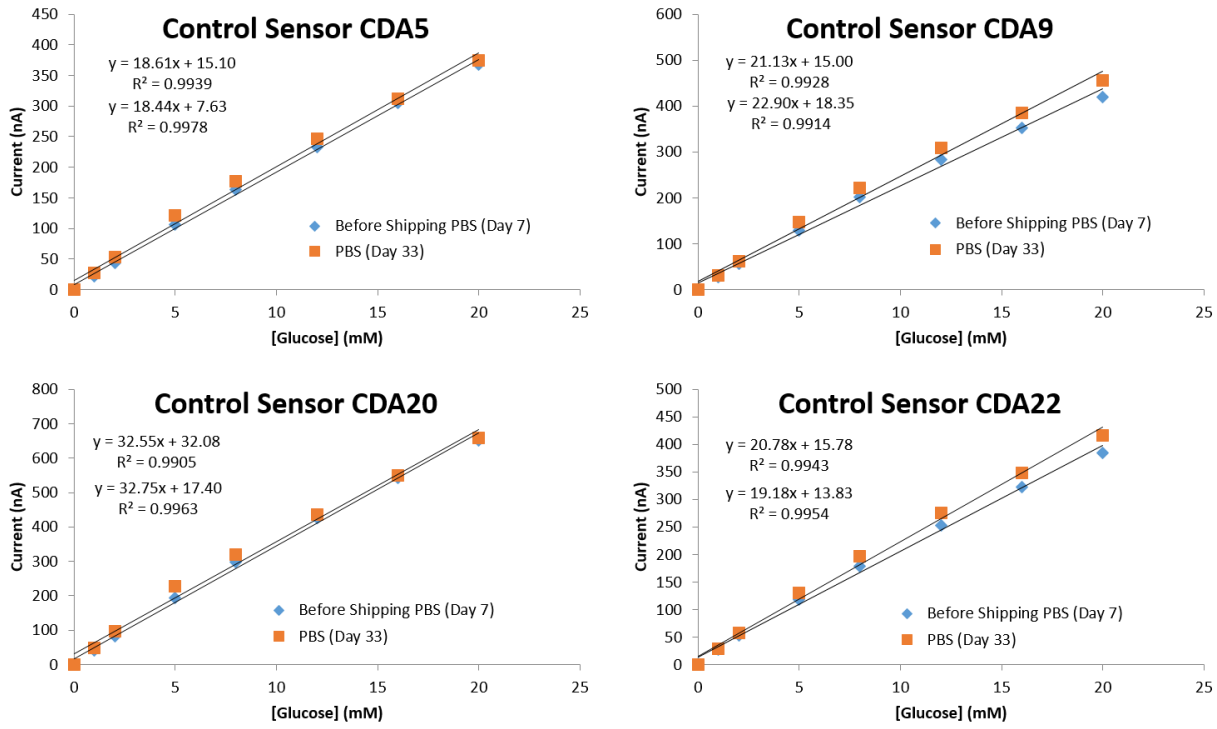

Figure 3.7. Glucose sensor calibration of the control sensors, which were not CD47 functionalized, but were re-calibrated simultaneously when the modified sensors were received.

Figure 3.8 shows a comparison of selectivity over electroactive interference species before and after CD47 functionalization. The lifetime of the CD47 sensors was much longer than the sensors evaluated in Chapter 2 (due to shipment and processing at CHOP), and thus the observed higher standard deviations for selectivity between the sensors may indicate that a combination of extended lifetime and the functionalization procedure did partially exhaust the effectiveness of the annealed Nafion layer of these sensors; however, the average interference response is still well within the 5% threshold deemed acceptable for blood glucose sensors.

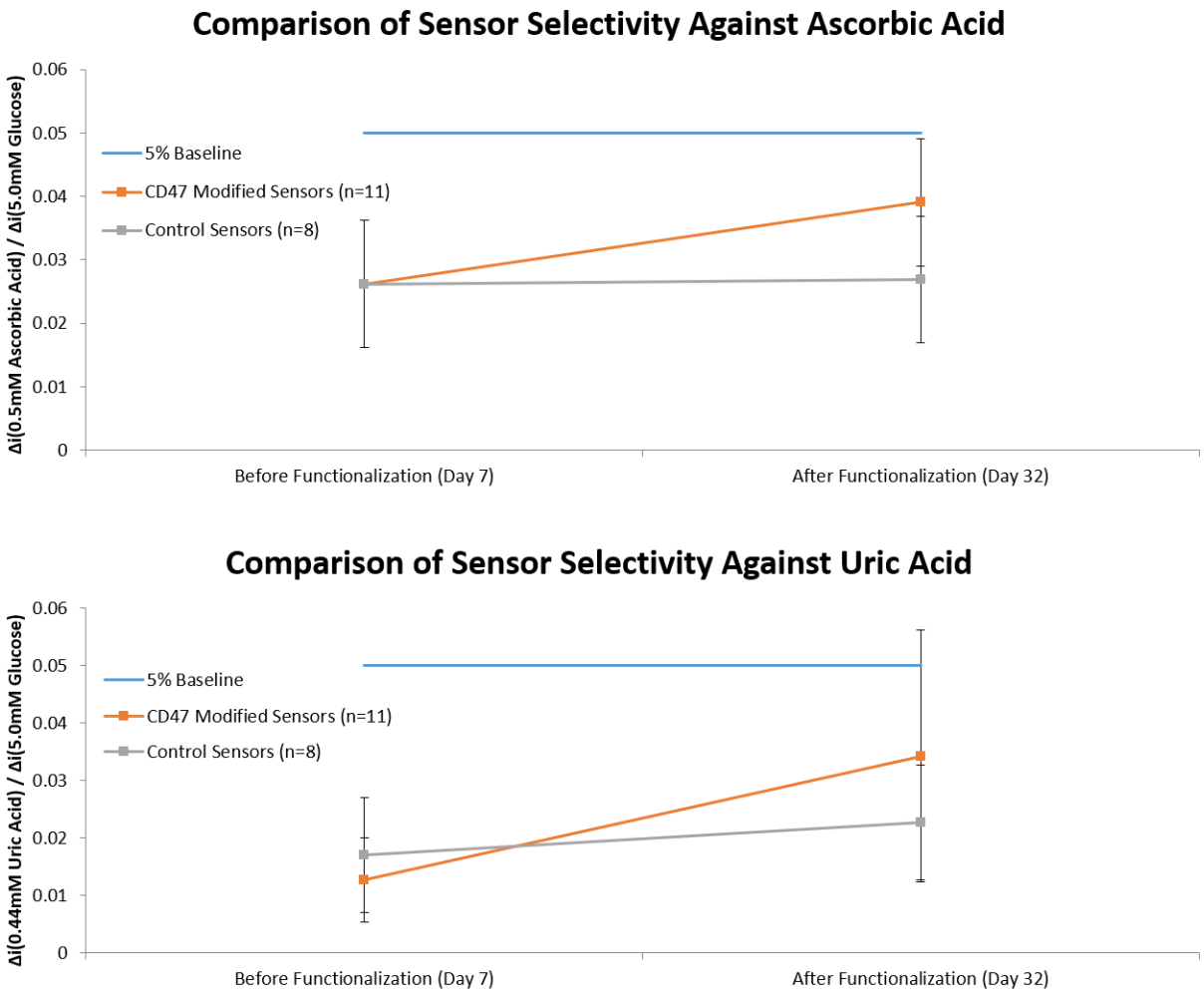

Figure 3.8. Comparison between CD47 functionalized sensors and control sensors of selectivity against negative electroactive interference species (ascorbic and uric acids). The upper plot displays selectivity of the sensor against 0.5 mM ascorbic, acid and the lower plot shows selectivity over 0.44 mM uric acid. The steady-state current resulting from these interference species should not exceed 5% of the steady-state current response from 5.0 mM glucose (blue line).

3.3.2 Discussion and Future Combination of In Vivo Studies

Dr. Stanley Stachelek and coworkers at CHOP confirmed the density of recombinant protein attachment was determined by conjugation with a FITC-tagged antibody specific for human CD47 via BD Biosciences (Franklin Lakes, NJ)[2]. The next logical step will be to determine whether

immobilized CD47 confers sufficient hemocompatibility to enable the glucose sensors not to activate the coagulation cascade when tested *in vivo.* Studies to conduct such studies are being planned. Another important question to answer is whether immobilized CD47 provides equivalent anti-platelet activity as sensors prepared only with nitric oxide releasing capability (see Chapter 4), or might sensors prepared with a combination of both immobilized CD47 and NO release be the most desirable approach to enhancing biocompatibility? To potentially pursue this approach, the nitric oxide releasing polymeric coating would need to be added first as an inner layer and then the CD47 could be functionalized on the outermost surface of a thin additional layer of polyurethane. Since NO is readily permeable through polyurethanes adding this layer should have little effect on the NO release flux of such a sensing device.

3.4 Conclusions

Intravenous needle-type glucose sensors coated with the E2As Elast-Eon polyurethane can be successfully functionalized on their outer surface with recombinant CD47 protein domains through a photopolymerization procedure to thiolate the polymer surface. This immobilization process, which takes approximately 1 h to form thiol reactive groups on the surface followed by 14 h incubation time at 4°C with the poly-lysine recombinant CD47[2], does not adversely influence the glucose response properties of such sensors. Indeed, sensors retain their linear response range and glucose oxidase activity after the surface functionalization procedure, and retain an acceptable level of selectivity over electroactive interference species through the use of an annealed Nafion inner layer.

3.5 Literature Cited

(1) Stachelek, S. J.; Finley, M. J.; Alferiev, I. S.; Wang, F. X.; Tsai, R. K.; Eckells, E. C.; Tomczyk, N.; Connolly, J. M.; Discher, D. E.; Eckmann, D. M.; Levy, R. J. *Biomaterials* **2011**, *32*, 4317.

(2) Finley, M. J.; Rauova, L.; Alferiev, I. S.; Weisel, J. W.; Levy, R. J.; Stachelek, S. J. *Biomaterials* **2012**, *33*, 5803.

(3) Jaiswal, S.; Jamieson, C. H. M.; Pang, W. W.; Park, C. Y.; Chao, M. P.; Majeti, R.; Traver, D.; van Rooijen, N.; Weissman, I. L. *Cell* **2009**, *138*, 271.

(4) Soto-Pantoja, D. R.; Stein, E. V.; Rogers, N. M.; Sharifi-Sanjani, M.; Isenberg, J. S.; Roberts, D. D. *Expert Opin Ther Tar* **2013**, *17*, 89.

(5) Hsu, Y. C.; Acuna, M.; Tahara, S. M.; Peng, C. A. *Pharm Res* **2003**, *20*, 1539.

(6) Tsai, R. K.; Discher, D. E. *J Cell Biol* **2008**, *180*, 989.

(7) Rodriguez, P. L.; Harada, T.; Christian, D. A.; Pantano, D. A.; Tsai, R. K.; Discher, D. E. *Science* **2013**, *339*, 971.

(8) Schutz, C. *Aging-Us* **2015**, *7*, 513.

(9) Bruns, H.; Bessell, C.; Varela, J. C.; Haupt, C.; Fang, J.; Pasemann, S.; Mackensen, A.; Oelke, M.; Schneck, J. P.; Schutz, C. *Clin Cancer Res* **2015**, *21*, 2075.

(10) Sosale, N. G.; Spinier, K. R.; Alvey, C.; Discher, D. E. *Curr Opin Immunol* **2015**, *35*, 107.

(11) Finley, M. J.; Clark, K. A.; Alferiev, I. S.; Levy, R. J.; Stachelek, S. J. *Biomaterials* **2013**, *34*, 8640.

(12) Brown, E. J.; Frazier, W. A. *Trends Cell Biol* **2001**, *11*, 130.

(13) Yan, Q. Y.; Major, T. C.; Bartlett, R. H.; Meyerhoff, M. E. *Biosens Bioelectron* **2011**, *26*, 4276.

(14) Yan, Q. Y.; Peng, B.; Su, G.; Cohan, B. E.; Major, T. C.; Meyerhoff, M. E. *Anal Chem* **2011**, *83*, 8341.

(15) Bindra, D. S.; Zhang, Y. N.; Wilson, G. S.; Sternberg, R.; Thevenot, D. R.; Moatti, D.; Reach, G. *Anal Chem* **1991**, *63*, 1692.

(16) Batchelor, M. M.; Reoma, S. L.; Fleser, P. S.; Nuthakki, V. K.; Callahan, R. E.; Shanley, C. J.; Politis, J. K.; Elmore, J.; Merz, S. I.; Meyerhoff, M. E. *J Med Chem* **2003**, *46*, 5153.

(17) Geise, R. J.; Adams, J. M.; Barone, N. J.; Yacynych, A. M. *Biosens Bioelectron* **1991**, *6*, 151.

(18) Gifford, R.; Batchelor, M. M.; Lee, Y.; Gokulrangan, G.; Meyerhoff, M. E.; Wilson, G. S. *J Biomed Mater Res A* **2005**, *75a*, 755.

(19) Brisbois, E. J.; Handa, H.; Major, T. C.; Bartlett, R. H.; Meyerhoff, M. E. *Biomaterials* **2013**, *34*, 6957.

(20) Zhang, Y. N.; Hu, Y. B.; Wilson, G. S.; Moattisirat, D.; Poitout, V.; Reach, G. *Anal Chem* **1994**, *66*, 1183.

CHAPTER 4

IMPROVED THROMBORESISTANCE AND ANALYTICAL PERFORMANCE OF INTRAVASCULAR AMPEROMETRIC GLUCOSE SENSORS USING NITRIC OXIDE RELEASE COATINGS WITH PRELIMINARY *IN VIVO* EXPERIMENTS

4.1 Introduction

Accurate monitoring and control of blood glucose play critical roles in the treatment of patients with diabetes millitus. Benchtop point-of-care devices are the current standard for many hospitals and medical care facilities, and finger prick glucometers are widely used for personal and home glucose measurements. While these devices yield discrete blood glucose values, trends of rapidly increasing/decreasing glucose concentrations often go unobserved when such devices are used. Some commercially available systems provide continuous glucose monitoring of interstitial fluid using implanted electrochemical sensors. However, due to the ~10-15 minute lag time between changes in blood glucose concentration and changes in interstitial fluid glucose,[1] in practice these devices can only supplement, rather than fully replace, discrete blood measurements.

---

*Note: Sections from this chapter are adapted from the following publication by this Ph.D. candidate: A. K Wolf, Y. Qin, T. C. Major, M. E. Meyerhoff, "Improved Thromboresistance and Analytical Performance of Intravascular Amperometric Glucose Sensors using Optimized Nitric Oxide Release Coatings," *Chinese Chemical Letters*, (2015) Volume 26, pages 464-468.

Intravenous amperometric glucose sensors may provide a better alternative platform for continuous blood glucose measurements, especially within a hospital environment. Such monitoring could not only decrease potential complications for diabetic patients, but also offers better outcomes for non-diabetic patients, both benefiting from tight glycemic control. Indeed, tight glycemic control is a requirement for many patients in intensive care units (ICUs) to achieve targeted treatment and better patient outcomes. The amperometric glucose sensors described in this work are designed to be implanted intravenously in critical care patients through existing IV port access or inserted into a catheter. Continuous measurement from these devices would provide medical staff with the ability to see trends in rising and falling blood glucose, allowing them to select better treatment options. Miniaturized electrochemical blood glucose sensors have been previously reported in literature, and have been developed into commercialized products for measurement in subcutaneous interstitial/brain fluid matrices; however, these sensors can quickly lose analytical accuracy due to thrombus formation on their surfaces when placed within the bloodstream of hospitalized patients.[2,3] Via the formation of thrombus with encapsulated platelets, the local glucose concentration near the surface of the sensor can be reduced by metabolic activity of platelets and other trapped cells and, therefore, the sensor reads a false glucose value compared to the level of glucose within the plasma phase of the blood. The well-known antithrombotic and anti-inflammatory properties of nitric oxide (NO) provide a useful method of potentially enhancing the hemocompatibility of a blood contacting surface. Incorporating NO releasing donor molecules into a sensor's outer polymeric coatings allows it to mimic the functions of endothelial cells lining the inner walls of all blood vessels, which endogenously release NO at localized fluxes of 0.5 – 4.0 $x10^{-10}$ mol cm^{-2} min^{-1}.[4] This approach has previously been shown to reduce clot formation on the surface of intravenous glucose sensors and preserve their *in vivo* performance.[5,6] Herein we

extend this earlier work by further optimizing the NO release formulation and the outer glucose restriction layer used to prepare such devices to achieve more optimal linearity and *in vivo* performance.

4.2 Experimental

4.2.1 Materials

Glucose oxidase (Type VII, from *Aspergillus niger*), d(+)-glucose, glutaraldehyde, bovine serum albumin (BSA), fetal bovine serum (filtered, sterilized), hemoglobin(lyophilized, from bovine blood), iron (III) chloride ($FeCl_3$), 37% hydrochloric acid (HCl), Nafion (5 wt% solution in lower aliphatic alcohols/H_2O mixture), 1,3-diaminobenzene, resorcinol, tetrahydrofuran (THF), N,N'-dibutyl-1,6-hexanediamine (DBHD) were all obtained from Sigma-Aldrich (St. Louis, MO). Sodium phosphate dibasic heptahydrate ($Na_2HPO_4 \cdot 7H_2O$), sodium phosphate monobasic monohydrate ($NaH_2PO_4 \cdot H_2O$) were purchased from Amresco, Inc. (Solon, OH). Sodium chloride (NaCl) is a product of Research Products International Corp. (Mt. Prospect, IL). Potassium chloride is from Fisher Scientific (Pittsburgh, PA). Teflon-coated platinum/iridium and silver wires are products of A-M Systems (Sequim, WA). E2As Elast-Eon polyurethane was a gift from Aortech Biomaterials (Weybridge, Surrey, UK). Diazeniumdiolated DBHD (DBHD/N_2O_2) was synthesized by treating DBHD with 80 psi nitric oxide (NO) gas purchased from Cryogenic Gases (Detroit, MI) at room temperature for 24 h, as previously described.[5] Accu-Chek SmartView testing strips and the associated Accu-Chek Nano hand-held glucose meter are commercially available products from Roche Diagnostics (Risch-Rotkreuz, Switzerland)

4.2.2 Sensor Fabrication

Glucose sensor design (see Fig. 4.1) was based on previous configurations[5-8] by first cutting a 1-mm length cavity in the Teflon coating of a platinum/iridium wire (outer diameter = 0.2 mm). A Nafion coating was then applied to the cavity, and then the wires that feature an annealed Nafion inner selective membrane were placed in a Fisher Scientific Isotemp oven set to 170°C for 1.5 h and then gradually cooled to 35°C to enhance sensor selectivity against negatively-charged electroactive interference species, such as ascorbic and uric acid, as described in Section 2.2.2 of this thesis. Non-annealed sensors were dried at 37.5°C, rather than annealed. Then, *via* a CV electropolymerization process (cycling voltage between 0 and +0.830 V at 0.002 V/s for 18 h) a layer of polymerized resorcinol and *m*-phenylenediamine[6,9] was applied to the cavity to help further reject neutral electroactive interference species, such as acetaminophen, from reaching the inner Pt/Ir surface. A silver/silver chloride (Ag/AgCl) wire electrode was tightly wrapped around the sensor to serve as an electrochemical reference, and heat-shrinkable polyester tubing was applied to secure the reference wire in place. Glucose oxidase was then immobilized within the cavity using glutaraldehyde. An outer polymer layer was then applied to the sensor's surface using a wire loop: a 2% (wt/vol) Elast-Eon E2As polyurethane in THF was applied with a wire loop as a top coat to modulate the NO release and also control the sensor's linear detection range for glucose by restricting glucose diffusion into the immobilized enzyme layer. E2As polyurethane was chosen for these studies since it had been previously used with positive success as an NO release coating to prevent platelet activation and clotting within a rabbit model for extracorporeal circulation.[10] Additional outer layers were then applied to the sensor's surface using a wire loop: an ester-capped polylactic acid layer containing diazeniumdiolated dibutylhexyldiamine (2:1, wt:wt) (Fig. 4.1c) was applied to provide the sensor NO releasing behavior, and then an additional

2% (wt/vol) Elast-Eon E2As polyurethane in THF (Fig. 4.1b) was applied as a top coat to modulate the NO release and also control the sensor's linear detection range for glucose by restricting glucose diffusion into the immobilized enzyme layer. A diagram of the fully-assembled sensor is shown in Fig. 4.1a. Control sensors were prepared using a similar procedure except that no diazeniumdiolated dibutylhexyldiamine was doped within the PLA coating.

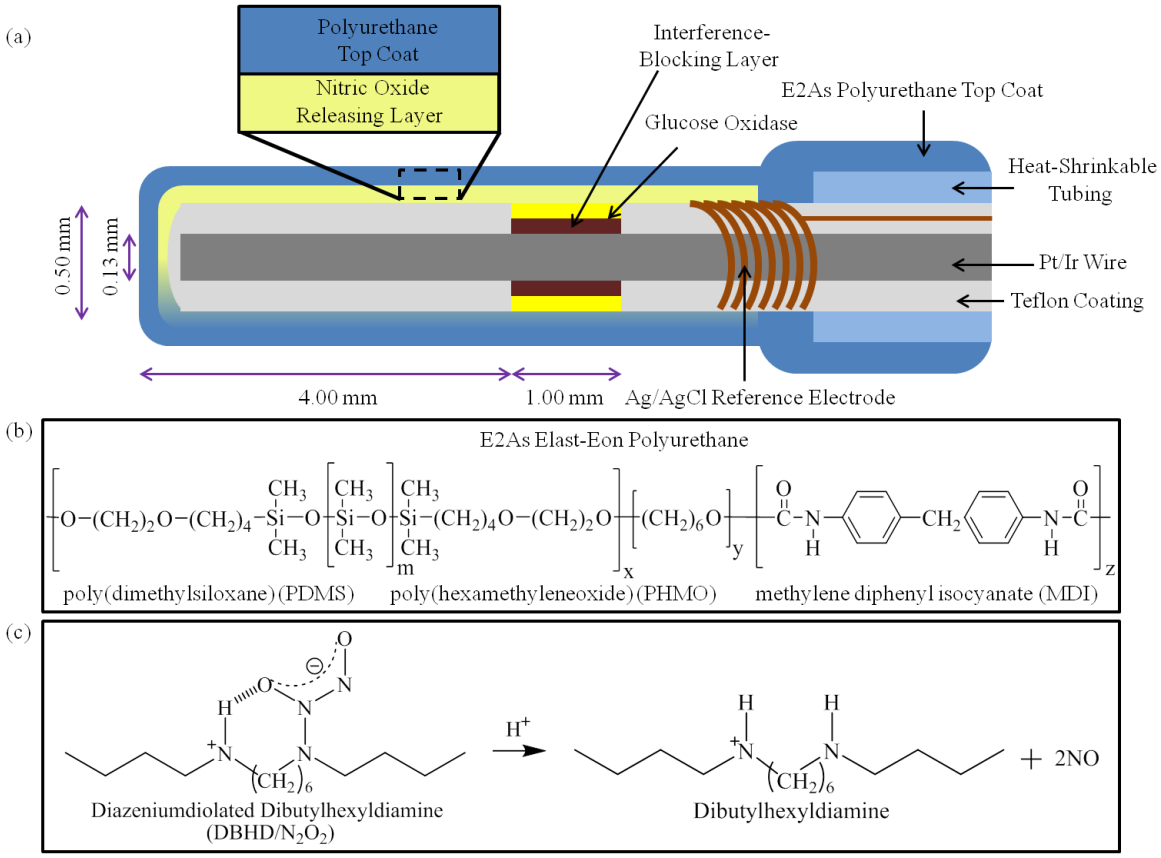

Figure 4.1. (a) Needle/catheter type glucose sensor design; (b) E2As Elast-Eon polyurethane used for the sensor outer layer; (c) Lipophilic diazeniumdiolated dibutylhexyldiamine and the proton-driven mechanism for nitric oxide release.

4.2.3 In Vitro Analytical Performance of Annealed Glucose Sensors

Glucose sensors were calibrated using 4-channel BioStat potentiostats (ESA Biosciences Inc., Chelmsford, MA). The potential applied to the inner Pt/Ir wire was +0.600 V vs. Ag/AgCl reference in a 0.1 M phosphate buffered saline (PBS), pH 7.4, test solution at 37.5°C. *In vitro* glucose calibrations were conducted in both phosphate buffered saline (PBS) and fetal bovine serum, as the bovine serum was identified as an intermediate matrix between buffered saline solution and the whole blood of an *in vitro* experiment. Total glucose concentration of the serum was assessed using a commercial AccuChek SmartView glucometer.

4.2.4 In Vitro Assessment of NO Release

Nitric oxide released from these glucose sensors was monitored via chemiluminescence using a Sievers Nitric Oxide Analyzer (NOA) 280i (Boulder, CO). Measurement occurred when the sensors were immersed in 0.1 M PBS, pH 7.4, at 37.5°C and the NO release data were collected. Long-term NO release was monitored by collecting daily release measurements to ensure that flux (based on surface area) was above the 0.5 x 10^{-10} mol cm^{-2} min^{-1} minimum threshold for endogenous NO release from endothelial cells.[4]

4.2.5 In Vivo Protocol for Evaluation of Sensor Performance During 7h Implantation Within Rabbit Veins

In vivo 7h rabbit experiments were conducted through the assistance of surgical specialist Terry Major (a member of the Dr. Robert H. Bartlett lab in the University of Michigan Department of Surgery). The rabbits were anesthetized for the duration of the procedure. Briefly, three sensors (typically two NO release, and one non-NO release control) for each rabbit were inserted into the two jugular veins and one femoral vein, and sutured in place. To assess the glucose calibration

accuracy, the discrete venous blood glucose values, measured by an ALB-800 Flex Radiometer blood gas analyzer every 30 min, were recorded and compared with the continuous measurements provided by the sensors. Several bolus injections of 50% dextrose solution were given intravenously to modulate the rabbit's venous glucose concentration. At the conclusion of the experiment, the sensors were explanted and photographed to examine the extent of surface clotting that had developed. Post-experimental glucose calibrations (in 0.1M PBS and/or bovine serum) as well as post-experimental NO release measurements were also conducted. A continuous time-trace of the sensor's measurements is reported, based on both a one-point calibration from a discrete Radiometer measurement made early in the experiment as well as an *in vitro* calibration curve conducted in bovine serum prior to the experiment.

4.2.6 In Vivo Protocol for Evaluation of Sensor Performance During 20h Implantation Within Porcine Blood Vessels

In vivo 20 h porcine experiments were conducted through the assistance of surgical specialists Drs. Megan Coughlin, Alvaro Rojas Pena, and Joseph Church and animal specialists Salvatore Aiello and Elena Perkins (members of the Dr. Robert H. Bartlett lab in the University of Michigan's Department of Surgery). The pigs were anesthetized for the duration of the procedure. Briefly, the NO releasing sensors corresponding to Figures 4.6, 4.7 and 4.8 were inserted into the jugular vein, and sutured in place. (In this case, the femoral venous access sites for these experiments were used for testing a colleague's intravenous glucose sensors simultaneously.) To assess the glucose calibration accuracy, the discrete venous blood glucose values, taken by an ALB-800 Flex Radiometer blood gas analyzer each hour, were recorded and compared with the continuous measurements provided by the sensors. Several bolus injections of 50% dextrose solution were given intravenously to modulate the rabbit's venous glucose concentration. At the

conclusion of the experiment, the sensors were explanted and photographed to examine the extent of surface clotting that had developed. Post-experimental glucose calibrations (in 0.1M PBS and/or bovine serum) as well as post-experimental NO release measurements were also conducted. A continuous time-trace of the sensor's measurements is reported, based on a two-point calibration from discrete *in vitro* Radiometer measurements made early in time after the start of each animal experiment.

4.2.7 Glucose Sensor Surface Investigation with SEM and Diffusion Cell Assessment of Membrane Potential

To investigate the outer polyurethane layers' topography as well as the structure of the NO releasing PLGA/DBHD/N_2O_2 layer, SEM images were taken of the surface profile and cross-sectional areas of sample glucose sensors on an Amray 1910 FEG-SEM. Thicker versions of the E2As Elast-Eon polyurethane and a sandwich membrane composed of a layer of PLGA and DBHD/N_2O_2 between two layers of E2As Elast-Eon were cast and placed into glass diffusion cells. In one type of experiment, the both halves of the diffusion cell were filled with 0.1 M PBS with a membrane clamped into place between them, and a commercial reference electrode was placed on each side. When one side was replaced with bovine serum, any potential change was recorded in order to assess whether an unintended potential developed across the polyurethane membrane when the aqueous environments on each side were asymmetrical. A Lawson Labs multi-channel potentiostat was used to measure the open circuit potentials of each electrode.

In a second type of experiment, both halves of the diffusion cell were filled with 0.1 M PBS with a membrane clamped into place between them, and a fabricated glucose sensor (described in Chapter 2) was placed into one half-cell. A high concentration of glucose was injected into the

half-cell not containing the glucose sensor and the current reading from the sensor was monitored with a BioStat to detect glucose able to diffuse across the thicker membrane. The solutions in each section cell were well stirred.

4.2.8 In Vitro Investigations of Intravenous Medications on Glucose Oxidase Activity

Based on poor analytical performance of sensors during the 20 h porcine experiments, several additional benchtop measurements were conducted to examine potential interferences from intravenous drugs administered to the pig during the longer-term experiments. These drugs serve as anesthetics or pressors to maintain the animal's blood pressure. Injections of dopamine, vercuronium bromide, heparin, and epinephrine (each separately) were made into cells containing 10 mM glucose to check for any major changes in sensor output current, either as electroactive species or as an inhibitor of glucose oxidase activity. An experiment was also conducted by replacing a 0.1 M PBS solution containing NO releasing sensors (without glucose oxidase) with concentrated oxyhemoglobin to examine if the oxyhemoglobin scavenged an appreciable amount of local NO, causing any background current due to NO oxidation at the surface of the inner Pt working electrode to decrease.

4.3 Results and Discussion

4.3.1 In Vivo Evaluation of Sensor Performance During 7 h Implantation Within Rabbit Veins

NO releasing glucose sensors were soaked in phosphate buffered saline (PBS) or bovine serum at physiological conditions (pH 7.4, 37.5^{o}C) to hydrate the polyurethane layer for restricted glucose diffusion and to activate the NO release with protons within the PLA layer. The PLA controls the local pH of the NO releasing layer by supplying protons as it slowly hydrolyzes. Ideally performing sensors release NO at a stable flux at physiological levels found for endothelial

cells ($0.5 – 4.0 \times 10^{-10}$ mol cm^{-2} min^{-1}) for the duration of the sensor's functional lifetime. Nitric oxide release from the surface of the sensors was measured by chemiluminescence using a Sievers Nitric Oxide Analyzer (NOA) 300i. The NO release profile over 7 d of the optimized sensors used for the *in vivo* experiment can be seen in Fig. 4.2a. The sensors maintained NO release above 0.5 x 10^{-10} mol cm^{-2} min^{-1} over this period while stored in bovine serum solution (containing glucose at physiological levels). Without the addition of PLA, the NO release profile would exhibit an initial burst followed by a much sharper daily decay. As indicated in Fig. 4.1c, the NO release mechanism from diazeniumdiolated dibutylhexyldiamine is dependent upon a steady supply of protons. In our previously published *in vivo* glucose sensor experiments, a 50:50, acid-capped poly(lactic-*co*-glycolic acid) (PLGA) was used to formulate the NO release layer to control local pH at the sensor surface. The innate acid-terminated polymer chains of this material coupled with the co-polymer structure yield relatively rapid hydrolysis rates; thus, the NO release profile based on PLGA begins with a large burst of NO on day 1 with a characteristic decay over subsequent days. In contrast, the PLA used in the studies reported herein has ester-capped end groups, which slows the hydrolysis rate, and therefore provides a more stable NO release profile for the duration of testing. This ensures that NO release will remain greater than 0.5×10^{-10} mol cm^{-2} min^{-1} until after the 7^{th} day of sensor lifetime.

E2As Elast-Eon, a polymer composed of a mixed soft segment of poly(-dimethylsiloxane) and poly(hexamethylene oxide) with a methylene diphenyl isocyanate (MDI) hard segment, was used as the outermost coatings in the fabrication of the glucose sensors because it has been reported to exhibit excellent intrinsic biocompatibility and biostability, with low levels of blood protein adhesion.[11,12] Since the inherent hemocompatibility of this material should enhance the overall thromboresistance properties from the NO release devices, E2As was selected as a replacement

for PurSil Thermoplastic silicone polyether used in our previous *in vivo* glucose sensor designs.[6] In benchtop studies, the E2As coated sensors displayed the desired control over the linear glucose detection range (slowing glucose diffusion to enzyme layer so sensor is not limited by oxygen levels); the NO release through this layer was also quite acceptable for this *in vivo* study. The linear range for amperometric glucose response of the NO release sensors was also measured in two types of solutions (PBS and bovine serum) *in vitro* before and after the *in vivo* implantation to evaluate their performance and recovery. Ideally, a sensor should have linear response not only within the standard resting blood glucose range of 4.4 – 6.6 mM, but it should also provide accurate measurements within the hypoglycemic and hyperglycemic ranges (1.0 -20.0 mM). The sensor should also be selective over other electroactive species present in blood that interfere with the electrochemical oxidation of hydrogen peroxide at the sensor's operating potential of +0.600 V (*vs*. Ag/AgCl). The glucose calibration curves for a representative sensor tested *in vitro* within both PBS and bovine serum (Fig. 2b) demonstrate that the sensor has a similar linear range in both environments, although a higher calibration intercept and decreased sensitivity are observed in serum, which may result from the presence of additional unknown interfering species within that commercial serum matrix. Response times for sensors intended for continuous monitoring should also be as short as possible so that they quickly react to rapid blood glucose concentration changes. Accordingly, the typical response times for the sensors employed in the *in vitro* serum calibration experiment shown in Fig. 4.2b were 5 min (with response time defined as the time required for the signal to achieve 95% of its final steady-state amperometric value after change in glucose concentration).

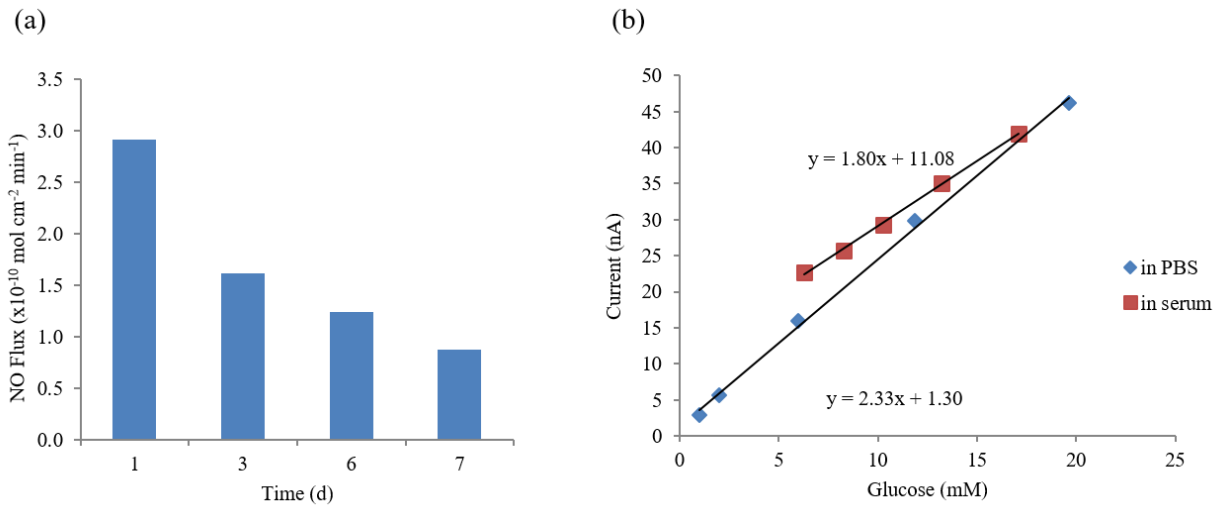

Figure 4.2. (a) Nitric oxide release fluxes of sensors stored in bovine serum at 37.5°C for three days prior to day 1 testing, and day 7 measurements were conducted after *in vivo* implantation; (b) Calibration curves of representative sensor in both PBS and bovine serum at 37.5°C before *in vivo* implantation.

When implanted into rabbit jugular veins, the glucose sensors were used to measure the *in vivo* blood glucose level and generate an amperometric time trace (Fig. 4.3a). When a bolus of 50% dextrose solution was given intravenously to modulate the rabbit's venous glucose concentration, the NO releasing sensor responded to the resulting change in blood glucose with a proportional increase in anodic current. Also, as observed in Fig.4.3b, after the 7 h *in vivo* experiment the NO releasing sensor does not develop significant clotting on its surface; hence, when the sensor's surface is in direct contact with the blood, and the observed current will remain proportional to the true blood glucose value. In contrast, the control sensor without NO release quickly developed a surface clot, as shown in Fig. 4.3b. The contrast between the clotting patterns of the control and NO release sensors is very similar to results obtained from previous glucose sensors that were evaluated *in vivo via* rabbit studies.[6] Therefore, this behavior is representative of the expected clotting that will be observed when additional sensors with the optimized outer layers are tested within future *in vivo* animal studies. The cells within the clot (*e.g.*, platelets) consume glucose in

the localized sensing area and this also creates an additional diffusion barrier, resulting in very low currents for the control sensor when placed *in vivo*. It should be noted that due to anesthesia, the rabbit's glucose levels start at hyperglycemic levels (13.8 mM), and then drop with time until dextrose is infused.

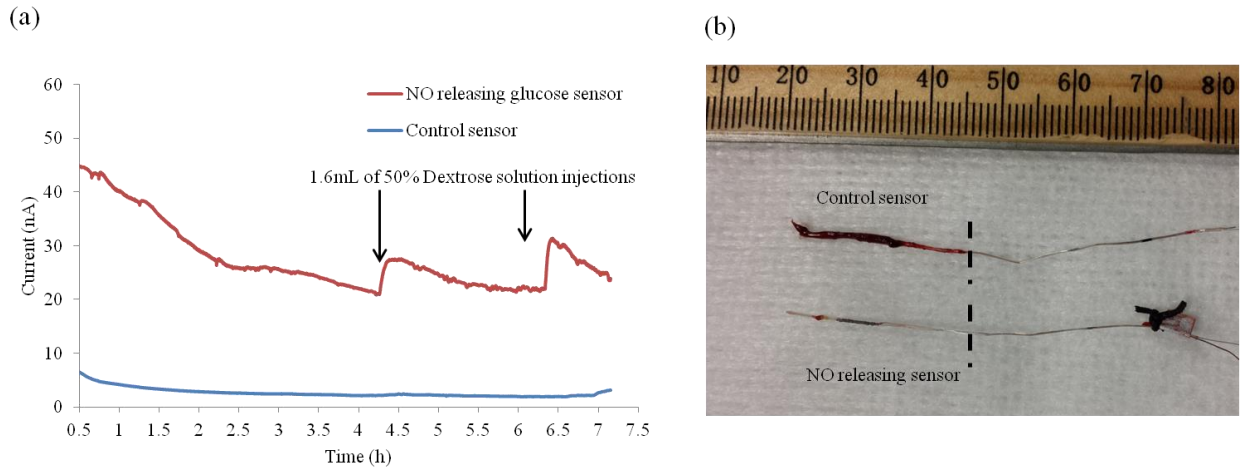

Figure 4.3. (a) Raw current time trace of *in vivo* implanted sensors. Two injections of 50% dextrose were given to modulate the blood glucose of the rabbit; (b) Photos of the control (top) and NO release (bottom) glucose sensors after the *in vivo* experiment. The portions of the sensors to the left of the dashed lines were actually inside the veins.

To assess the glucose calibration accuracy, the discrete venous blood glucose values, taken with the ALB-800 Flex Radiometer blood gas analyzer, were compared with the continuous measurements provided by the sensors. Both a one-point calibration based upon the venous blood glucose at the 1 h time-point and the *in vitro* calibration of the NO releasing sensor in bovine serum were used to convert the raw current values to corresponding glucose concentrations. In Fig. 4.4**,** the discrete venous blood glucose values are compared with the continuous glucose measurements, converted by a one-point calibration and the *in vitro* bovine serum calibration for the NO releasing sensor and by a one-point calibration for the control sensor. The NO releasing sensor quickly responds when a bolus of 50% dextrose is given intravenously, and the calibrated glucose values

more closely match those of the blood gas analyzer than those of the control sensor. The delay in response time to the dextrose boluses and the deviations from the venous blood glucose concentration by the control sensor are likely due to the heavy surface clot formation (Fig. 3b).

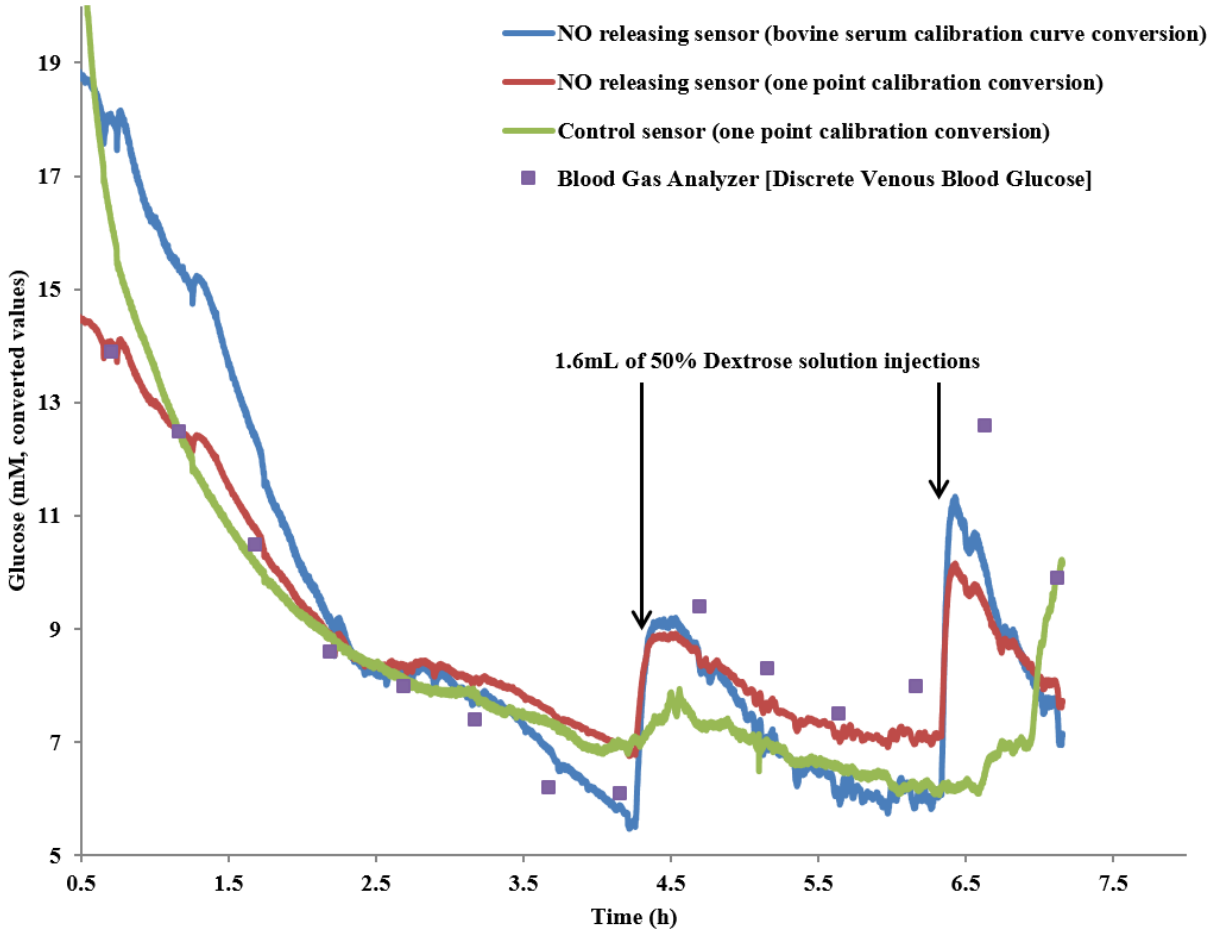

Figure 4.4. Comparison of glucose concentration values obtained from benchtop blood gas analyzer and the converted current values measured by the continuous sensor. One conversion of current to glucose concentration (mM) was made with the calibration curve in bovine serum (Fig. 4.2); the other conversion was a one point calibration taken at the 1 h time point.

Thus, NO release provides the sensor with resistance to *in vivo* thrombosis, allowing the sensor to maintain continuous analytical functionality and measurement accuracy for the duration of its implantation. The one-point *ex-vivo* Radiometer instrument blood gas calibration and the bovine

serum calibration both yielded similar values when used to convert the raw current values obtained from the NO-releasing sensor.

4.3.2 In Vivo Evaluation of Sensor Performance During 20 h Implantation Within Porcine Blood Vessels

In a similar manner as the NO release sensors fabricated for the 7 h rabbit studies, sensors intended for porcine implantation were first soaked in phosphate buffered saline (PBS) or bovine serum at physiological conditions (pH 7.4, 37.5^{o}C) to hydrate the polyurethane layer for restricted glucose diffusion and activate the NO release. Previously reported *in vivo* data for glucose sensors did not show dextrose modulation on the sensor's continuous time trace plot.[13] The 20 h porcine experiment is more than twice the duration of previous *in vivo* data collection from intravenous glucose sensors. Other long term glucose implantation involves subcutaneous placement and an initial adjustment time before data collection to account for decreased vascularization and foreign body encapsulation at the implant site. Several small design modifications were made to better suit them for the extended implantation time, including an extra 5.0 μL layer of NO releasing layer (PLGA/ DBHD/N_2O_2) applied specifically over the cross-linked glucose oxidase cavity and Ag/AgCl reference wire coil. Early experiments showed that even though NO release prevented major thrombosis on the sensor surface, minor clotting could occur specifically on top of the enzyme cavity, perhaps where local (surface) NO concentration was the smallest owing to electrochemical NO oxidation adjacent to the enzyme layer. In addition, the glucose sensor's total length was extended from 12 cm to 22 cm to accommodate placement in the larger animal and ensure that electrode leads could be properly attached to the potentiostat. Figure 4.5 shows a comparison of glucose calibration for two NO releasing sensors conducted in 0.1M PBS versus bovine serum for the porcine sensors.

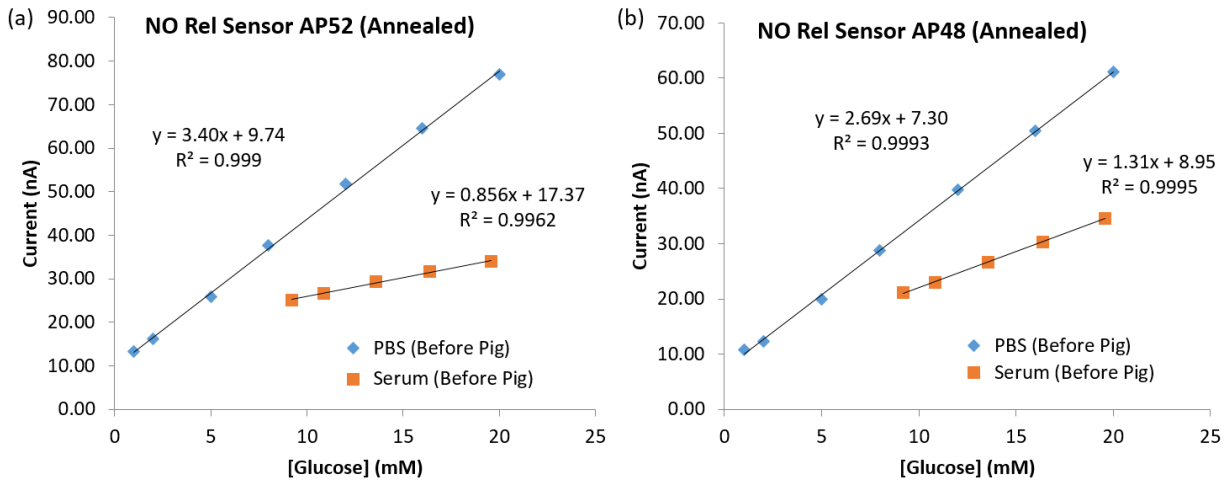

Figure 4.5. Respective glucose calibrations in 0.1 M PBS and bovine serum for two NO releasing glucose sensors (a & b) that were evaluated for *in vivo* analytical performance in Fig 4.6. The slope from the serum calibration and an average of the intercepts from the PBS and serum calibrations were used to convert raw current from the sensors into glucose concentration values in Fig. 4.6a.

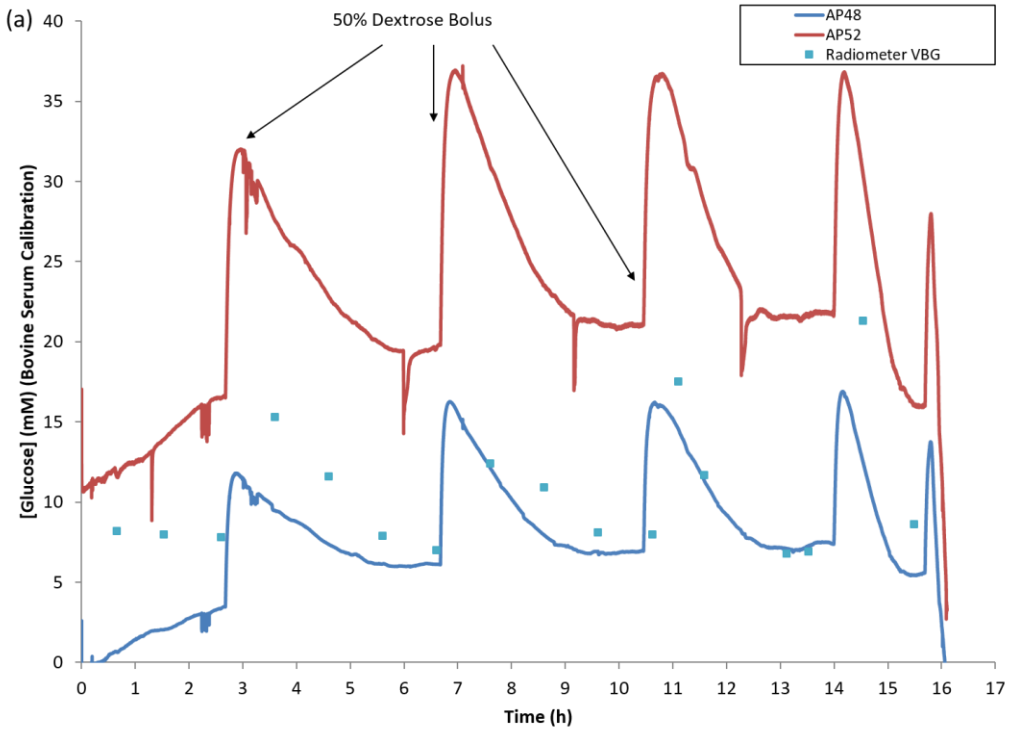
(a)
50% Dextrose Bolus
AP48
AP52
Radiometer VBG
[Glucose] (mM) (Bovine Serum Calibration)
Time (h)

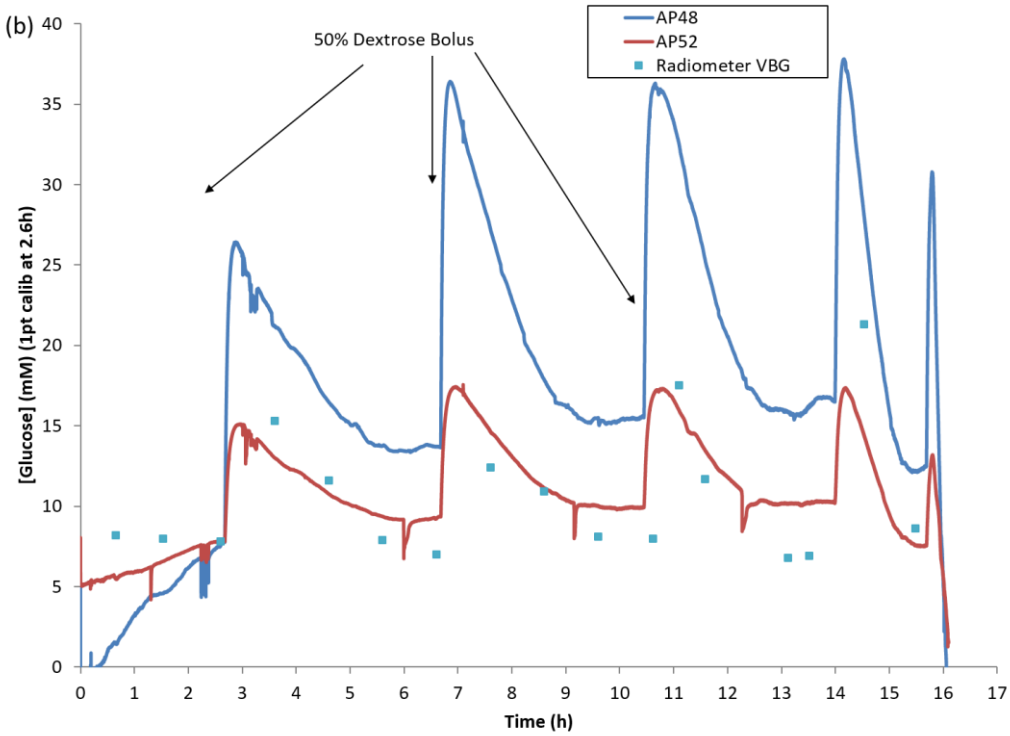
(b)
50% Dextrose Bolus
AP48
AP52
Radiometer VBG
[Glucose] (mM) (1pt calib at 2.6h)
Time (h)

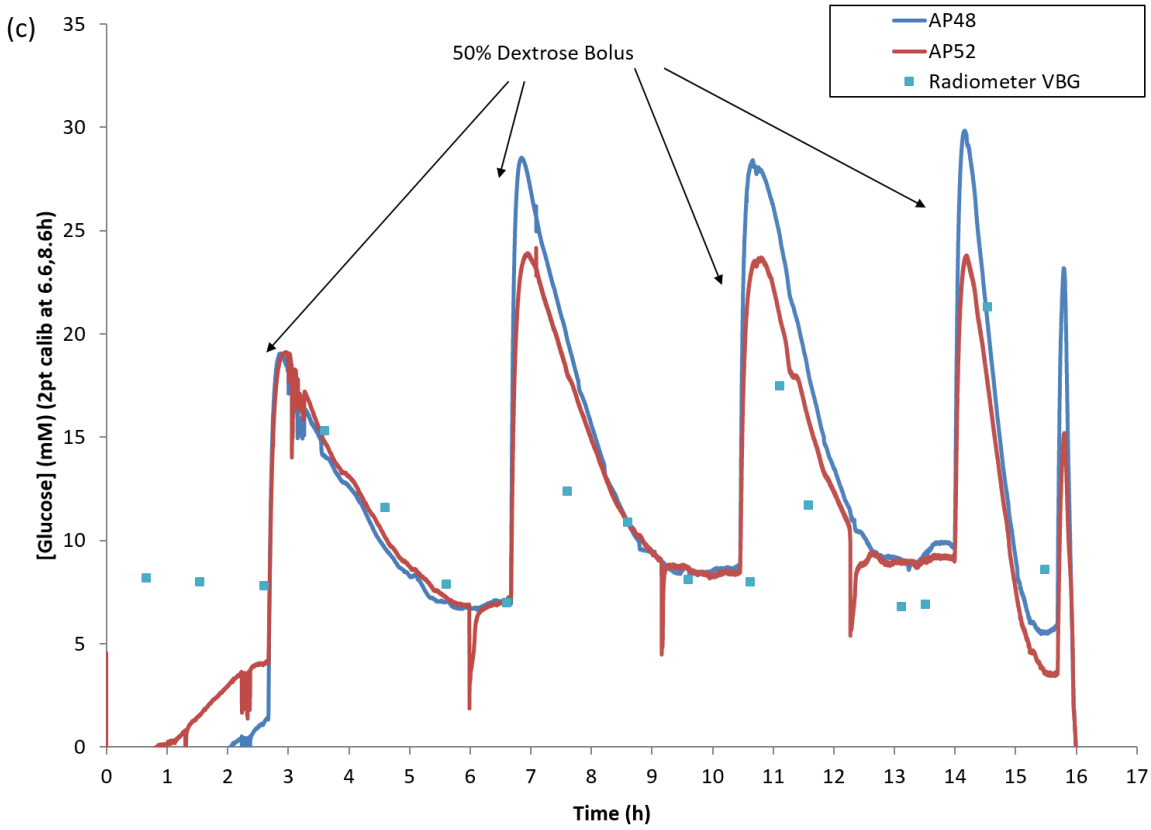

Figure 4.6(a-c). *In vivo* intravenous glucose measurement time-traces from two NO releasing glucose sensors during porcine implantation and three methods of data interpretation: (a) pre-implantation serum calibration (see Fig. 4.5), (b) a 1-point calibration from a Radiometer blood glucose value taken at 2.6 h, and (c) a 2-point calibration from Radiometer blood glucose values taken at 6.8 and 8.6 h. The discrete hourly Radiometer analyzer glucose values are plotted as square markers.

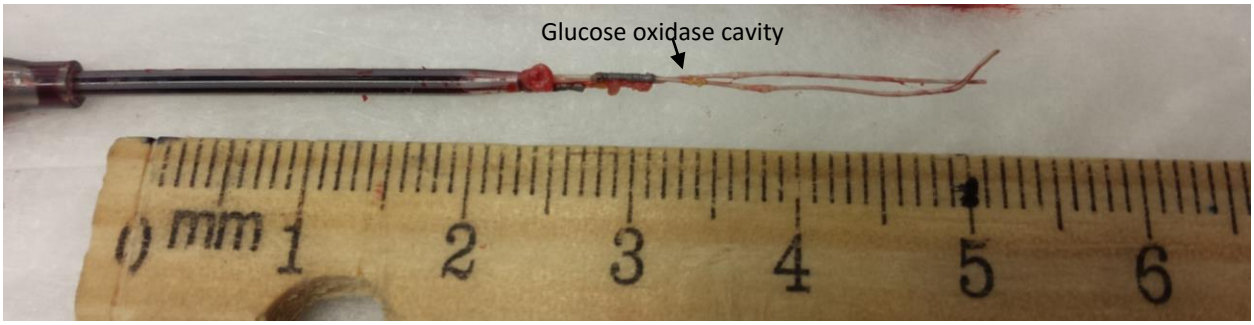

Figure 4.7. Explanted NO releasing glucose sensors from the *in vivo* porcine measurements taken in Figure 4.6. Minimal clotting is observed on the sensor surface, except where the close proximity placement of two sensors formed a "bridge clot".

During the 20 h of intravenous porcine blood glucose measurements (Fig. 4.6a-c), the NO releasing glucose sensors tracked the rising and falling patterns of the blood glucose levels as 50% dextrose bolus injections were administered. Blood glucose was allowed to stabilize (typically at 7-8 mM) before any dextrose was given. Unfortunately, the pig in this experiment died unexpectedly from low blood pressure before the 20 h duration was complete. The linear equation obtained from the calibration in serum (Fig 4.5b), which was used to convert the raw sensor current values into glucose concentrations in Figure 4.6a, did not yield accurate glucose values within an acceptable error of those measured discretely at hourly time points. The predicted glucose values based on the serum calibration have a large error in comparison to the Radiometer values, indicating that the slope and intercept of the sensor in the porcine vein are very different from those measured in serum. If the sensors cannot easily be calibration in serum prior to implantation, the next best model would be a one-point calibration from a Radiometer value early in the experiment. The Radiometer blood glucose value from 2.6 h into the experiment was used to convert the raw sensor current into glucose concentration values in Figure 4.5b. Converted glucose concentration values close to this one-point calibration point may have less error from the true glucose concentration values, but values at the end of the experiment have a greater degree of error. This could indicate drifting behavior in the sensor sensitivity during extended 20 h *in vivo* which is not observed *in vitro* or in the shorter 7 h *in vivo* rabbits.

Thus, a two-point calibration from discrete blood glucose values taken at the 6.1 h and 8.6 h time points provided the best conversion of raw sensor current values into accurate venous glucose concentrations in Figure 4.6c. Measurements early in the *in vivo* study are the most preferred to use for such an *in vivo* calibration approach, since this would allow the sensor to be calibrated

quickly after implantation, and hopefully this calibration would remain accurate for the remainder of the implantation period. Ideally, all discrete points should fit closely to the lines consisting of the continuous measurements within the bloodstream. However, experimentally, calibrations conducted from discrete blood measurements taken in between the 6-9 h time period after implantation yielded the most accurate blood glucose values from the sensor. The data from the sensor predicts glucose values higher than those measured by the Radiometer analyzer, especially in the final hours of the experiment. This could indicate drifting behavior of the sensors between the time the two-point calibrations were taken and the measurements at the end of the experiment. This behavior was not observed in the shorter rabbit experiments, and it was not possible to conduct longer-term implantation in anesthetized rabbits for durations longer than 7 h; therefore, it was not clear if this behavior arose from differences in physiology between rabbits and pigs, differences in anesthesia protocol/intravenous drugs administered specifically to the pig, or it was simply a function of the longer duration of the animal experiment. When the sensors were explanted from the pig vein, they were examined for surface clotting as observed in Figure 4.7, very little surface clotting was observed, likely a result from both small surface area and active NO release chemistry. Since these two sensors were placed in the same angiocatheter for implantation within the same vein, a small "bridge clot" developed between the two sensors with reduced blood flow between the sensors due to their close proximity.

Results from an additional *in vivo* experiment in a pig are shown in Figure 4.8. With a two-point calibration (from blood-gas measurements taken at 6.1 h and 9.0 h), the sensor tracks the increasing and decreasing blood glucose values during the modulations by dextrose injections. From hour 4.0 until 15.0, the values from the glucose sensor closely match the discrete *in vitro* Radiometer glucose concentrations, but somewhat higher glucose concentrations than expected

are observed from the implanted sensor during the final hours of implantation. Although the analytical performance of these NO release IV glucose sensors still require further efforts to improve analytical accuracy, these experiments are the first reported use of NO release intravenous glucose sensors for continuous *in vivo* measurement exceeding the previous 7 h time period in rabbits.

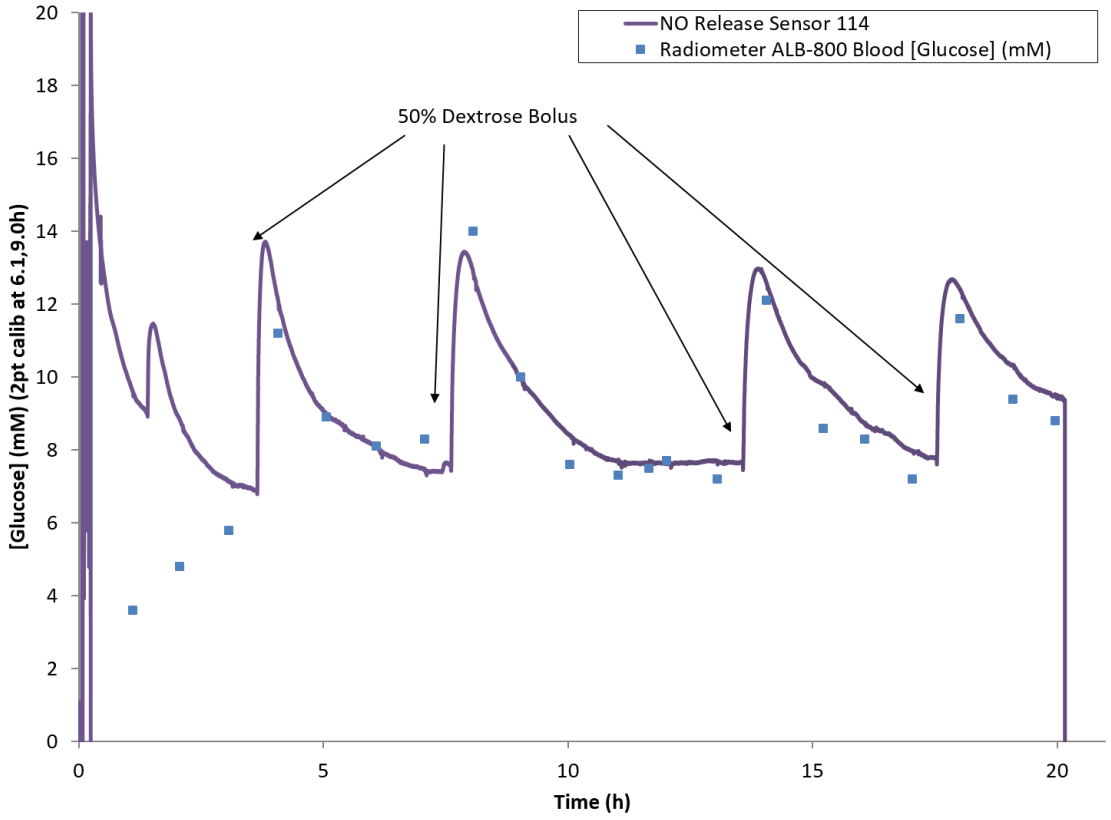

Figure 4.8. *In vivo* intravenous glucose measurement time-trace from an NO releasing glucose sensors during porcine implantation. A two-point calibration from the discrete bench-top blood-gas analyzer was used to convert raw current measurements from the sensor into blood glucose concentration values. The discrete hourly blood-gas analyzer glucose values are plotted as squares. The continuous measurements from the sensor best fit the discrete measurements from the Radiometer blood gas analyzer in the middle implantation, from 4-15 h.

Further *in vitro* studies (see Sections 4.3.3 and 4.3.4, below), were conducted to investigate changes in the calibration background (hemoglobin scavenging of NO), or if intravenous drugs

administered during the pig experiments could influence the glucose sensor sensitivity, that could account for this discrepancy in sensor behavior. In other words, it is important to understand what causes the large change in sensitivity of the NO release glucose sensors when they are implanted in pig blood vessels, which resulted in the need to wait 6-9 h periods to calibrate the sensors based on two separate *in vitro* blood glucose measurements.

4.3.3 Diffusion Cell Assessment of Membrane Potential and Glucose Sensor Surface Investigation with SEM

In an effort to determine if an additional potential develops across the outer membrane of the glucose sensor when in environments different than 0.1 M PBS (i.e., such a membrane potential could change the applied voltage to the Pt electrode, leading to decreased sensitivity to hydrogen peroxide), a series of diffusion cell experiments were designed. First, each side of the diffusion cell contained 0.1 M PBS and a reference electrode measured the open circuit potential (OCP) across the membrane (Fig. 4.9a). Separating the two cells was a membrane either of E2As Elast-Eon polyurethane, or a sandwich membrane composed of a layer of PLA/DBHD/N_2O_2 between two layers of E2As. Then the solution on one side would be replaced with bovine serum (Fig 4.9b) to see if a potential developed across the membrane. If a large potential was observed immediately, or developed over time, it could indicate that a membrane potential was causing only part of the +0.600V vs. Ag/AgCl potential to be correctly applied to the inner Pt electrode surface. A decreased applied potential would result in a smaller, possibly drifting, current response and reduced analytical accuracy.

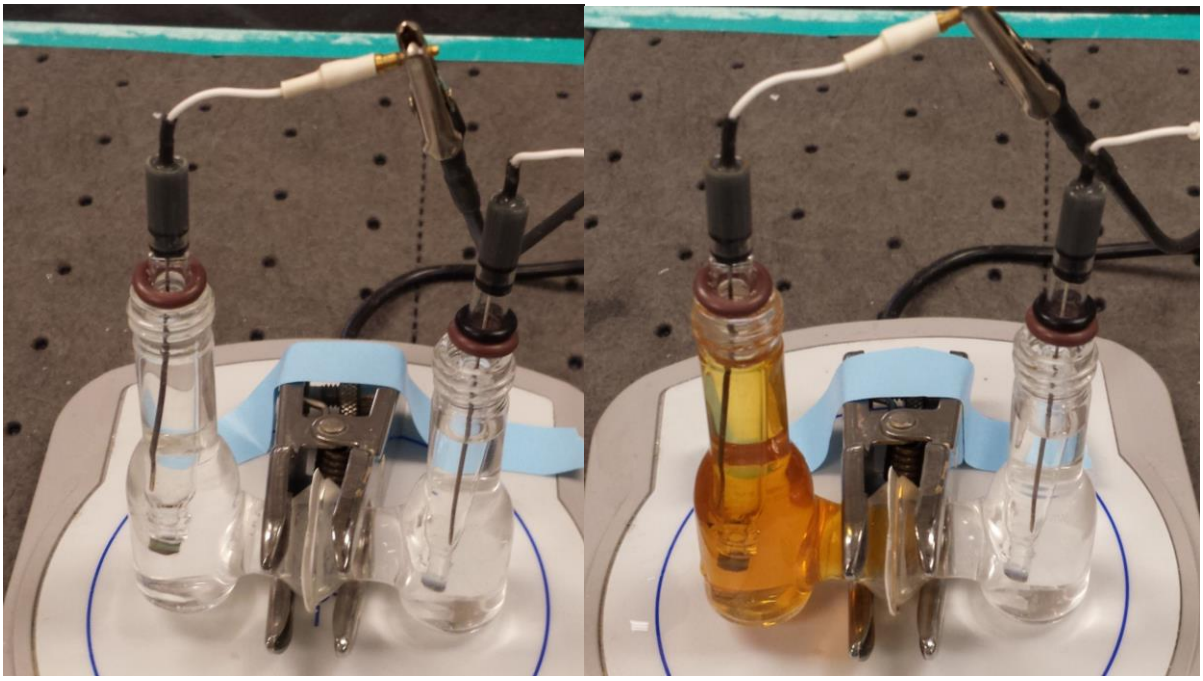

Figure 4.9. Diffusion cell experiment to detect a membrane potential developing across an E2As membrane In (a) both sides of the diffusion cell contain 0.1 M PBS and a commercial reference electrode In (b) the left side solution has been changed to bovine serum.

Figure 4.10 shows the difference in OCP between the two reference electrodes when the separating membrane is pure E2As. The difference between the initial and the new OCP was -0.95 mV after the addition of the bovine serum, indicating that E2As alone, as a homogeneous membrane did not give rise to a significant membrane potential when it came into contact with a serum solution.

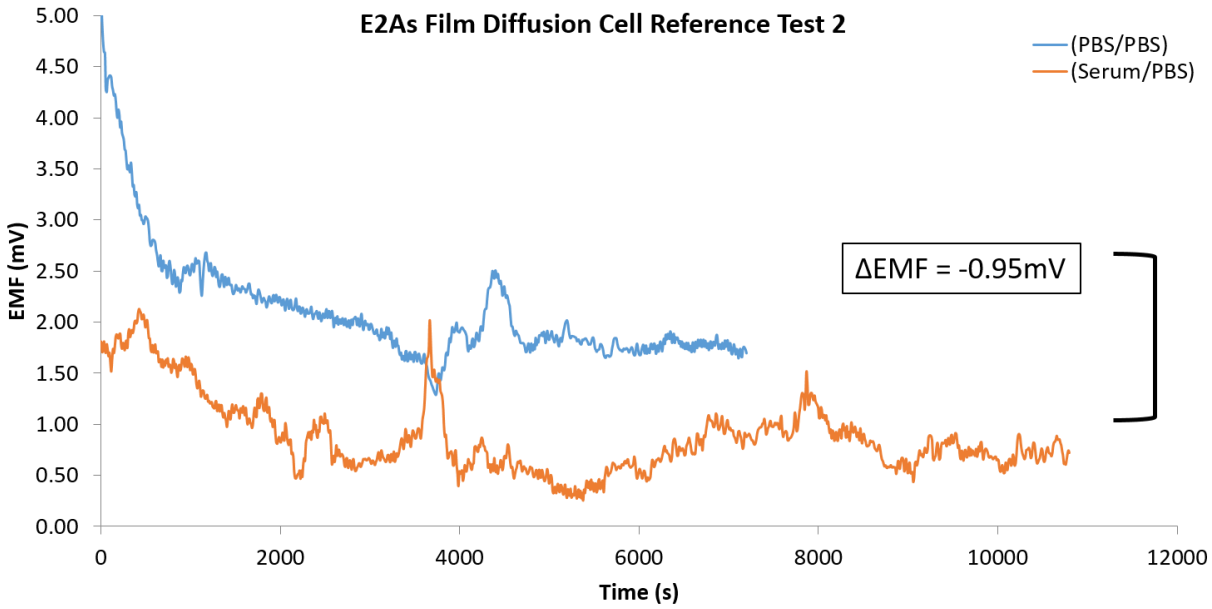

Figure 4.10. Open circuit potential difference between the two sides of the diffusion cell separated by a membrane of pure E2As when both sides have a symmetrical configuration with 0.1 M PBS filling solution versus the OCP measured when one side's solution was changed to bovine serum.

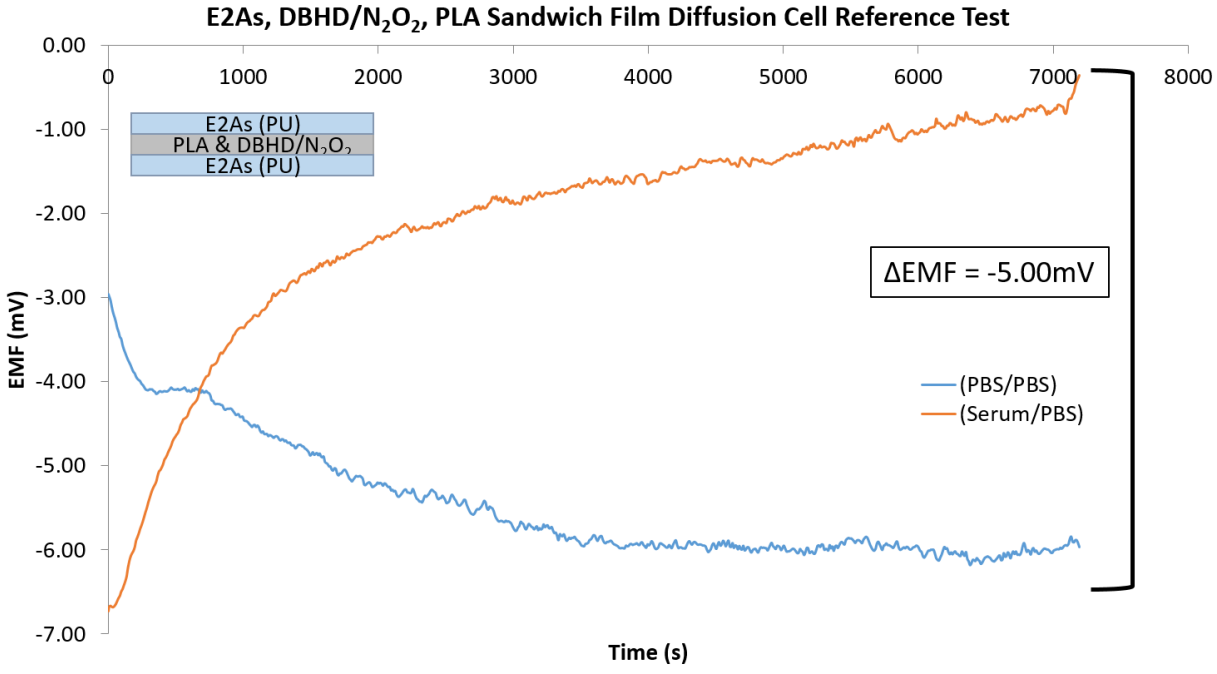

Figure 4.11. Open circuit potential difference between the sides of the diffusion cell separated by a sandwich membrane of PLA/DBHD/N_2O_2 between two layers of E2As when both sides have a symmetrical configuration with 0.1 M PBS filling solution versus the OCP measured when one side's solution was changed to bovine serum.

In Figure 4.11 it can be seen that a sandwich membrane, designed to better mimic the outer layers found on the glucose sensors gives rise to a largeer potential difference when one side of the diffusion cell is filled with bovine serum. A difference in open circuit potential of -5.0 mV, which develeoped from the switch from PBS to bovine serum is larger than one observed when using a homogeneous E2As membrane, but this small 5.0 mV decrease in applied potential would still not account for the magnitude of calibration drift observed in the *in vivo* experiments.

To investigate the bulk diffusion properties of the glucose sensors' outer layers that restrict glucose diffusion and thereby give the sensor linear response, another diffusion cell experiment was conducted. In this case, a functioning glucose sensor was placed into one side of the diffusion cell (containing 0.1 M PBS) and a 1.0 mL of 2.0 M glucose was injected into the PBS on the opposite side. A quick response from the sensor would indicate rapid diffusion, likely through larger diffusion channels or membrane pores. In contrast, a slow sensor response would instead indicate very small channels or pores. However, no significant response was recorded from the glucose sensor, even after measuring for >1 d, giving evidence to the hypothesis that small pinholes in the very thin membranes coating the glucose sensors are likely responsible for glucose diffusion restriction, providing the sensors with their linear response function to glucose over an extended concentration range.

A series of SEM images were taken of the exterior E2As surface as well cross-sectional images of the sensor to identify surface pinholes (Fig 4.12a) and the structure of the PLA/DBHD/N_2O_2 releasing layer (4.12b). Figure 4.12a highlights some of the small 1-μm size pinholes found in the E2As surfaces of glucose sensors. Pinholes of this size would account for restricted diffusion of glucose into the glucose oxidase layer, giving the sensors linear response. Distribution of these

pinholes over a given area could also help account for variations between individual sensors when they are assembled and fabricated by hand. The SEM in Figure 4.12b is one taken from a cross-section of an NO releasing glucose sensor. The outer E2As membrane is quite smooth, other than the presence of pinholes that link to the NO releasing layer below it, but the structure of the PLA/ DBHD/N_2O_2 layer has a porous nature. Given that the PLA/ DBHD/N_2O_2 layer is approximately 10x the thickness of the E2As layer, one can explain why glucose sensors with thick NO releasing layers (to maximize NO release duration) have longer response times (to achieve steady-state current values) than sensors fabricated with thinner NO releasing layers or outer layers of only E2As polyurethane.

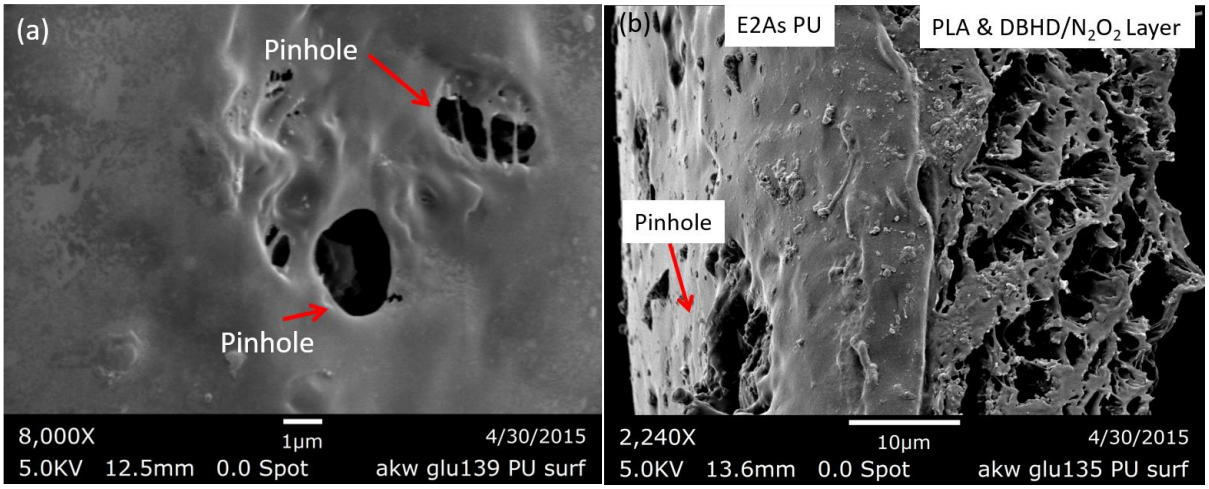

Figure 4.12. SEM images of glucose sensor outer layers showing (a) pinholes in the 5 µm thick E2As outermost top coat and (b) the porous structure of the PLA & DBHD/N_2O_2 layer responsible for NO release activity.

4.3.4 In Vitro Investigations of Intravenous Medications on Glucose Oxidase Activity

After observing experiments in which glucose sensors lost significant sensitivity over the course of the IV implantation in pigs, as evidenced by increasingly smaller response to similar bolus injections of Dextrose, a series of *in vitro* investigations were conducted to determine if

intravenous drugs given through the jugular vein access to maintain a state anesthesia or raise the pig's blood pressure were adversely affecting glucose oxidase activity of the sensors. For these experiments, glucose sensors were placed in 0.1 M PBS, a baseline was recorded, and the solution was brought to 10 mM glucose. Once a steady-state current was achieved for this concentration of glucose, several injections of the given intravenous drug were administered at a similar concentration to those given during the pig experiment. By conducting these tests at a 10 mM glucose concentration, while H_2O_2 was actively being produced by the immobilized glucose oxidase, a drug's potential inhibition of glucose oxidase activity or reaction with hydrogen peroxide should be rapidly observable. A second calibration with fresh PBS and two 5 mM glucose injections conducted immediately after was designed to reveal if non-recoverable damage had occurred to the glucose oxidase activity. Figure 4.13 a-d shows four such calibrations where four primary drugs (which typically were administered during the 20 h porcine *in vivo* studies): dopamine, vecuronium bromide, epinephrine, and heparin were injected into reaction cells containing functioning NO release glucose sensors. Since there was no observable drop in current after the injection of each of these drugs, it was concluded that all four had no significant effects on glucose oxidase activity and were thus not responsible for the decreased current response from *in vivo* sensors.

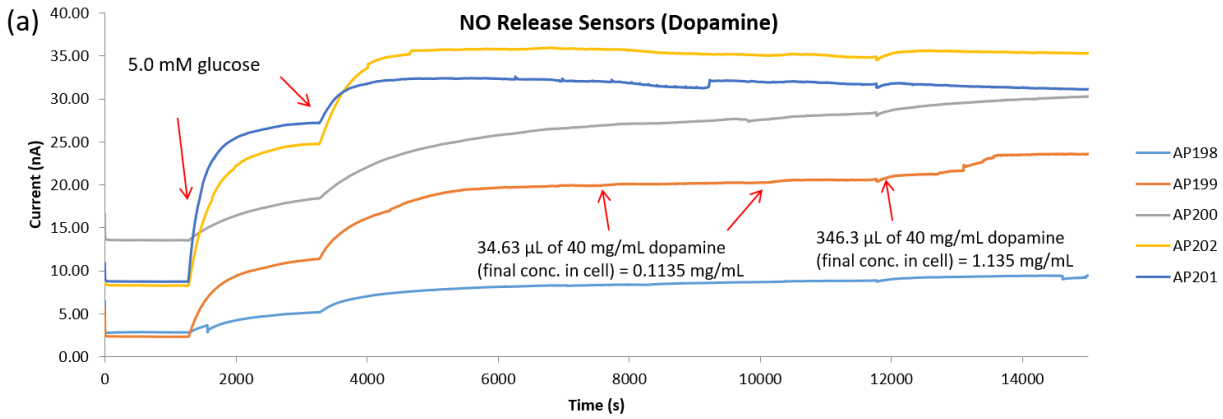
(a)
NO Release Sensors (Dopamine)
5.0 mM glucose
34.63 µL of 40 mg/mL dopamine
(final conc. in cell) = 0.1135 mg/mL
346.3 µL of 40 mg/mL dopamine
(final conc. in cell) = 1.135 mg/mL
Current (nA)
Time (s)
AP198
AP199
AP200
AP202
AP201

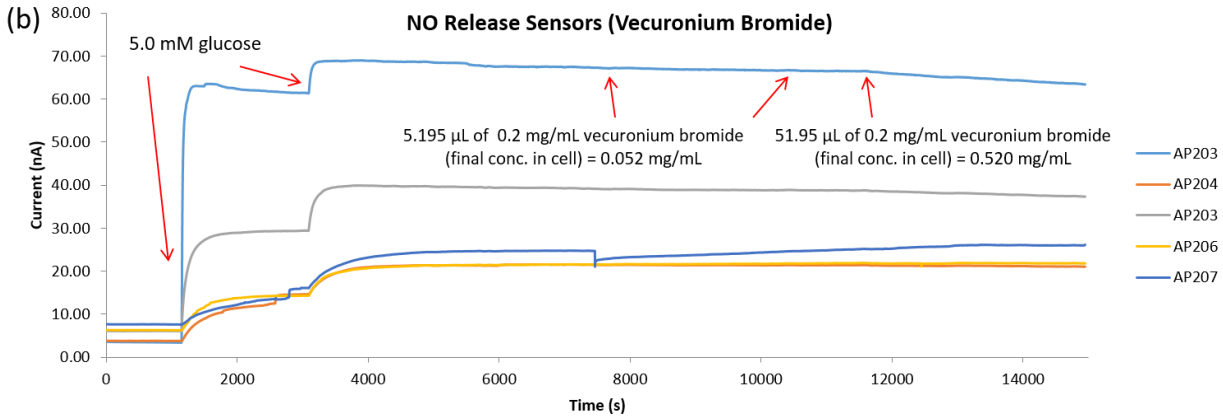
(b)
NO Release Sensors (Vecuronium Bromide)
5.0 mM glucose
5.195 µL of 0.2 mg/mL vecuronium bromide
(final conc. in cell) = 0.052 mg/mL
51.95 µL of 0.2 mg/mL vecuronium bromide
(final conc. in cell) = 0.520 mg/mL
Current (nA)
Time (s)
AP203
AP204
AP203
AP206
AP207

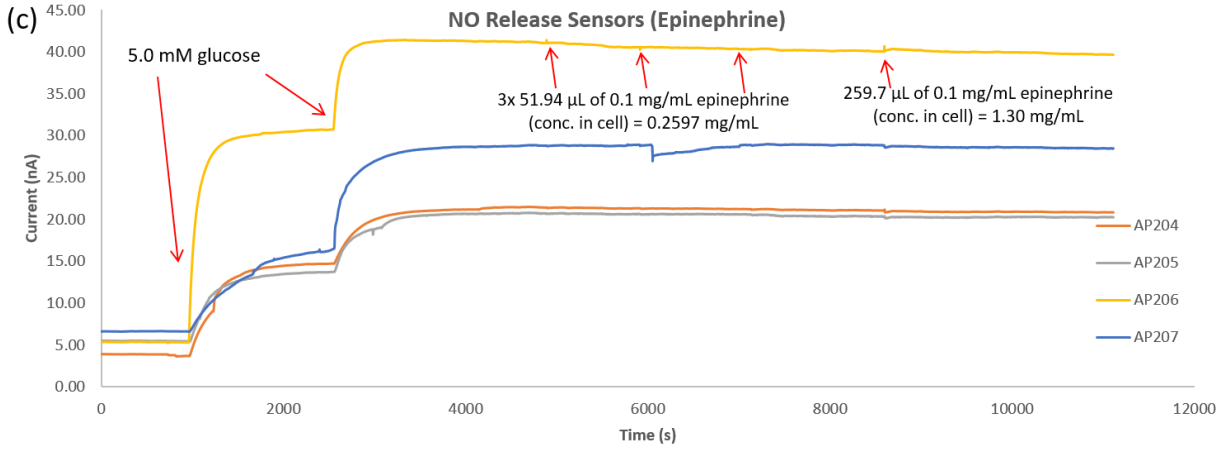
(c)
NO Release Sensors (Epinephrine)
5.0 mM glucose
3x 51.94 µL of 0.1 mg/mL epinephrine
(conc. in cell) = 0.2597 mg/mL
259.7 µL of 0.1 mg/mL epinephrine
(conc. in cell) = 1.30 mg/mL
Current (nA)
Time (s)
AP204
AP205
AP206
AP207

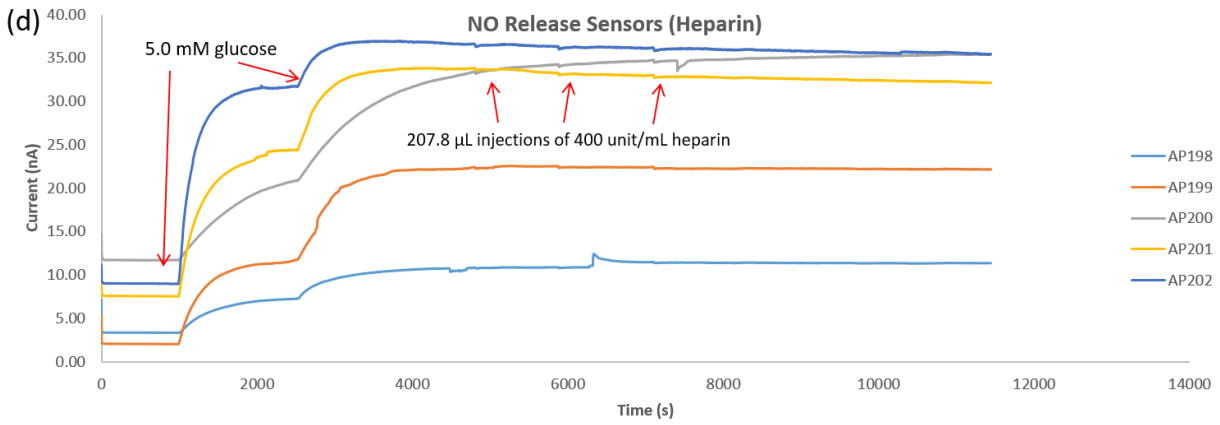

Figure 4.13. *In vitro* calibrations exploring the effects of intravenous drugs administered during the 20 h porcine experiments: (a) dopamine, (b) vecuronium bromide, (c) epinephrine, and (d) heparin on glucose oxidase activity of NO release glucose sensors.

Another possible explanation for discrepancies between glucose sensors in bovine serum and actual *in vivo* implantation is the possible NO scavenging by hemoglobin, since serum has the majority of hemoglobin-containing red blood cells removed. In a non-scavenging environment, excess NO produced from the PLA/DBHD/N_2O_2 layer can be oxidized at the platinum electrode surface at the operating potential of +0.600 V vs. Ag/AgCl, generating a nonzero background. If enough of this NO were potentially scavenged by hemoglobin, this would cause a reduced background signal, and therefore, a smaller than expected intercept for the linear calibration equation. A simple experiment designed to test this hypothesis is shown in Figure 4.14a-b. First, NO release sensors were fabricated without glucose oxidase, so that the source of the sensor background was due to NO oxidation alone. Then, oxyhemoglobin was produced from lyophilized hemoglobin and sodium dithionite in 0.1 M PBS while keeping the solution at 37.5°C to avoid current changes due to rapid changes in solution temperature. A UV Visible absorbance spectrum (Figure 14a) was used to calculate the concentration of oxyhemoglobin, and the 0.1 M PBS solution containing the sensors was replaced with the hemoglobin solution.

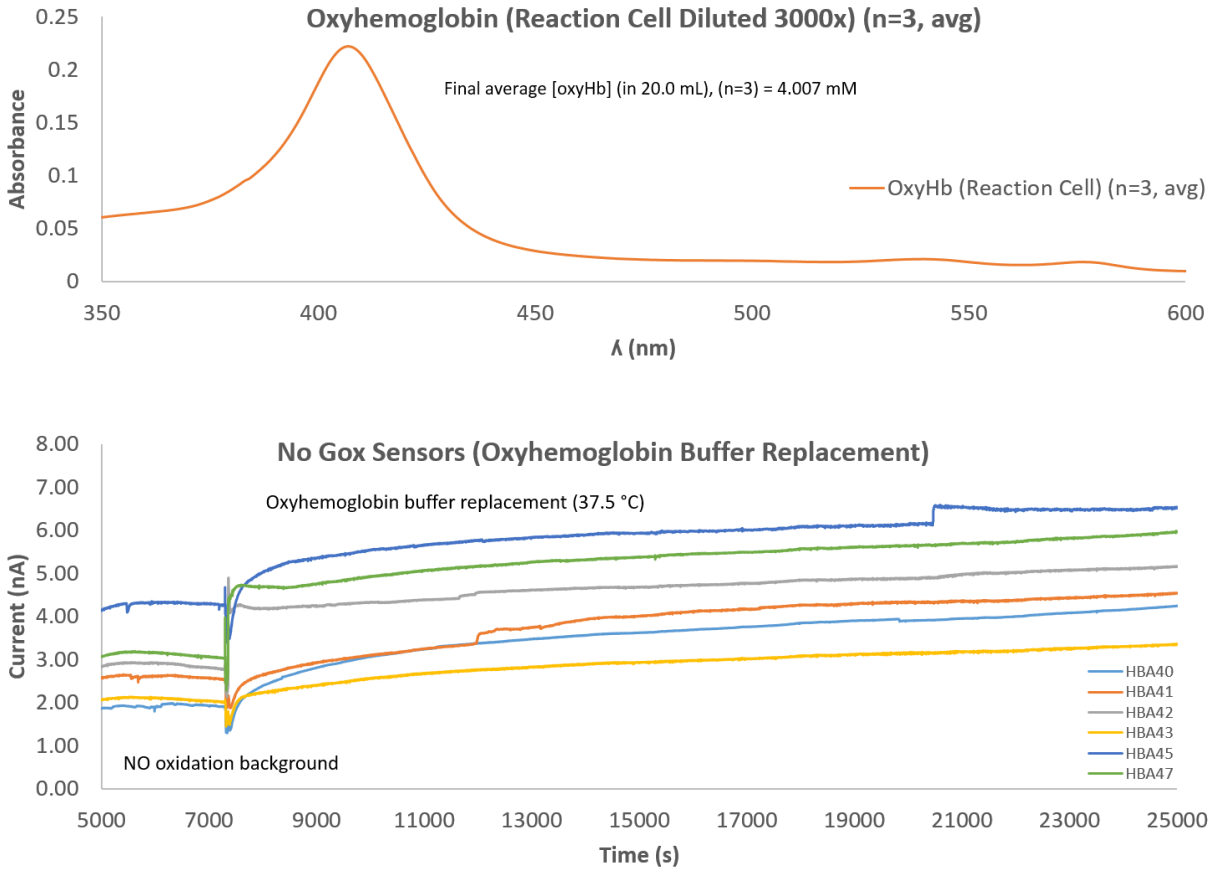

Figure 4.14. Effect of oxyhemoglobin on NO oxidation background. A solution of 4.01mM oxyhemoglobin in 0.1 M PBS was measured via UV-visible spectrometry (a) and was placed into a cell containing NO release sensors (with no glucose oxidase) to observe oxyhemoglobin effects on the background current generated from nitric oxide oxidation.

Although there was an initial decrease in current signal when the hemoglobin buffer first came into contact with the active sensors, the current response did not remain below the initial background NO oxidation baseline. Instead, a slow drift to a baseline potential higher than the initial background was observed. For most of these sensors, the total change was < 2 nA, which is a small Δi in comparison to changes in current from a glucose injection. This small current increase most likely occurred due to the presence of electroactive interference species in the lyophilized hemoglobin powder.

The original protocol for glucose sensor fabrication called for two hours set aside for crosslinking of the glucose oxidase enzyme (in BSA suspension) onto the sensor cavity with glutaraldehyde.[6] More recently, it was observed that by extending this crosslinking time overnight (> 10 h) improved the sensors long-term stability in *in vitro* bovine serum. Thus, a set of sensors fabricated with extended glutaraldehyde crosslinking time was evaluated for analytical performance in bovine serum. Following an overnight soak in serum of 8 h, the sensors were calibrated for glucose linearity ranging from the baseline serum glucose concentration of 6.6 mM to 21.2 mM via sequential injections of 2.0 M glucose in PBS. Additional bovine serum that was not spiked with additional glucose was used to dilute the serum and modulate the glucose concentration to lower levels. First 5.0 mL, then 10.0 mL, and finally 20.0 mL of unspiked serum were used for these dilutions. The sensor responses to these glucose concentration modulations are shown in Figure 4.15. There are variations in responses between individual sensors, but all sensors responded accordingly to the changes in glucose concentration. Previously, extended time glucose measurements in bovine serum proved problematic. Growth of aerobic bacteria would form a film or viscous layer within the serum sample, depleting the oxygen and either increasing the viscosity or causing the serum to partition into layers, resulting in glucose signal currents that rapidly declined. However addition of 30 mg of sodium azide to the bovine serum helped prevent bacterial growth and allow for much longer measurements in the same serum solution. For 8 h prior to and 47 h after the bovine serum calibrations, the sensors were placed into bovine serum with a constant concentration of 6.61 mM and 6.72 mM glucose, respectively. These experiments showcase the stability of the sensor's steady-state current over an extended period of measurement (Figure 4.15 a-b).

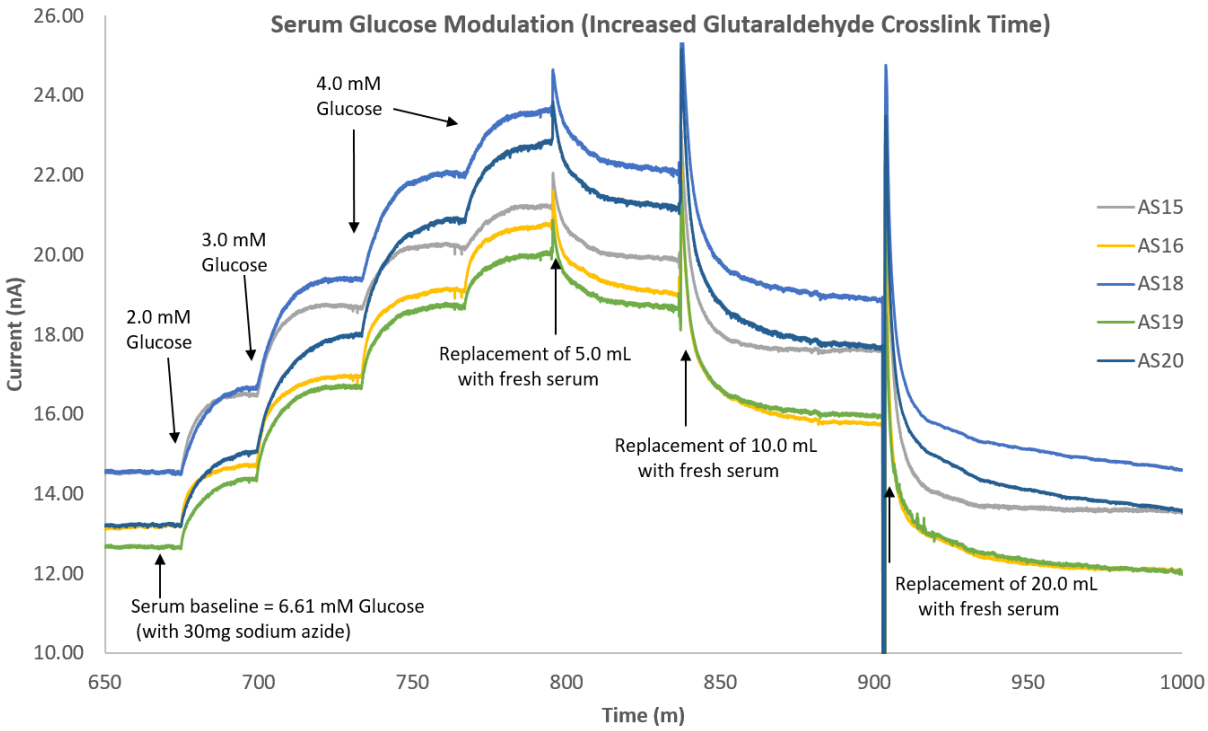

Figure 4.15. *In vitro* assessment of NO release glucose sensors (with extended glutaraldehyde crosslinking time) response to increasing and decreasing glucose concentrations in bovine serum through injections of glucose stock solution and dilutions of stock glucose, respectively.

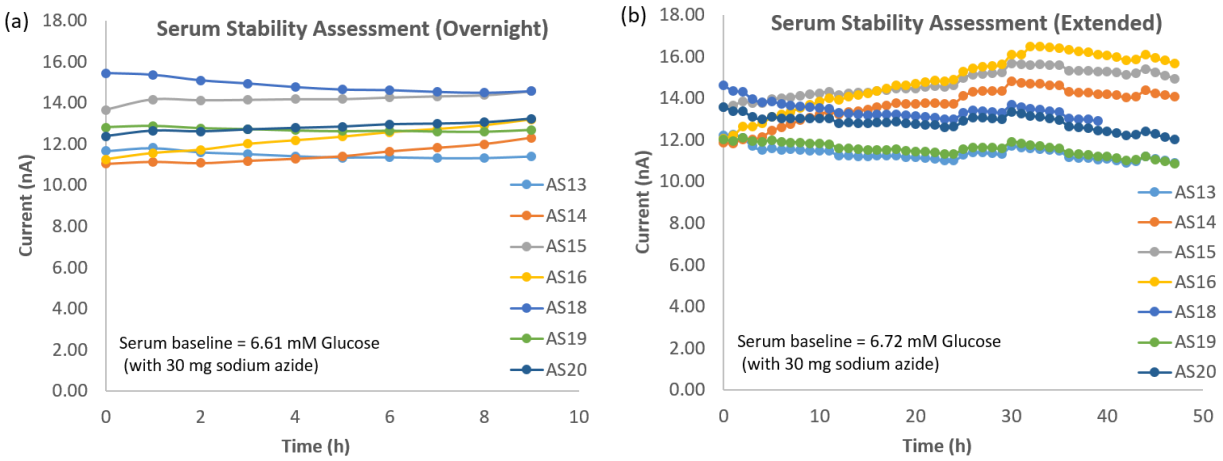

Figure 4.16. *In vitro* bovine serum measurements of glucose steady-state response current for extended durations. (a) represents an 8 h overnight serum signal stability assessment taken prior to the glucose modulations in Figure 4.15. (b) represents an extended multi-day serum signal stability assessment conducted immediately following the calibrations in Figure 4.15.

From these results, future NO release glucose sensors intended for evaluating *in vivo* analytical performance should adopt the extended glutaraldehyde crosslinking time. Use of sodium azide should allow more reliable calibrations in bovine serum, especially those lasting longer than several hours.

4.4 Conclusions and Future Directions

In summary, the incorporation of E2As Elast-Eon as an outer coating and ester-capped PLA as a layer containing the NO release diazeniumdiolate species appears to provide an ideal combination coating to create improved intravascular electrochemical glucose sensors. The use of E2As material serves a critical role by maintaining linear response to venous blood glucose concentrations up to 20.0 mM through its restriction of glucose diffusion to the glucose oxidase layer. The PLA serves to maintain a local acidic environment within the layer containing diazeniumdiolated DBHD, so that NO release is prolonged. The resulting NO release profile is sufficient to allow the continuous monitoring electrochemical glucose sensors to mimic the behavior of endothelial cells, granting them resistance to surface clot formation. This thromboresistance is integral to preserve *in vivo* analytical performance and functionality. The accuracy of NO-releasing glucose sensors was assessed by implantation within rabbit veins. Modulation of the animal's venous blood glucose with dextrose bolus infusions can be used to help determine glucose sensor response time. Control sensors quickly developed surface clots that increase sensor response time and decrease their measurement accuracy. Nitric oxide release functionality helps prevent surface clot formation, which preserves fast sensor response times and accuracy in measuring glucose concentrations when results are compared with whole blood analyzer values obtained with discrete blood samples drawn from the animal. In this preliminary

study, optimizing the NO release formulation and outer glucose restriction layer used to fabricate these devices has yielded improved *in vivo* performance.

This chapter reports the first use of NO release intravenous glucose sensors for extended *in vivo* porcine studies using the 20 h porcine model, exceeding the previous 7-h threshold of the rabbit model. Although additional future optimization is needed to improve the analytical accuracy of these sensors to the level of those found for the 7 h rabbit experiment, it can be concluded that the NO release chemistry still serves to enhance the thromboresistance of blood contacting sensor surfaces. The two point calibration yielded the most accurate conversion of the sensor's raw data to glucose values, but for future *in vivo* studies, it would be more ideal to use a one-point calibration, taken early in the experiment. Additional *in vitro* experiments were conducted to identify and rule out potential sources of drift and measurement inaccuracy in the porcine model, but no clear root cause could be identified for the more significant sensor calibration drift in these experiments.

Evaluation of membrane potentials developing across the polymers composing the outer layers of the glucose sensors revealed a negligible potential differential from only the E2As polyurethane, when in contact with bovine serum and a slight negative potential arising from a combination E2As and PLA/DBHD/N_2O_2 membrane. Neither source likely contributes significant shifts in applied potential to the inner Pt working electrode of the sensors. A bulk glucose diffusion test hinted that thick polyurethane membranes do not readily allow transit of glucose; instead, tiny pinholes in the thin layers of these polyurethanes used to coat glucose sensors are more likely responsible for glucose diffusion restriction and linear calibration behavior. This hypothesis was confirmed through SEM imaging of the glucose sensor surface.

Extensive investigations to examine the effects of four key intravenous medications given during an *in vivo* porcine protocol on glucose oxidase activity revealed that dopamine, vercuronium bromide, epinephrine, and heparin do not cause any temporary or permanent inhibition of glucose sensor function. Similarly, introduction of a large concentration of hemoglobin, which acts as a rapid NO scavenger in whole blood, did not scavenge enough local NO in the vicinity of the Pt electrode cavity of the glucose sensors to significantly reduce the NO oxidation background signal.

Following *in vitro* tests hinting that increased time allotted for the crosslinking reaction of glutaraldehyde yielded sensors with increased stability in bovine serum, a series of extended steady-state stability tests and glucose calibrations were conducted on sensors allowed to crosslink overnight, nearly 5x the time originally reported. It is suspected that this additional crosslinking time offers additional resistance of the immobilized glucose oxidase enzyme to damaging substrates or inhibiting molecules encountered in whole blood. The sensors fabricated with the revised crosslinking protocol showed long-term stability at a constant serum glucose concentration as well as continuous time trace measurements that followed rising and falling serum glucose concentrations. Additional NO release glucose sensors fabricated from the designs presented herein, especially those undergoing *in vivo* testing, should capitalize on the benefits provided by an increased crosslinking period.

For future *in vivo* experiments, it is expected that both the thromboresistance and improved analytical measurement accuracy will be observed with additional sensors utilizing diazeniumdiolate-based NO release, E2As polyurethane outer membranes, annealed Nafion, and extended glutaraldehyde crosslinking as novel design elements.

4.5 Literature Cited

(1) Boyne, M. S.; Silver, D. M.; Kaplan, J.; Saudek, C. D. *Diabetes* **2003**, *52*, 2790.
(2) Wisniewski, N.; Reichert, M. *Colloids Surf B Biointerfaces* **2000**, *18*, 197.
(3) Frost, M.; Meyerhoff, M. E. *Anal Chem* **2006**, *78*, 7370.
(4) Vaughn, M. W.; Kuo, L.; Liao, J. C. *Am J Physiol-Heart C* **1998**, *274*, H2163.
(5) Batchelor, M. M.; Reoma, S. L.; Fleser, P. S.; Nuthakki, V. K.; Callahan, R. E.; Shanley, C. J.; Politis, J. K.; Elmore, J.; Merz, S. I.; Meyerhoff, M. E. *J Med Chem* **2003**, *46*, 5153.
(6) Yan, Q. Y.; Major, T. C.; Bartlett, R. H.; Meyerhoff, M. E. *Biosens Bioelectron* **2011**, *26*, 4276.
(7) Yan, Q. Y.; Peng, B.; Su, G.; Cohan, B. E.; Major, T. C.; Meyerhoff, M. E. *Anal Chem* **2011**, *83*, 8341.
(8) Bindra, D. S.; Zhang, Y. N.; Wilson, G. S.; Sternberg, R.; Thevenot, D. R.; Moatti, D.; Reach, G. *Anal Chem* **1991**, *63*, 1692.
(9) Geise, R. J.; Adams, J. M.; Barone, N. J.; Yacynych, A. M. *Biosens Bioelectron* **1991**, *6*, 151.
(10) Brisbois, E. J.; Handa, H.; Major, T. C.; Bartlett, R. H.; Meyerhoff, M. E. *Biomaterials* **2013**, *34*, 6957.
(11) Cozzens, D.; Luk, A.; Ojha, U.; Ruths, M.; Faust, R. *Langmuir* **2011**, *27*, 14160.
(12) Simmons, A.; Padsalgikar, A. D.; Ferris, L. M.; Poole-Warren, L. A. *Biomaterials* **2008**, *29*, 2987.
(13) Yan, Q. Doctor of Philosophy Dissertation (Chemistry), University of Michigan, 2011.

CHAPTER 5

TOWARD ENHANCING THE BIOCOMPATABILITY OF COMMERCIAL INTRAVENOUS INTERMITENTLY MONITORING GLUCOSE SENSORS VIA TRANSIENT NITRIC OXIDE RELEASE

5.1 Introduction

At present, no commercial product exists in the United States market (having attained FDA approval) for real-time measurement of blood glucose levels for the intended use of tight glycemic control. The GlucoClear Peripheral IV Sensor (Fig. 5.1), developed by Edwards Lifesciences, is a device that measures blood glucose intermittently, by drawing a small volume of intravenous blood back over the sensor every 5 min through a 20 gauge IV catheter[1-3]. When the device is not undergoing blood sampling or blood glucose measurement mode, a pump continually flushes the line with a glucose calibrating solution. The glucose sensor component used within the system is based on a commercially-licensed Dexcom glucose sensor,[4,5] designed to function for up to 72 h. By using Flavin Adenine Nucleotide (FAD) as a co-enzyme for the immobilized glucose oxidase and a multilayer hydrogel membrane, the sensor gains selectivity over potential interference species, while providing a the sensor linear behavior and glucose diffusion restriction through a polyurethane insulating layer. The sampling line catheter contains two adjacent sensing electrodes, one with the enzyme, and the second without, to create an internal measurement reference and further ensure the selectivity of the observed current response. However, without

added thromboresistance functionality, the blood contacting portion of the device can develop clots, preventing accurate glucose measurement. In this product, available on the European commercial glucose sensor market, addition of heparin to the continuously-flushing/calibrating solution helps prevent blood clotting for the duration of the device lifetime; however, use of a nearly continuous heparin infusion has hindered FDA-approval for US markets, owing to the potential bleeding risks of infusing even low doses of heparin into intensive care unit patients.

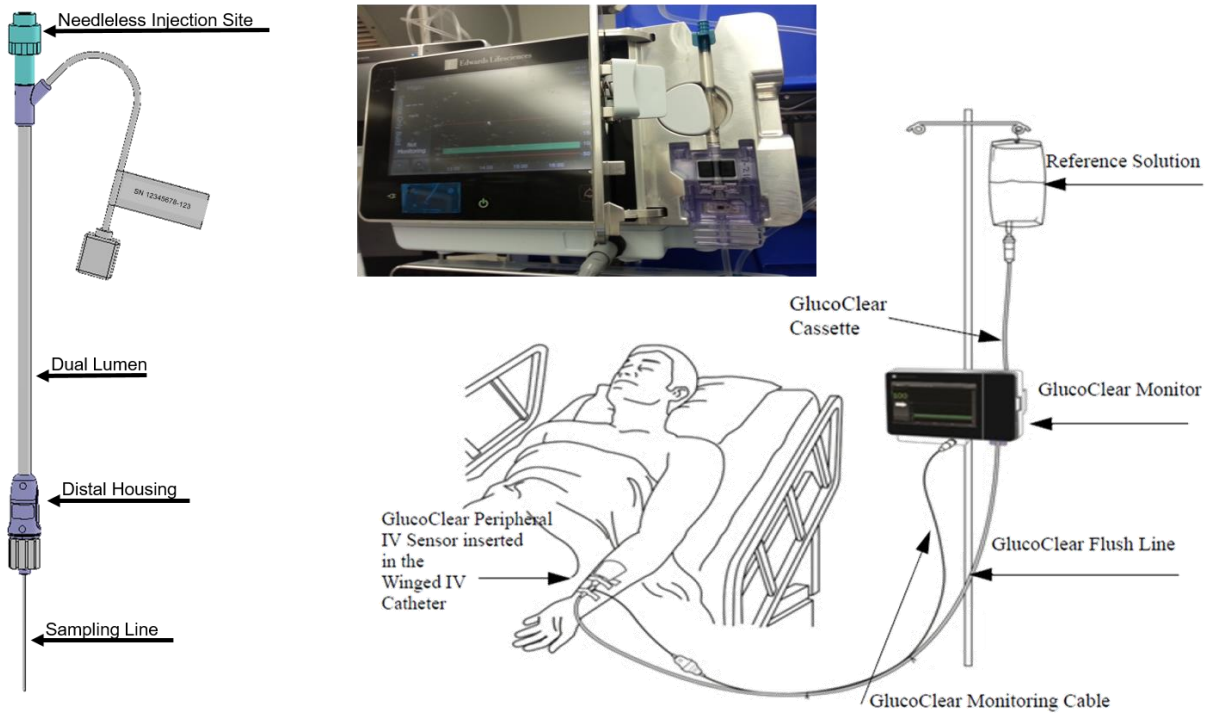

Figure 5.1. The Edwards Lifesciences GlucoClear System, featuring: the sensor housing (left) containing the intravenous sampling line with dual-electrode configuration, the solution pump and monitor (top right), and the entire system (bottom right).[1-3]

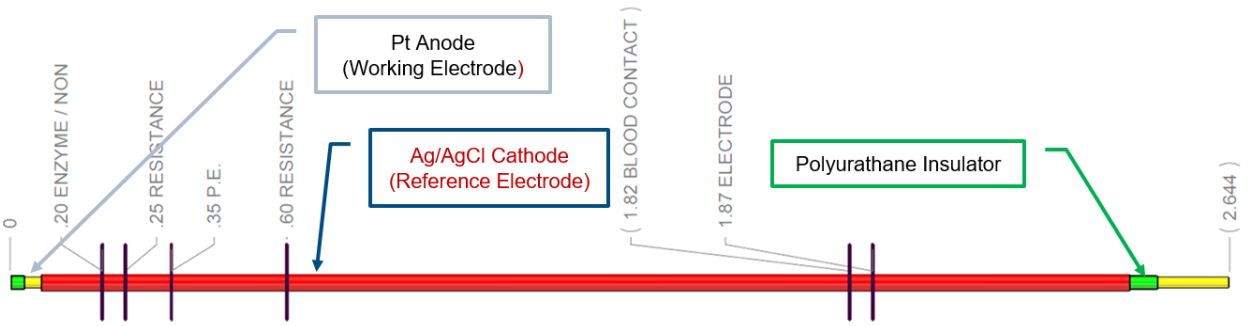

Figure 5.2. A diagram of the Edwards glucose sensors. Each sampling line contains two of these sensors, one with an enzyme layer, and one without enzyme (to serve as an internal reference).

A research engineer from Edwards approached our laboratory with the idea of a collaboration project that would combine nitric oxide (NO) release chemistry with the GlucoClear system as an alternative method of imparting thromboresistance to the sensor. If this could be accomplished, it would obviate the need to add heparin into the calibrating/flush solution. *S*-Nitroso-*N*-acetylpenicillamine (SNAP), an *S*-nitrosothiol, has been previously reported to provide stable NO release in an E2As polyurethane.[6-8] Active NO release incorporated into blood contacting polymer surfaces functions to mimic the endogenous NO flux of 0.5×10^{-10} mol cm^{-2} min^{-1} by endothelial cells lining all blood vessels, which helps in preventing platelet activation.[9] By incorporating SNAP-based NO release into the catheter tubing of the sample line of the Edwards system, clot formation on the catheter surface could be reduced or prevented without a need for heparin infusion. An even higher priority is preventing clot formation on the sensor surface. Based on the design of GlucoClear system, the sensor spends the majority of the time in contact with the calibrating solution, which makes it unique from the other continuously-monitoring intravenous sensors discussed in Chapter 4 of this dissertation. Since this solution will not scavenge NO immediately, as is the case whole blood, NO should be able to diffuse from the catheter wall source, through the aqueous calibrating solution (since no hemoglobin will be in this region after the flush with the calibrating solution), and partition into the thin polyurethane coating on the

sensors during the calibration phase. When the device undergoes the blood draw phase, this transient NO accumulated within the polyurethane layer of the sensor should be able to provide temporary NO release from the sensor surface, and therefore impart some thromboresistance. The goal of this preliminary study was to assess whether creating a NO release catheter into which the GlucoClear sensors are placed, could provide a level of NO release to the surface of the sensors.

5.2 Experimental

5.2.1 Materials

Individual glucose sensors, pellethane tubing, and sensor housings were a generous gift from Edwards Lifesciences. *N*-Acetyl-DL-penicillamine, tetrahydrofuran, iron(III) chloride ($FeCl_3$), and ethylenediaminetetraacetic acid were obtained from Sigma-Aldrich (St. Louis, MO). Sodium phosphate dibasic heptahydrate ($Na_2HPO_4 \cdot 7H_2O$), sodium phosphate monobasic monohydrate ($NaH_2PO_4 \cdot H_2O$) were purchased from Amresco, Inc. (Solon, OH). Sodium chloride (NaCl) is a product of Research Products International Corp. (Mt. Prospect, IL). Potassium chloride, sulfuric acid, methanol, and dichloromethane were from Fisher Scientific (Pittsburgh, PA). Teflon-coated silver wires were products of A-M Systems (Sequim, WA). Standard silicone tubing, composed of Dow Corning Silastic pharmaceutical/biomedical grade, with platinum-cured silicone, was produced by HelixMark Medical, LLC (Carpinteria, CA) and purchased through VWR International (Chicago, IL).

5.2.2 SNAP Synthesis

SNAP was synthesized using a modified version of a previously reported method.[6,7,10] Briefly, an equimolar ratio of NAP and sodium nitrite was added to a 1:1 mixture of water and methanol containing 2 M HCl and 2 M H_2SO_4. After 30 min of stirring, the reaction vessel was cooled in an ice bath to precipitate the green SNAP. These SNAP crystals were then dried and isolated with vacuum filtration and stored in a -20°C freezer until needed.

5.2.3 SNAP Loading of Sensor Housing Tubing

To load the synthesized SNAP into lengths of commercial tubing, the SNAP was first dissolved into a solvent or solvent mixture that was capable of both swelling the tubing as well as having a desired solubility for SNAP. In the case of the pellethane tubing originally used in the Edwards GlucoClear system[1], a 0.9/0.1 mixture of methanol:dicholomethane with 200 mg/mL SNAP served as the impregnation solution, since tetrahydrofuran (THF) dissolves pellethane. The tubing samples were soaked overnight, briefly rinsed with DI water, and then dried in a hood vacuum under a cardboard cover for 24 h.

Due to insufficient loading of the pellethane tubing, HelixMark silicone rubber tubing was suggested as an alternative housing/catheter tubing for the sensors. SNAP can be loaded into silicone rubber efficiently by using THF as a solvent[6-8]. Due to crosslinking in the silicone rubber structure, THF swells such tubing rather than dissolving the material due to the crosslinked structure of silicone rubber, and also has a high solubility for SNAP, making it the ideal solvent for loading silicone rubber. Again, 200 mg/mL SNAP in THF solutions were injected into glass swelling chambers containing tubing samples for the loading. Initially, the loading time was 24 h,

but given the small diameter and thickness of the tubing wall (1.65 mm o.d., 0.76 mm i.d., 0.445 mm wall thickness), loading time was reduced to 2 h for later experiments.

5.2.4 Nitric Oxide Release Measurements

Transients of nitric oxide released from these Edwards glucose sensors after they were placed in solution within the NO release tubing was monitored via chemiluminescence using a Sievers Nitric Oxide Analyzer (NOA) 280i (Boulder, CO). The source SNAP impregnated SR catheters were soaked in 0.1 M PBS, pH 7.4, containing 100 μM EDTA in a 37.5°C oven. The Edwards commercial glucose sensors were also soaked in 0.1 M PBS, pH 7.4 with 100 μM EDTA. One at a time, sensors were placed inside the SNAP-loaded tubing for a 5 min charging time, allowing NO to diffuse from the catheter surface to the polyurethane surface of the sensors and favorably partition into that layer. At the end of the charging period, they were placed into an amber glass NOA reaction cell containing 0.1 M PBS, pH 7.4 with 100 μM EDTA, and the NO released from sensors could be measured and recorded by the NOA as function of time. The data were converted from raw ppb gas phase concentration values to flux units (based on an approximation of the sensor surface area) to compare it to the 0.5×10^{-10} mol cm^{-2} min^{-1} minimum threshold for endogenous NO release from endothelial cells.[9] The NO release of the source catheter was also measured during the experiments.

The glucose sensing functionality of the commercial sensors was also assessed via calibrations using 4-channel BioStat potentiostats (ESA Biosiences Inc., Chelmsford, MA). The potential applied to the inner Pt wire was +0.600 V vs. Ag/AgCl reference in a 0.1 M phosphate buffered saline (PBS), pH 7.4, test solution at 37.5°C.

5.3 Results and Discussion

5.3.1 NO Release from Pellethane and Silicone Rubber Tubing

Pellethane tubing was first considered for SNAP-loading, given that it is the original material used in the Edwards GlucoClear system[1]. However, it became readily apparent from initial NO release measurements that only a very small amount of SNAP can be loaded into this tubing, perhaps due to a low solubility of SNAP within the polymer phase. In Figure 5.3, the flux from the pellethane source catheters begins below 0.5 flux units, and is exhausted 3 d after initial soaking in PBS. This plot served as evidence to consider an alternate polymer material for the catheters.

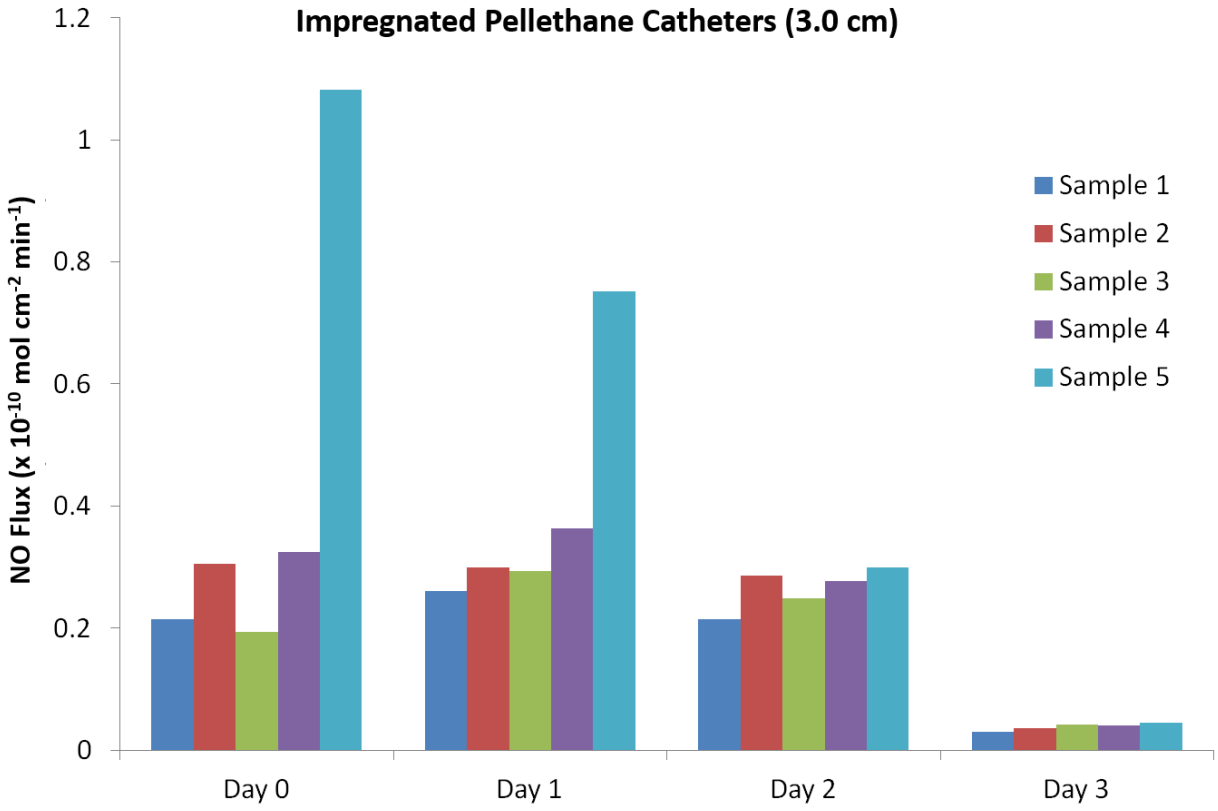

Figure 5.3. NOA measurement of NO release from SNAP-loaded pellethane tubing showing the need to use an alternate material or polymer for efficient SNAP loading and adequate levels of NO release.

SNAP loading of silicone rubber tubing yielded far better NO release properties. As shown in Figure 5.4, the silicone rubber HelixMark tubing shows NO release above 0.5 flux units for most of their 9 d NO release lifetime after initial soaking in PBS for 2 h. The ideal length of catheter needed for use with the Edwards system was 55 cm, so segments >55 cm were loaded with SNAP. Portions from different regions of the catheter were measured to ensure consistent loading throughout the catheter's entire length. An average NO flux for n=5 catheters is reported.

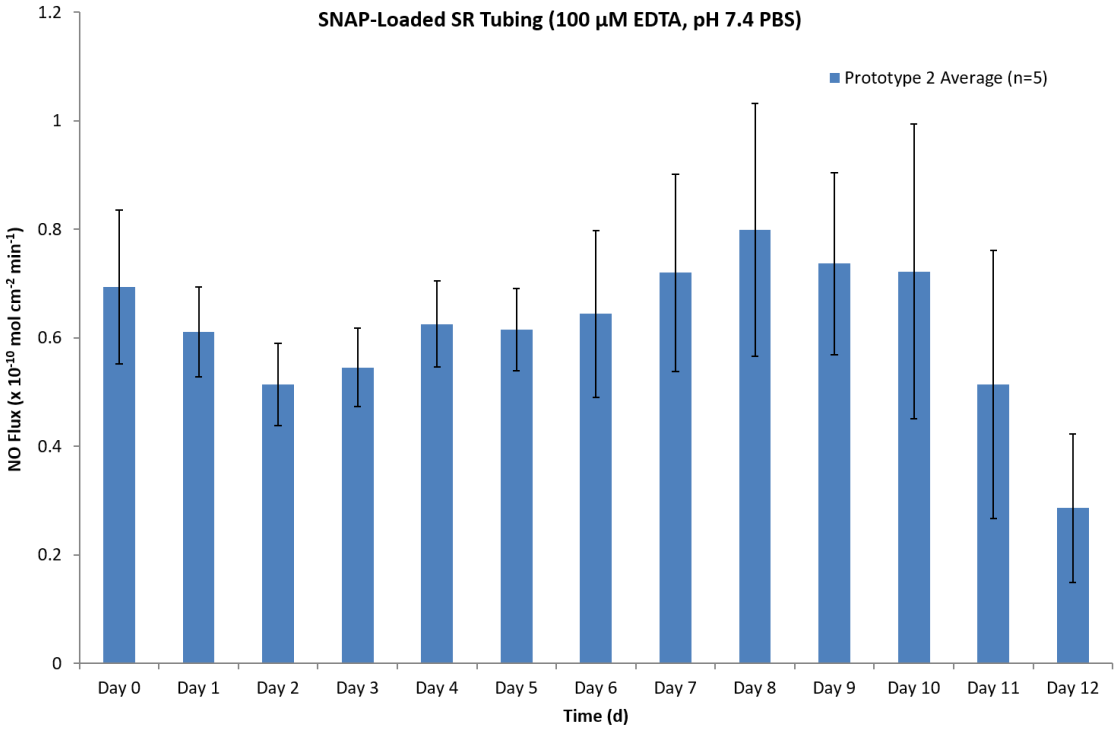

Figure 5.4. NOA cataloging of NO release from SNAP-loaded silicone rubber tubing when stored in 0.1 M PBS, pH 7.4, at 37.5 °C. Release remained at or above 0.5 flux until 9 d after initial buffer exposure.

5.3.2 Transient NO Charging of Glucose Sensors

Following the confirmation that SNAP-loaded silicone rubber tubing could be successfully manufactured into NO releasing tubing, it was possible to assess if an appreciable amount of NO could partition into the polyurethane layer of the Edwards sensors if they were placed within a SNAP-loaded SR tubing for 5 min charging time (in the presence of PBS buffer that filled the tubing). Figure 5.5a shows the transient NO release from Edwards commercial sensors after 5 min of charging within the source SNAP-loaded catheter. NO release lasts for 5-6 min at or above a flux of 0.5×10^{-10} mol cm^{-2} min^{-1} indicating that NO was successfully able to partition into Edwards sensor, likely the outer polyurethane layer. Figure 5.5b shows the NO release of the source SNAP-loaded SR catheter, at its baseline NO release, which was about 68 ppb or 1.0 flux units.

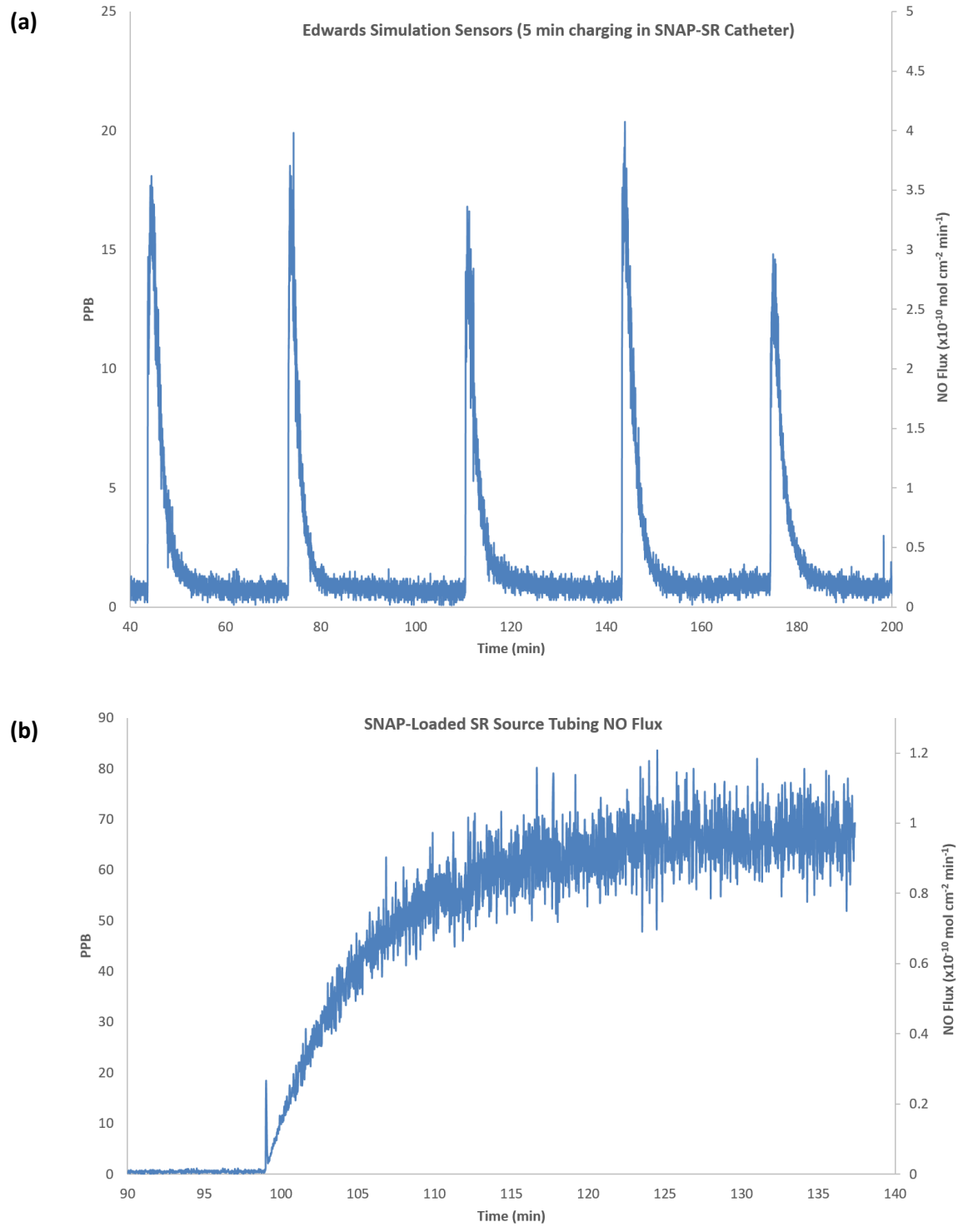

Figure 5.5. (a) Transient nitric oxide release from the surface of the Edwards commercial glucose sensors following 5 min soaking inside a SNAP-loaded silicone rubber catheter in 0.1 M PBS, pH 7.4, 37.5°C. (b) Nitric oxide release from the source SNAP-loaded SR catheter of 68 ppb, or around 1.0 flux units.

The efficiency of the transient NO charging appears to be a function of the NO release from the source catheter to a greater extent than the amount of time allow for charging. Since the polyurethane layer on the sensors is very thin, there should be a threshold of a maximum concentration of NO able to partition into the polyurethane layer based on the thickness of that layer, such that beyond a certain charging time, no additional transient NO could partition into the polyurethane layer no matter what duration the soaking/charging occurred. In Figure 5.6a, additional testing was conducted to examine NO charging of the Edwards sensors; however, the maximum NO release spikes did not match those of Fig. 5.5a though they still released transient NO at or above 0.5 flux for 5-8 minutes. However, as shown in Figure 5.6b, for these follow-up experiments, the source SNAP-loaded SR catheter had an NO release about one half that of the earlier test. Several repetitions of such studies were conducted, and the data behavior more often resembled that of Fig. 5.6a-b rather than Fig 5.5a-b. This could result from the efficiency of the SNAP loading of the source catheter. If the THF solvent used for loading was old and no longer anhydrous from exposure to air and water vapor for an extended amount of time, this could cause the swelling and SNAP partitioning into the silicone rubber to be less efficient, or cause the SNAP to begin decomposing to release NO prior to the actual loading process. It is also suspected that due to the thin wall thickness of the source catheter, beyond a certain time point, additional SNAP cannot be loaded.

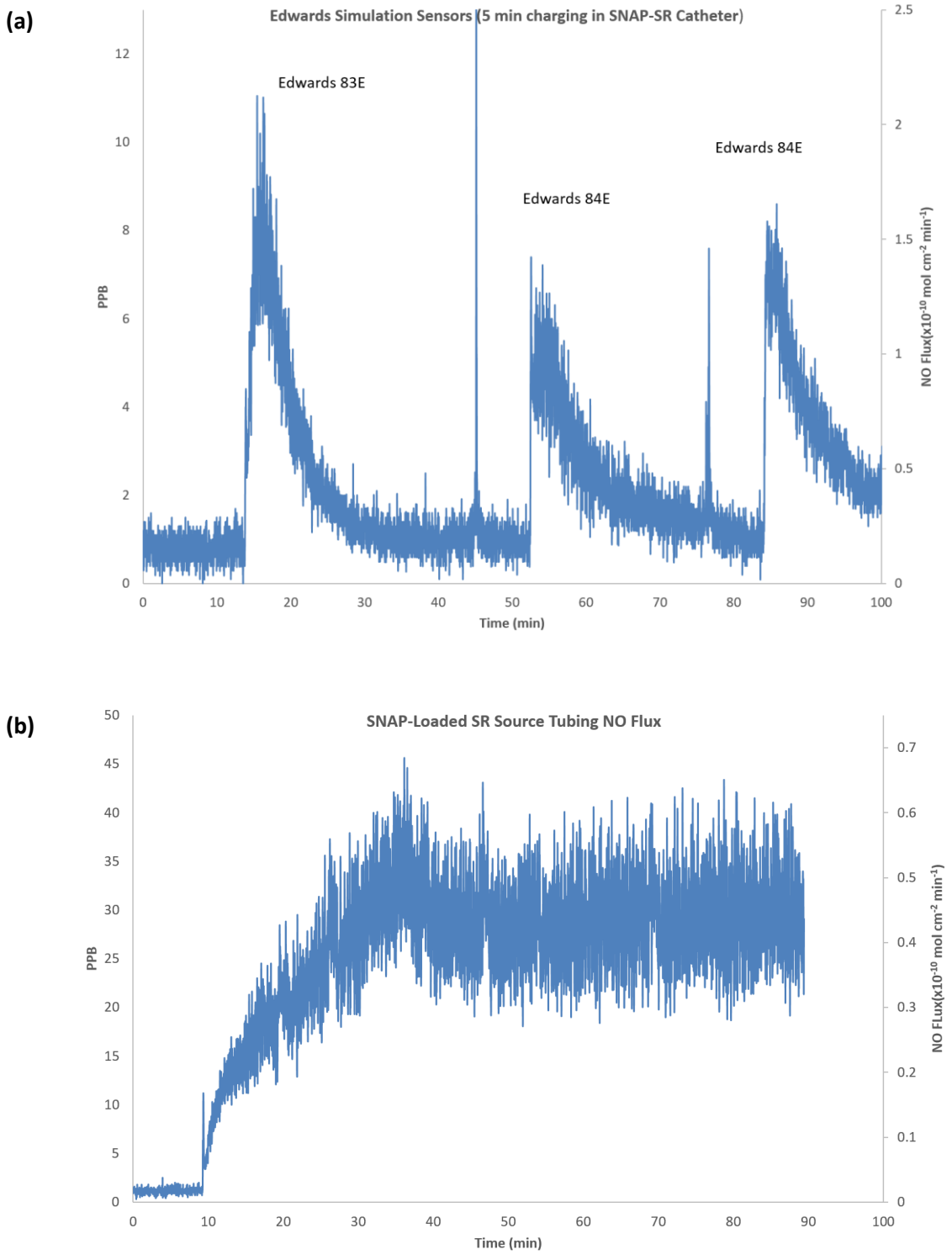

Figure 5.6. (a) Additional experiment showing transient NO release from the surface of the Edwards commercial glucose sensors following 5 min soaking inside a SNAP-loaded silicone rubber catheter in 0.1 M PBS, pH 7.4, 37.5°C. (b) Nitric oxide release from the source SNAP-loaded SR catheter of 30 ppb, or 0.45 flux units.

A simple model of NO diffusion was assembled as a collaboration with Hang Ren of the Meyerhoff lab using the COMSOL Multiphysics® modeling software. As observed in Figure 5.7 (a), the model represents the NO concentration gradient from the inner diameter of the SNAP-loaded source catheter to the outer polyurethane layer of the Edwards sensor. It assumes a charging time of 5 min, an NO diffusion coefficient (D) equal to 1.2×10^{-6} cm^2 s^{-1}, and a partition coefficient (K) for NO into polyurethane of 2.5. The concentration decreases slightly from 2.83 to 2.71 $\times 10^{-5}$ M from the inner surface of the source catheter to the polyurethane surface. An expanded view of the thin polyurethane layer can be seen in Figure 5.7b, and here the NO is able to build a higher concentration of 6.77×10^{-5} M than that present in the surrounding PBS solution, based on the favorable partitioning of NO into polyurethane. It can also be seen that the concentration gradient throughout the layer is consistent, although models assuming thicker polyurethane outer layers would likely have greater NO concentration in the area nearest to the surface. Without the presence of scavenging hemoglobin, it is certainly possible, based on this model, for transient NO to accumulate within the outer polyurethane surface of the glucose sensors, and to later be released back into solution. This would provide the sensors with some degree of thromboresistance when they are in direct contact with whole blood (as is the process in the Edwards GlucoClear system). However, by using silicone rubber tubing with a thicker wall and a similar inner diameter, it may be possible to boost the NO release of the source catheter to a higher level, and achieve a greater NO concentration within the polyurethane outer sensor layer and/or increase the duration of transient NO release from the sensor surface.

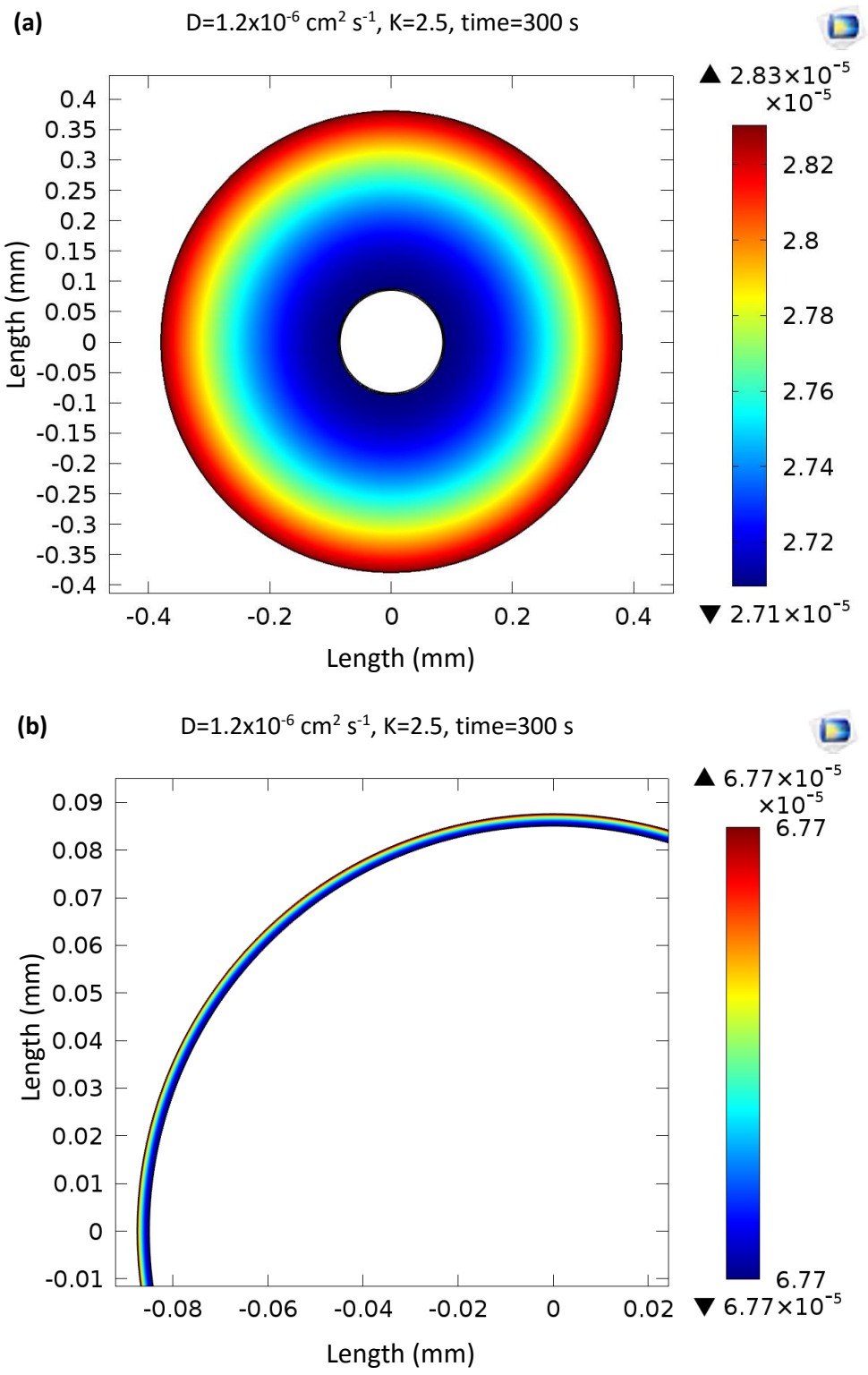

Figure 5.7. (a) Nitric oxide concentration gradient model from the inner surface of the SNAP-loaded source catheter to the polyurethane surface of the Edwards commercial glucose sensor. (b) Expanded NO concentration gradient model within that polyurethane surface of the Edwards commercial glucose sensor.

A second theoretical model illustrated in Figure 5.8a shows the NO concentration gradient assuming that the layer coating the glucose sensor was composed of silicone rubber, rather than polyurethane, but with the same charging time of 5 min. The concentration of NO again decreases from 2.79 to 2.67 x 10^{-5} M as one moves from the inner surface of the source catheter to the sensor surface. However, since the model for silicone rubber has a much more favorable partition coefficient (K) of 7, and an increased diffusion coefficient of 1.2 x10^{-6} cm^2 s^{-1}, the concentration within the sensor coating is around three times that of the polyurethane layer model, 1.87 x 10^{-4} M. Again, the layer is very thin, so the NO concentration within that silicone rubber layer is consistent throughout. One could make a prediction that if a polyurethane had silicone segments within its structure, like E2As,[11] perhaps more efficient transient NO accumulation could occur.

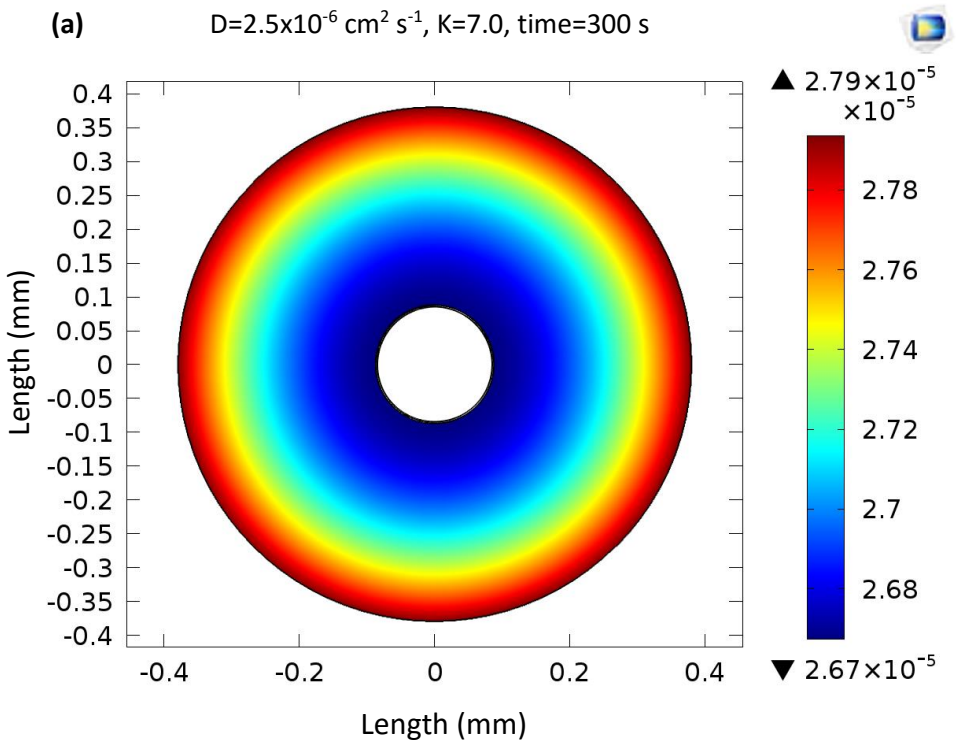

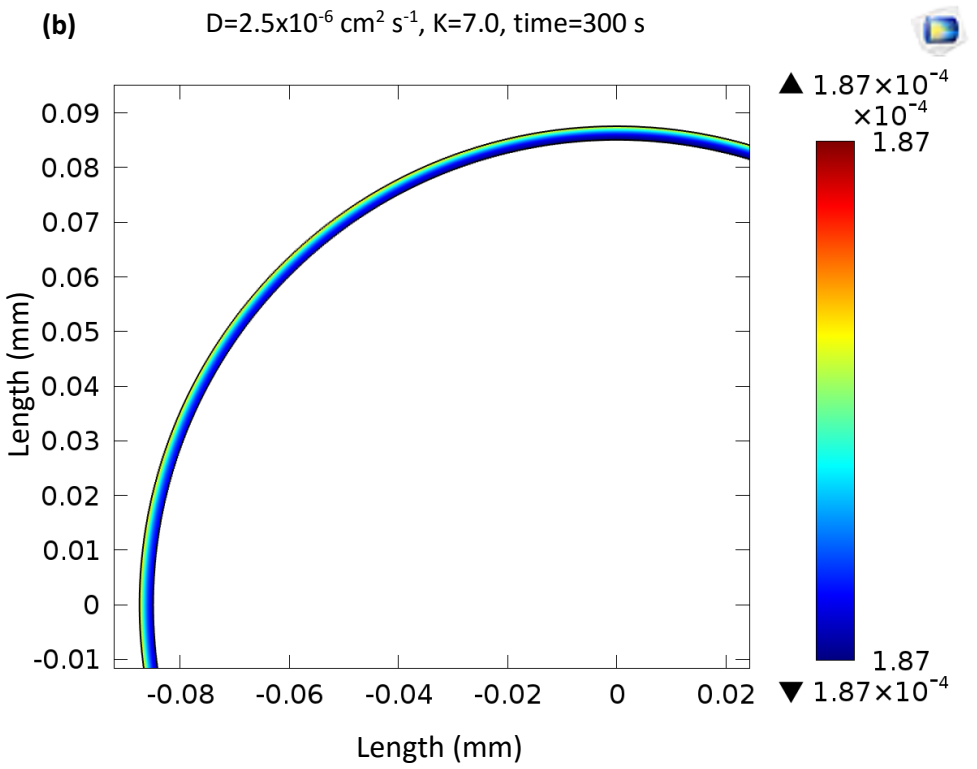

Figure 5.8. (a) Nitric oxide concentration gradient model from the inner surface of the SNAP-loaded source catheter to a theoretical silicone rubber surface the thickness of the Edwards commercial glucose sensor. (b) Expanded NO concentration gradient model within that silicone rubber surface of the Edwards commercial glucose sensor.

However, modeling of the NO release from such a surface, seen in Figure 5.9, suggests that transient NO from a 5 min charging time would be depleted much faster than the 5-8 min shown in the experimental data. This would indicate that the actual thickness of the outer layer of the Edwards commercial system is greater than the value used in the model, as a thicker layer could accumulate a greater reservoir of transient NO that would accordingly, take a longer time to exhaust. The actual diffusion constant and partitioning coefficient values are also very specific to chemical structure, such that they can vary between polyurethanes depending on the soft and hard segment composition.

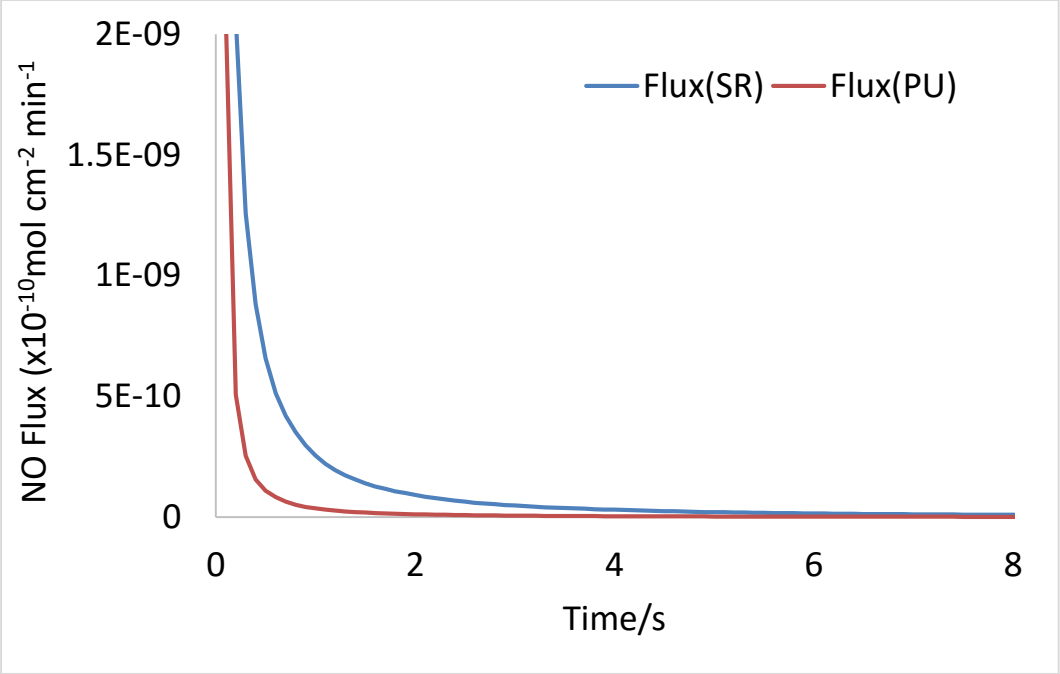

Figure 5.9. Comparison model of theoretical NO release from a polyurethane (PU)-based outer glucose sensor coating versus a silicone rubber (SR)-based coating. An outer sensor coating composed of segments more similar in structure to silicone rubber would likely show a longer duration of NO release. The actual thickness of the outer polyurethane is very likely greater than the thickness of the layers for the model, which would also result in more prolonged NO release.

5.3.3 Analytical In Vitro Performance of Edwards Glucose Sensors

The Edwards commercial glucose sensors are fabricated by machine process (Figure 5.10) rather than individually assembled by hand, resulting in greatly reduced variation in sensor response between individual sensors. In addition, the layers of polyurethane applied over the enzyme layers are both very thin and extremely consistent across a given lot, granting exceptionally fast response times for nearly every sensor. In comparison, hand-fabricated sensors with only polyurethane outer coatings (like those in Chapter 2) have significantly faster response times than those assembled with several coatings of NO releasing compounds, such as the PLA/DBHD/N_2O_2 glucose sensors described in Chapter 4. One specific advantage of using

indirect NO release through transient diffusion and partitioning is that the rapid response time of the sensor remains uncompromised, which can be quite challenging to achieve when sensors are prepared with a directly applied NO release coating on their surfaces (see Chapter 4).

In addition, it was of utmost importance to also conduct glucose calibrations of the sensors following the transient NO release testing to ensure that glucose oxidase activity, linear range, and response time were not damaged or adversely effected by the NO charging or release measurements. Figure 5.11 shows a typical glucose calibration of the Edwards sensors after NO release testing. Glucose oxidase activity and linear range are superb, and sensor response time is very rapid, demonstrating that the transient NO exposures do not affect analytical performance of the glucose sensors for their intended function.

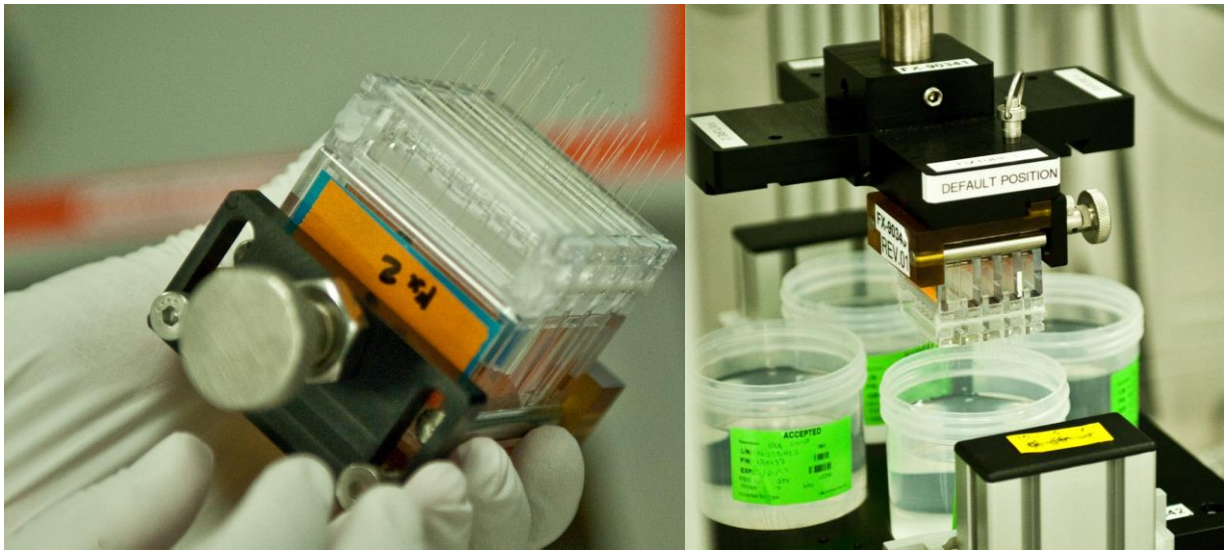

Figure 5.10. Outer layer layer-by-layer assembly array for Edwards commercial glucose sensors.

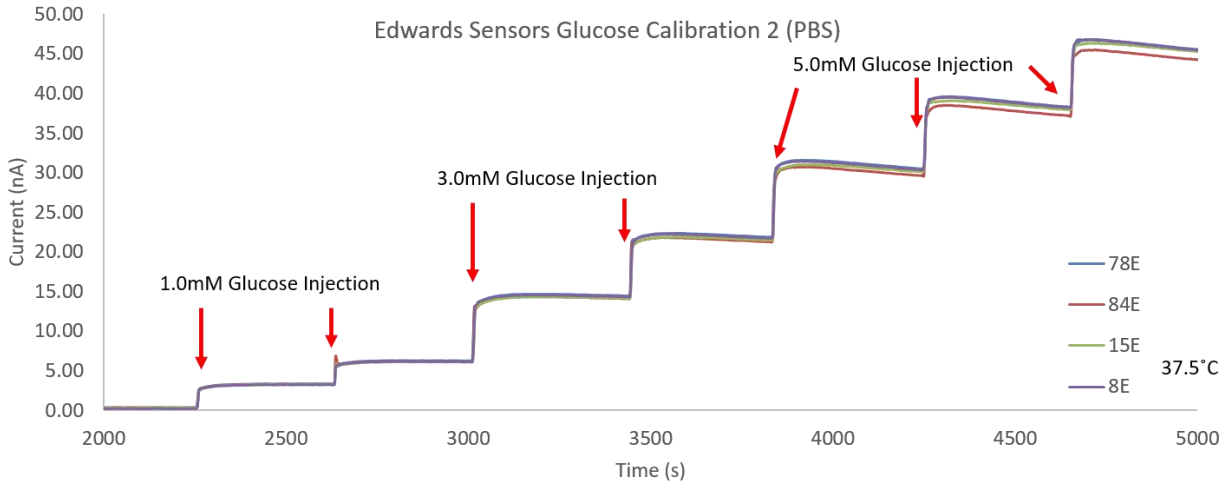

Figure 5.11. *In vitro* glucose calibration of Edwards commercial glucose sensors to assess preservation of glucose oxidase activity, sensor linearity, and sensor response time following transient NO release testing.

5.4 Conclusions and Future Directions

Incorporation of NO releasing chemistry offers a great advantage of thromboresistance to sensors intended for blood-contacting applications. Previously published work has focused primarily on coating glucose sensor with a NO releasing layer composed of diazeniumdiolated compounds or more robust *S*-nitrosothiols like SNAP. However, in this specific case, the Edwards GlucoClear system is only exposed to whole blood during a small portion of its lifetime, giving the flexibility to localize the source of NO release chemistry to the catheter housing of the sensor, rather than the sensor surface, as would be required of sensors in constant blood contact (due to rapid NO scavenging by hemoglobin in blood). Instead, if NO is able to diffuse through the aqueous catheter calibration solution and partition into the thin outer polyurethane layer of the commercial sensor for the 5 min interval between blood measurements, it can theoretically achieve a higher NO concentration than is found in the solution, due to favorable diffusion and partitioning into the polyurethane layer. Preliminary tests show that transient NO release accumulated from

this charging phase can then release for a duration of at least 5 min once the sensor is isolated from the source catheter, as would occur if the catheter were filled with blood. Additional optimization involving SNAP-loaded catheters of different sizes (resulting in different source NO flux values) or additional concentrations of SNAP-loading impregnation solutions could be conducted to determine the maximum values for peak and longest-lasting NO release. However, the experiments described in this chapter are proof-of-concept that glucose sensor thromboresistance through transient NO release is a worthwhile alternative to use of heparin for the intermittent-sampling GlucoClear device.

5.5 Literature Cited:

(1) Foubert, L. A.; Lecomte, P. V.; Nobels, F. R.; Gulino, A. M.; De Decker, K. H. *Diabetes Technol The* **2014**, *16*, 858.
(2) Foubert, L. 2013; Vol. 2015.
(3) Edwards Lifesciences Corporation: 2013; Vol. 2015.
(4) Tapsak, M. A. R. K. R., R. K.; Shults, M. C.; McClure, J. D.; Dexcom, Inc.: United States, May 22, 2002; Vol. US7226978 B2.
(5) Simpson, P. C. G., P.; Tapsak, M. A.; Carr-Brendel, V.; Dexcom, Inc.: United States, Jul 21, 2004; Vol. US7108778 B2.
(6) Ren, H.; Colletta, A.; Koley, D.; Wu, J.; Xi, C.; Major, T. C.; Bartlett, R. H.; Meyerhoff, M. E. *Bioelectrochemistry* **2015**, *104*, 10.
(7) Brisbois, E. J.; Handa, H.; Major, T. C.; Bartlett, R. H.; Meyerhoff, M. E. *Biomaterials* **2013**, *34*, 6957.
(8) Brisbois, E. J.; Davis, R. P.; Jones, A. M.; Major, T. C.; Bartlett, R. H.; Meyerhoff, M. E.; Handa, H. *J Mater Chem B* **2015**, *3*, 1639.
(9) Vaughn, M. W.; Kuo, L.; Liao, J. C. *Am J Physiol-Heart C* **1998**, *274*, H2163.
(10) Chipinda, I.; Simoyi, R. H. *J Phys Chem B* **2006**, *110*, 5052.
(11) Simmons, A.; Hyvarinen, J.; Odell, R. A.; Martin, D. J.; Gunatillake, P. A.; Noble, K. R.; Poole-Warren, L. A. *Biomaterials* **2004**, *25*, 4887.

CHAPTER 6

CONCLUSIONS AND FUTURE DIRECTIONS

6.1 Summary of Results for Dissertation Research

The benefits of tight glycemic control range from minimizing complications for diabetic patients to improving patient outcomes for all critically-ill patients, even those without diabetes. Monitoring a patient's blood glucose levels continuously or intermittently via electrochemical glucose sensors offers an advantage of detecting and predicting increasing/decreasing trends over benchtop blood analyzers, which only offer discrete time-point measurements from drawn samples taken every few hours.[1-3] Electroactive species present in the complex matrix of whole blood can cause inaccurate measurements stemming from the interference currents they can generate without the addition of selectivity-enhancing layers. Development of implantable glucose sensors has also been impeded by the body's immune and foreign body response to implanted devices, which often results in surface clotting and performance failure when such devices are placed intravenously. Therefore, development of methods to enhance the biocompatibility of implantable glucose sensors, with respect to selectivity for current response arising only from glucose as well as sensor surface functionalization to add thromboresistant capability, are of great research and commercial interest. Chapter 1 discussed the wide range of glucose sensing devices developed through

academic research or commercially produced products, and the wide variety of biocompatibility-enhancement strategies that have yielded various levels of effectiveness to date.

Previous intravenous glucose sensor designs required a combination of layers to provide sensor selectivity over electroactive interference species such as ascorbic acid, uric acid, and acetaminophen. Often, a Nafion layer was applied first, providing selectivity over negatively charged species such as ascorbic and uric acid. This would be followed by addition of a size exclusion layer, formed by the electropolymerization of 1,3-diamnobenzene and resorcinol within the pores of the Nafion layer.[4-9] However, studies of Nafion films, for applications other than implantable sensors, that were subjected to an annealing process showed increased rejection of large anionic species, indicative of reorganization of the internal sulfonate groups within the Nafion film structure, resulting in smaller hydrophilic channels.[10-12] Application of annealed Nafion layers to implantable glucose sensors could therefore enhance the sensor selectivity. Indeed, in Chapter 2, glucose sensors fabricated with annealed Nafion layers exhibited enhanced selectivity (over non-annealed films) over ascorbic and uric acid, reducing their interference signal contribution to ≤ 3 % of the signal measured for typical blood glucose concentration (5 mM) for a duration of 8 d. The variation in selectivity over ascorbic and uric acid between individual sensors was also smaller than glucose sensors fabricated by previously reported methods using a non-annealed Nafion selectivity-enhancing layer.[4,6,13,14]

In Chapter 3, a collaboration with researchers at the University of Pennsylvania who are experts on functionalizing blood-contacting polymeric surfaces with CD47 protein[15-17] led to the development of intravascular glucose sensors with CD47 successfully functionalized onto the E2As Elast-Eon polyurethane outer coating of these devices. The CD47 protein endogenously functions as a marker of self, being ubiquitously expressed within the cell membranes of many

cells. When it undergoes a temporary "handshake" interaction with its cognate receptor protein, SIRPα, expressed within the cell membranes of inflammatory cells (e.g., platelets, neutrophils, etc.), the inflammatory cells are not activated and immune response and coagulation cascades are not triggered.[18-24] Preliminary *in vitro* calibrations, conducted before and after CD47 immobilization, show that the steps required for immobilization protocol do not adversely influence the glucose response properties of such sensors. Glucose sensors surface-functionalized with recombinant human CD47 retain their linear response range and glucose oxidase activity after the surface functionalization procedure. In addition, testing of selectivity before and after CD47 functionalization, revealed that an acceptable level of selectivity over electroactive interference species based on the use of an annealed Nafion inner layer was also maintained throughout the immobilization procedure.

In Chapter 4, intravenous glucose sensors featuring a nitric oxide (NO) releasing layer composed of diazeniumdiolated N,N'-dibutyl-1,6-hexanediamine (DBHD/N_2O_2), an NO donor molecule, suspended in a pH-controlled poly(lactic acid) PLA matrix, were examined for continuous *in vivo* monitoring of glucose. This research expanded upon prior studies regarding the use of intravenous NO releasing glucose sensors implanted within rabbits.[4,6,14] In this new work, blood glucose concentration was modulated via intravenous injections of dextrose, and the sensor response was shown to correctly report the rising and falling blood glucose concentrations, which were compared alongside discrete time points of measured venous blood glucose values, as measured by a benchtop whole blood analyzer. In addition, the NO release glucose sensors of similar design were used in preliminary extended duration 20 h porcine studies to generate continuous time traces of venous blood glucose, as modulated with dextrose injections. Due to significant sensor calibration drift during the course of these 20 h porcine experiments, it was

difficult to convert the raw current values measured by the glucose sensors into venous blood glucose concentration values that matched with the discrete *in vitro* whole blood values. A two point calibration model for data interpretation, conducted several hours after the start of the experiment, proved to yield a better fit model for determining glucose concentration values than a model based on *in vitro* calibration in bovine serum prior to *in vivo* implantation or a one-point calibration taken from a discrete whole blood *in vitro* measurement at the start of the experiment. As a direct result of calibration difficulties for these 20 h *in vivo* studies, *in vitro* investigations were conducted to determine the underlying cause for the calibration drift. The intravenous drugs dopamine, vecuronium bromide, epinephrine, and heparin, which are administered to the pig throughout the course of the experiment to regulate metabolic functions, were individually determined not to adversely affect the glucose response properties of the sensors. Hemoglobin, an element found in whole blood in high concentrations (in red blood cells) but not in bovine serum was suspected to scavenge NO released at the sensing surface, thereby reducing the oxidation current background. However, an *in vitro* benchtop experiment showed that introduction of a 4.01 mM oxyhemoglobin solution did not result in a decreased background current response from the sensor ruling out this mechanism as the root cause of the calibration problems. Diffusion cell experiments ruled out the buildup of a membrane potential in serum as a source of drifting sensor signal due to changes in applied voltage to the underlying Pt working electrode of the implantable glucose sensor. SEM imaging determined that pinholes in the outer polyurethane membrane, rather than bulk diffusion across the layer, were likely responsible for the limited diffusion of glucose that provides the sensors their linear range. Eventually, it was determined that increasing the duration of time allotted for glucose oxidase to be crosslinked and immobilized during sensor fabrication from 2 h to >10 h increased the stability of glucose oxidase activity in a bovine serum

matrix. A series of extended *in vitro* calibrations in bovine serum as well as analysis over a >45 h period yielded enhanced current stability at a constant serum glucose concentration. NO release glucose sensors with increased crosslinking time displayed analytically accurate glucose measurements in bovine serum, with both increasing and decreasing concentration modulations after an extended (>8 h). This suggests that glucose sensors with increased cross-linking time will likely better resist *in vivo* calibration drift in future animal testing of the NO release glucose sensors.

In Chapter 5, a method to enhance the thromboresistance via NO release of a commercial system designed by Edwards Lifesciences to aid in tight glycemic control was examined. In its current form the system functions by drawing venous blood samples through an IV access and measuring blood glucose in those samples intermittently every 5 min *via* a glucose sensor placed within the catheter. When blood is not drawn back over the sensor, the sensor surface is in direct contact with a stream of aqueous solution containing a known glucose level (used for continual calibration of the sensors) as well as heparin (to prevent clot formation on the sensor surface). Since the majority of the time the sensors would be in the buffered, aqueous calibration solution, rather than in constant contact with whole blood, it was reasoned that incorporating active NO release within the catheter tubing that surrounds the electrochemical glucose sensor would be a viable alternative to attempting to directly apply an NO releasing coating to the sensor surface, thereby preserving the rapid sensor response time and low variability of behavior between individual, commercially-produced sensors. Without the presence of hemoglobin to act as a rapid NO scavenger, the NO released from the inner wall of the tubing could diffuse to the thin polyurethane outer surface of the glucose sensors and favorably partition into that material. If partitioning of NO into the polyurethane over the surrounding solution was favorable, the

polyurethane layer could be "charged" with an elevated concentration of transient NO, which could be subsequently released during the blood-contact phase of calibration. This would provide the sensor surface with enhanced thromboresistance obviating the need for heparin in the calibration solution. While the original pellethane catheter tubing used by Edwards to house the sensors in the GlucoClear system could not be effectively loaded with *S*-nitroso-*N*-acetylpenicillamine (SNAP), an NO releasing donor molecule, silicone rubber catheters of similar size can be loaded with SNAP and provide sustained NO release. Selection of silicone rubber catheters for this application was based on recently published results regarding a solvent swelling method to incorporate SNAP into silicone rubber tubing.[25] It was essential to determine if the source SNAP-loaded catheter could provide an adequate measure of NO sufficient to allow the secondary transient NO release from the glucose sensor surface. Placement of sample commercial sensors within SNAP-loaded SR tubing for a duration of 5 min to charge the polyurethane layer with transient NO revealed a sufficiently high enough NO concentration within the polyurethane which provided at least 5 min of NO release from the sensor surface. However, the magnitude of transient NO release did appear to depend upon the flux level from the SNAP-loaded source catheter surrounding the sensor, and a source catheter with less than desired surface flux yielded a proportionally lower transient NO release from the glucose sensors. Glucose calibrations conducted on these sensors following NO release testing confirmed no adverse effects to the glucose response properties of the sensor after exposure to the NO coming from the SNAP-doped catheter.

Diffusion and partitioning modeling of NO by COMSOL® Multiphysics via a collaboration with Hang Ren shed insight on the mechanics of this method of secondary NO release. The model is constructed using diffusion and partition coefficients for common polyurethane structures.

Modeling results revealed that a 5 min charging period of a glucose sensor within an NO releasing source catheter of given dimensions (i.d.) would accumulate an elevated concentration of NO as compared to the solution in the catheter surrounding the sensor. In addition, the NO concentration within that layer is expected to be uniform. A second model assuming a sensor outer layer with properties akin to silicone rubber showed a similar ability to uniformly charge the outer layer with NO, except that the transient NO could accumulate to an even higher concentration within the sensor's outer layer. Assuming that the commercial sensors were fabricated with a polyurethane layer with a high percentage of poly(dimethylsiloxane) segments and characteristics, its behavior would likely be an intermediate between the two models.

6.2 Future Work

Glucose sensors with annealed Nafion were shown to provide a significant increase in selectivity over the negatively charged interference species of ascorbic and uric acid as compared to previous fabrication techniques. In future research, one could conduct daily selectivity experiments for a longer duration (10-20 d) in order to determine the lifetime of this enhanced selectivity before significant degradation occurs to the annealed Nafion layer. *In vitro* experiments are the best way to evaluate selectivity, as the exact amount of the interference species can be controlled, although spiking a bovine serum sample or intravenously administering a bolus of interference species could be pursued to give an approximation of the actual *in vivo* selectivity (in the presence of blood components). If the sensor fabrication protocols for annealed Nafion are closely followed, the Nafion film and its selectivity character are quite reproducible; thus it is anticipated that these coatings should continue to maintain selectivity when used for *in vivo* experiments.

The majority of work conducted in Chapter 3 with the CD47 surface-functionalized glucose sensors serves as proof-of-concept, and the next logical progression will be to determine whether immobilized CD47 confers sufficient hemocompatibility to enable the glucose sensors not to activate the coagulation cascade when tested *in vivo.* Studies to assess the CD47's antithrombotic activity when immobilized on implantable chemical sensors are currently being planned. To answer an additional key question, a comparison study should be conducted to determine whether immobilized CD47 provides an equivalent level of anti-platelet activity as sensors prepared only with NO releasing capability. Perhaps sensors prepared with a combination of both immobilized CD47 and NO release will be the most desirable approach to enhancing biocompatibility (see Figure 6.1). To potentially pursue this approach, the NO releasing polymeric coating would need to first be applied as an inner layer and then CD47 could be functionalized on the outermost surface of a thin additional layer of polyurethane. Since NO is readily permeable through polyurethanes, the addition of this layer should have little effect on the NO release flux of such a sensing device. The critical component that will need to be controlled in this configuration is the length of time that the sensor is hydrated during the CD47 immobilization process, since NO release will occur over this period and hence decrease the overall NO reservoir remaining within the sensor. However, if the CD47 reaction times can be limited to 8 h or so, and the glucose sensors can be immediately dried thoroughly, the loss of NO will be minimal.

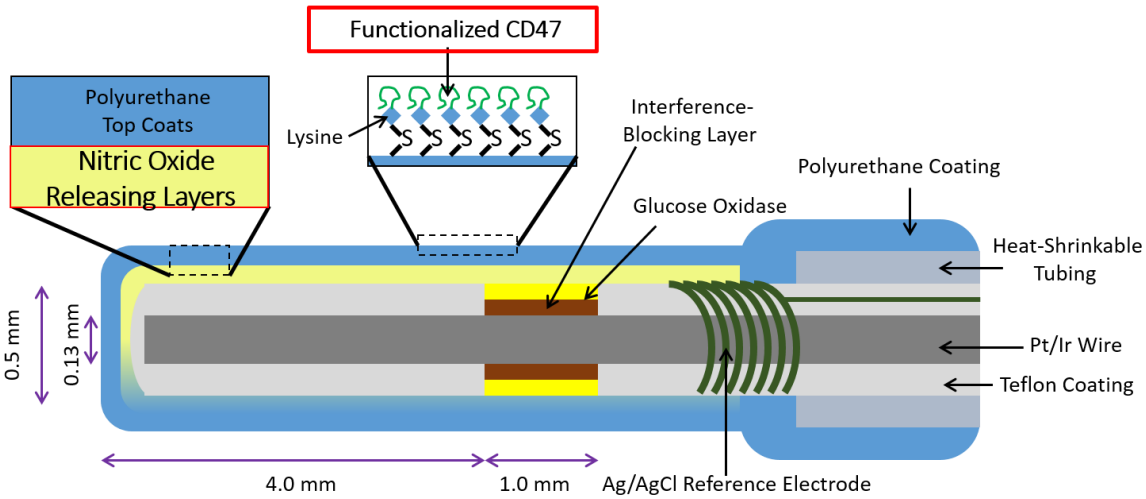

Figure 6.1. Glucose sensor incorporating an underlying NO releasing layer and then CD47 immobilization on the exterior of the outer polyurethane top coat.

Identification of increased glutaraldehyde crosslinking reaction time allotted to the glucose oxidase enzyme layer is a critical step to enhancing current signal stability in surrounding environments and should allow the continuation of long-term *in vivo* implantation studies for the NO release glucose sensors described in Chapter 4. Sensors fabricated with these protocol changes should experience significantly less calibration drift, resulting in a greater degree of analytical accuracy for *in vivo* blood glucose measurements with time. Additional *in vivo* data showing accurate continuous time trace measurements as blood glucose is modulated with intravenous dextrose are needed for publication of the 20 h *in vivo* studies. Other researchers within the Meyerhoff lab are developing variations on designs for NO release glucose sensors. Though it has been shown to be a more stable NO donor, SNAP cannot be directly used in place of DBHD & N_2O_2 for the needle type glucose sensors, due to insufficient duration of NO release. Dr. Xuewei Wang, a postdoctoral fellow in the Meyerhoff laboratory, has developed a catheter-based glucose sensor that does not directly have an NO releasing layer applied to its surface. Rather, glucose

sensors with only polyurethane coatings are placed inside small pre-swelled and pre-SNAP-loaded catheters, which do provide NO release for >14 d, while maintaining glucose response properties. A similar approach using a dual-lumen silicone rubber catheter, where one lumen contains a glucose sensor (without an NO releasing layer) and the other lumen generates NO electrochemically from nitrite reduction. If additional difficulties arise from *in vivo* testing of the specific NO release glucose sensor design detailed in Chapter 4, these other NO release strategies could be further developed.

Continuation of the preliminary testing in Chapter 6 could immediately involve the SNAP-loading of additional silicone rubber catheters, preferably of increased wall thickness, to determine if a loaded catheter with an increased surface source NO flux could further increase the concentration of transient NO accumulated and released from the Edwards sensor's polyurethane layer. If the specific type of polyurethane used to fabricate the sensors can be determined, a more specifically tailored computer model could be constructed, reflecting its specific NO diffusion and partition coefficients. Eventually, a mimic of the whole Edwards GlucoClear system could be assembled with peristaltic pumps and heparinized blood, to serve as an *in vitro* simulation of analytical performance of the proposed design. The effectiveness of transient NO as an anti-thrombotic agent could be determined via use of the a pumping system connected to an *in vivo* animal, which would sample blood intermittently using a flow profile employed in the Edwards commercial system.

6.3 Literature Cited

(1) Wilinska, M. E.; Hovorka, R. *Clin Chem* **2014**, *60*, 1500.
(2) Van Herpe, T.; De Moor, B.; Van den Berghe, G.; Mesotten, D. *Clin Chem* **2014**, *60*, 1510.
(3) Boyd, J. C.; Bruns, D. E. *Clin Chem* **2014**, *60*, 644.
(4) Yan, Q. Y.; Major, T. C.; Bartlett, R. H.; Meyerhoff, M. E. *Biosens Bioelectron* **2011**, *26*, 4276.
(5) Bindra, D. S.; Zhang, Y. N.; Wilson, G. S.; Sternberg, R.; Thevenot, D. R.; Moatti, D.; Reach, G. *Anal Chem* **1991**, *63*, 1692.
(6) Yan, Q. Y.; Peng, B.; Su, G.; Cohan, B. E.; Major, T. C.; Meyerhoff, M. E. *Anal Chem* **2011**, *83*, 8341.
(7) Gifford, R.; Batchelor, M. M.; Lee, Y.; Gokulrangan, G.; Meyerhoff, M. E.; Wilson, G. S. *J Biomed Mater Res A* **2005**, *75a*, 755.
(8) Geise, R. J.; Adams, J. M.; Barone, N. J.; Yacynych, A. M. *Biosens Bioelectron* **1991**, *6*, 151.
(9) Carelli, I.; Chiarotto, I.; Curulli, A.; Palleschi, G. *Electrochim Acta* **1996**, *41*, 1793.
(10) Kwon, O.; Wu, S. J.; Zhu, D. M. *J Phys Chem B* **2010**, *114*, 14989.
(11) Singhal, N.; Datta, A. *J Phys Chem B* **2015**, *119*, 2395.
(12) Evans, C. M.; Singh, M. R.; Lynd, N. A.; Segalman, R. A. *Macromolecules* **2015**, *48*, 3303.
(13) Wisniewski, N.; Reichert, M. *Colloids Surf B Biointerfaces* **2000**, *18*, 197.
(14) Yan, Q. Doctor of Philosophy Dissertation (Chemistry), University of Michigan, 2011.
(15) Stachelek, S. J.; Finley, M. J.; Alferiev, I. S.; Wang, F. X.; Tsai, R. K.; Eckells, E. C.; Tomczyk, N.; Connolly, J. M.; Discher, D. E.; Eckmann, D. M.; Levy, R. J. *Biomaterials* **2011**, *32*, 4317.
(16) Finley, M. J.; Rauova, L.; Alferiev, I. S.; Weisel, J. W.; Levy, R. J.; Stachelek, S. J. *Biomaterials* **2012**, *33*, 5803.
(17) Finley, M. J.; Clark, K. A.; Alferiev, I. S.; Levy, R. J.; Stachelek, S. J. *Biomaterials* **2013**, *34*, 8640.
(18) Jaiswal, S.; Jamieson, C. H. M.; Pang, W. W.; Park, C. Y.; Chao, M. P.; Majeti, R.; Traver, D.; van Rooijen, N.; Weissman, I. L. *Cell* **2009**, *138*, 271.
(19) Soto-Pantoja, D. R.; Stein, E. V.; Rogers, N. M.; Sharifi-Sanjani, M.; Isenberg, J. S.; Roberts, D. D. *Expert Opin Ther Tar* **2013**, *17*, 89.
(20) Hsu, Y. C.; Acuna, M.; Tahara, S. M.; Peng, C. A. *Pharm Res* **2003**, *20*, 1539.
(21) Tsai, R. K.; Discher, D. E. *J Cell Biol* **2008**, *180*, 989.
(22) Rodriguez, P. L.; Harada, T.; Christian, D. A.; Pantano, D. A.; Tsai, R. K.; Discher, D. E. *Science* **2013**, *339*, 971.
(23) Bruns, H.; Bessell, C.; Varela, J. C.; Haupt, C.; Fang, J.; Pasemann, S.; Mackensen, A.; Oelke, M.; Schneck, J. P.; Schutz, C. *Clin Cancer Res* **2015**, *21*, 2075.
(24) Sosale, N. G.; Spinier, K. R.; Alvey, C.; Discher, D. E. *Curr Opin Immunol* **2015**, *35*, 107.
(25) Ren, H.; Colletta, A.; Koley, D.; Wu, J.; Xi, C.; Major, T. C.; Bartlett, R. H.; Meyerhoff, M. E. *Bioelectrochemistry* **2015**, *104*, 10.